

7-11-2016

# Protein-Polymer Nanocomposites for Enzymatic Catalysis in Hostile Media

Omkar V. Zore

*University of Connecticut*, [omkar.zore@uconn.edu](mailto:omkar.zore@uconn.edu)

Follow this and additional works at: <https://opencommons.uconn.edu/dissertations>

---

## Recommended Citation

Zore, Omkar V., "Protein-Polymer Nanocomposites for Enzymatic Catalysis in Hostile Media" (2016). *Doctoral Dissertations*. 1136.  
<https://opencommons.uconn.edu/dissertations/1136>

# **Protein-Polymer Nanocomposites for Enzymatic**

## **Catalysis in Hostile Media**

Omkar V. Zore, PhD

University of Connecticut, 2016

### **Abstract**

Recently use of protein-polymer nanocomposites in biocatalysis is becoming the area of interest for wide varieties of applications. Our lab focuses on development and design of the protein-polymer conjugates and then synthesizing nanocomposites using 2D nano-layered materials such as graphene oxide (GO) and graphene. These nanocomposites can be used in plethora applications such as solar cells, biofuel cells, bio-batteries and in biocatalysis for various industrial applications. The whole world is facing an energy crisis situation and we urgently need alternative to fuel source. Therefore, well thoughtful synthesis and design of protein-polymer nanocomposites are need of an hour. Preliminary part of this study is focused on production of protein-polymer conjugate and then assembly of these conjugates on GO or graphene. Then the characterization and evaluation for biocatalysis and other valuable applications.

Four major goals that form the basis of this thesis are- 1. Synthesis and characterization of the enzyme-polymer nanocomposites using simple and green method using biocompatible materials to stabilize enzymes. 2. Synthesize enzyme-polymer conjugates for biocatalysis in organic media. 3. Synthesis of bienzyme-polymer conjugates and nanocomposites for biocatalysis at low pH conditions, high temperatures and in presence of denaturant such as sodium

dodecyl sulfate (SDS). 4. Production of multienzyme-polymer conjugates and nanocomposites for biocatalysis and biofuel cell applications.

**Protein-Polymer Nanocomposites for Enzymatic  
Catalysis in Hostile Media**

**Omkar V. Zore**

B. Pharm., Institute of Chemical Technology, 2011

A Dissertation

Submitted in Partial Fulfillment of the  
Requirements for the Degree of Doctor of Philosophy  
at the  
University of Connecticut

2016

Copyright by

Omkar V. Zore

2016

**APPROVAL PAGE**

**Doctor of Philosophy Dissertation**

**Protein-Polymer Nanocomposites for Enzymatic Catalysis in Hostile Media**

**Presented by**

**Omkar V. Zore**

Major Advisor \_\_\_\_\_

**Dr. Rajeswari M. Kasi**

Associate Advisor \_\_\_\_\_

**Dr. Challa V. Kumar**

Associate Advisor \_\_\_\_\_

**Dr. Ashis Basu**

**University of Connecticut**

**2016**

## **ACKNOWLEDGEMENTS**

I would like to thank bunch of people that helped me get through this landmark in my life. Firstly, thank you Raji, for getting me into the group and having faith in me. I was from pharmacy background still you kept trusting me and had confidence in me. In tough times, you always helped to boost my confidence and helped me focus on the research. I will always cherish the memories for being part of Kasi research group for 5 years. Also, I would like to wish you best in our research projects.

Dr. Kumar, thank you so much for giving me a lab space in Kumar lab. Also, thank you for advising me and asking me those tough questions in group meeting that helped me develop as a person as well as a researcher. I will always remember your phrase –“science is not a religion, so do not blindly believe it.” You have been inspirational in all aspects of research. I wish you good health and best luck for research. I will miss our lab a lot.

I would like to thank Dr. Basu for collaborating with me and being on my committee. Also, guiding me in one of my research papers. Also, a big thanks goes to Dr. He and Dr. Selampinar for being on my committee. I especially want to thank Dr. Selampinar for my initial few years at Uconn where I got to learn from you the work ethics.

I will thank my previous lab members and mentors, Dr. Victoria, Dr. Prashant, Dr. Vindya, Dr. Inoka, Kyle and Marc, It was fun working with you and I missed you in my journey of PhD. Also I will thank current group members- Ajith, Clive, Bobbi,

Cat, Ananta, Kyle, Lalit, Jingwen, Melissa, Megan, Athina, Dennis, Reuben, Samiksha, Xixian, also my undergrads- Pat, Shailaja and Faith you guys are the best and with you PhD was somewhat fun. I thank you all for being part of my PhD journey. Also, thank you to my 'Coffee Club' members- Ajith, Clive, Abhay and Amit, It was fun to have a coffee in the afternoon with you guys which kept me going for the rest of my day doing research. I am going to miss you all a lot.

I would like to thank my family members who were big part of where I am today. I want to thank my Aai (mother), Baba (father), Ajoba (grandfather) and Aji (grandmother), I thank you all for everything. I want to thank Baba especially for encouraging me time to time whenever I felt let down. Thank you Aai, for being there, your emotional support meant a lot to me. Words are not enough. Also, I want to thank special person in my life, Payal, my girlfriend, thank you so much, for listening to me when I was behaving mad, thank you for understanding me. I know it's tough to be with me. Again words are not enough and I am sure we will be together soon. Love you Aai, Baba, Ajoba, Aji and Payal. Also, thank you my little siblings, Yash and Aashi, I hope this thesis will be inspirational to you.

Lastly, I want to dedicate this thesis to my Ajoba, I was saddened by his death exactly two weeks before my thesis oral defense. I would have loved if you were with me to hear this good news of me becoming a Dr. in Chemistry. I know it was your dream and I will miss you the most. You were the most inspirational person I ever came across in my life. You beat all the odds in life and you were a true fighter. I love you.

If I missed thanking someone, I take opportunity to thank them too.



## **TABLE OF CONTENTS**

<b>List of Tables</b>	<b>xii</b>
<b>List of Charts</b>	<b>xiii</b>
<b>List of Schemes</b>	<b>xiv</b>
<b>List of Figures</b>	<b>xvi</b>
<b>Chapter 1: introduction</b>	<b>1</b>
1.1 Introduction	1
1.2 Wrapping as a strategy	2
1.3 Protein-polymer conjugates: synthesis and characterization	3
1.4 Entropy control	7
1.5 Protein-polymer nanocomposites for biocatalysis and other applications	9
1.6 Overview of Thesis	10
 <b>Chapter 2: Efficient Biocatalysis in Organic Media with Hemoglobin and Poly (Acrylic Acid) Nanogels</b>	 <b>15</b>
2.1 Abstract	15
2.2 Introduction	16
2.3 Experimental	22
2.3.1 Materials	22
2.3.2 Synthesis of Hb-PAA conjugates	22
2.3.3 Synthesis of Hb-PAA ester conjugates	22
2.3.4 Circular dichroism (CD) studies	23
2.3.5 Activity studies	23

2.3.6 Calculating $K_M$ and $V_{max}$ values	24
2.3.7 Dynamic light scattering (DLS)	24
2.3.8 Transmission electron microscopy (TEM)	25
2.3.9 Infrared spectroscopy	25
2.3.10 Zeta potential studies	25
2.4 Result and discussion	26
2.4.1 Synthesis	26
2.4.2 Zeta potential studies	26
2.4.3 Infrared spectroscopy (IR)	29
2.4.4 TEM and DLS	29
2.4.5 Protein structure in the conjugates	32
2.4.6 Activity studies	40
2.4.7 $K_M$ and $V_{max}$ studies	49
2.5 Conclusion	56
2.6 References	57

### **Chapter 3: Bienzyme-Polymer-Graphene Oxide Quaternary Hybrid**

#### **Biocatalysts: Efficient Substrate Channeling at Chemically and Thermally**

<b>Denaturing Conditions</b>	61
3.1 Abstract	61
3.2 Introduction	62
3.3 Experimental	67
3.3.1 Materials	67
3.3.2 Synthesis of GO	67

3.3.3 Synthesis of bienzyme-PAA and bienzyme-PAA/GO conjugates	69
3.3.4 Zeta potential studies	69
3.3.5 Agarose gel electrophoresis	69
3.3.6 Circular dichroism (CD) studies	70
3.3.7 Transmission electron microscopy	70
3.3.8 Activity studies	70
3.3.9 Activity study with denaturant (SDS) and at high temperature (65 °C)	
3.3.10 Kinetics studies	71
3.4 Results	72
3.4.1 Synthesis	72
3.4.2 Agarose gel electrophoresis	73
3.4.3 Zeta potential studies	74
3.4.4 Circular dichroism (CD) studies	79
3.4.5 Transmission electron microscopy	85
3.4.6 Activity studies	87
3.4.6.1 Activity studies at room temperature and pH 7.4	87
3.4.6.2 Activity studies at different pH's in presence and absence of a chemical denaturant	88
3.4.6.3 Activity studies at 65 °C	94
3.4.7 Kinetics studies	97
3.5 Discussion	102

3.6 Conclusion	110
3.7 References	111
<b>Chapter 4: Biocompatible Multienzyme-Polyacrylic Acid Conjugates for High Temperature Catalysis</b>	<b>115</b>
4.1 Abstract	115
4.2 Introduction	116
4.3 Experimental	120
4.3.1 Materials	120
4.3.2 Synthesis of MEC's	120
4.3.3 Parallel synthesis of 5-P	120
4.3.4 Sequential synthesis of 5-S	121
4.3.5 Zeta potential studies	121
4.3.6 Agarose gel electrophoresis	121
4.3.7 Circular dichroism (CD)	122
4.3.8 Transmission electron microscopy	122
4.3.9 Dynamic light scattering	122
4.3.10 Catalytic activity measurements	123
4.3.10.1 Glucose oxidase (GOx) activity	123
4.3.10.2 Horseradish peroxidase (HRP) activity	123
4.3.10.3 Lipase (Lip) activity	124
4.3.10.4 Acid phosphatase (AP) activity	124
4.3.10.5 Lactate dehydrogenase (LDH) activity	125
4.3.11 Activity studies at high temperature (65 °C)	125

4.3.12 Kinetic studies	125
4.4 Results	127
4.4.1 Synthesis of MEC's	127
4.4.1.1 Synthesis of 5-P	128
4.4.1.2 Synthesis of 5-S	128
4.4.2 Agarose gel electrophoresis	129
4.4.3 Zeta potential studies	129
4.4.4 Transmission electron microscopy (TEM)	132
4.4.5 Dynamic light scattering (DLS)	132
4.4.6 Circular dichroism (CD) studies	134
4.4.7 Activity studies	137
4.4.7.1 Activity studies at room temperature	137
4.4.7.2 Activity studies at 65 °C	140
4.4.8 Kinetic studies	143
4.5 Discussion	148
4.6 Conclusion	155
4.7 References	156
<b>Chapter 5: Summary and Proposal of Future Work</b>	<b>159</b>
5.1 Summary	159
5.2 Proposal of future work	162
5.2.1 Biocatalysis	162
5.2.2 Sensing	163
5.2.3 Biofuel cell application	163



## List of Tables

**Table 2.1.** Size (hydrodynamic diameter) of conjugates and Hb using Dynamic Light Scattering in PB (10 mM. pH 7.4) at room temperature.

**Table 2.2.** Determination of  $K_M$ ,  $V_{max}$ ,  $k_{cat}$  and  $k_{cat}/K_M$

**Table 3.1.** Different conjugates and the mass percent of enzymes, PAA and GO used for synthesis.

**Table 3.2** Catalytic constants  $K_M$ ,  $V_{max}$ ,  $K_{cat}$  [Turnover Number (TON)] and catalytic efficiency of conjugates and corresponding unmodified protein.

**Table 3.3.** Comparison of substrate channeling efficiency of current catalytic system with other relevant reports.

**Table 4.1:** DLS data of MEC's, enzyme-PAA and enzymes illustrating the size of the samples. Data is gathered at pH 7.4 PB at 25 °C.

**Table 4.2:** Kinetic parameters such  $K_M$ ,  $V_{max}$ ,  $K_{cat}$  and catalytic efficiency of all the enzymes, enzyme-PAA, 5-P and 5-S. All the kinetic parameters were gathered in pH 7.4, 10 mM Tris/ phosphate buffer.

## List of Charts

**Chart 3.1:** Key properties of glucose oxidase (GOx) and Horseradish Peroxidase (HRP).

**Chart 4.1.** Key properties of glucose oxidase (GOx), horseradish peroxidase (HRP), lactate dehydrogenase (LDH), acid phosphatase (AP) and Lipase (Lip).



## List of Schemes

**Scheme 1.1:** Synthesis strategy for the protein-polymer conjugates. Hemoglobin (HB) will be used as model protein and PAA as a model polymer. EDC is used as a crosslinker to form Hb-PAA conjugates which is covalently conjugated to Alcohols (Ethanol/propanol) to form Hb-PAA-Eth/prop.

**Scheme 1.2:** Stabilization of the native state (N) and destabilization of the denatured state (D) would enhance the thermodynamic stability of the enzyme (Left). When the conformational entropy of the enzyme is lowered by confinement of the enzyme with a thin polymer shell (right), there will be a corresponding increase in  $\Delta G$ , when  $\Delta H$  is kept constant. The latter is thought to depend on the primary sequence of the enzyme and hence, unaltered in this scheme. The net result is an increase in the thermodynamic stability of the polymer-encased enzyme.

**Scheme 2.1:** Synthesis of Hb-PAA nanogel by -COOH activation with EDC followed by the esterification of Hb-PAA.

**Scheme 3.1:** Synthesis of GOx-HRP-PAA/GO conjugate using GOx and HRP bienzyme and PAA and GO. HRP and GOx structures are shown above; PAA as green line and GO is represented as a sheet. EDC chemistry is used to crosslink amine groups on the enzymes with the polymer COOH groups.

**Scheme 4.1:** Two different routes to synthesize MEC's. In Route 1 (A) individual enzyme-PAA conjugates were synthesized using EDC chemistry and then they were further crosslinked to make 5-P. In Route 2 (B), PAA and all 5 enzymes were mixed and stirred for 20 minutes and finally they are crosslinked using EDC to

make 5-S. In above figures enzymes- GOx, HRP, AP, LDH and Lip were represented by yellow, green, blue, black and red circles, respectively and PAA was shown by brown string. 5-P and 5-S were illustrated as shown in A and B respectively.

## List of Figures

**Figure 2.1.** (a) Zeta potentials of Hb-PAA conjugates, (b) IR spectra of Hb-PAA (green line), Hb-PAA-Eth (red broken line) and Hb-PAA-1-prop (black line), and the esters showed the characteristic carbonyl stretch at  $1720\text{ cm}^{-1}$  and  $1710\text{ cm}^{-1}$ , respectively, while the acid carbonyl of PAA indicated a strong band at  $1699\text{ cm}^{-1}$ .

**Figure 2.2.** Zeta potential saturation plot for Hb-PAA-Eth (red line) and Hb-PAA-1-prop (black line).

**Figure 2.3.** IR spectra for Hb (blue line) and PAA (brown line). PAA showed C=O stretch at  $1699\text{ cm}^{-1}$  whereas Hb shows no peak in same region.

**Figure 2.4.** TEM images of (a) Hb-PAA-Eth (b) Hb-PAA (c) Hb. All samples were stained with uranyl acetate. Hb-PAA and Hb-PAA-Eth formed nanogels while Hb showed discrete particles.

**Figure 2.5.** a) Soret absorption bands of Hb, Hb-PAA, Hb-PAA-Eth and Hb-PAA-1-prop in PB (pH 7.4, 10 mM). b) Soret CD bands of Hb, Hb-PAA, Hb-PAA-Eth and Hb-PAA-1-prop in PB (pH 7.4, 10 mM). All spectra were normalized with respect to their corresponding protein concentrations ( $1\text{ }\mu\text{M}$ ) and path lengths (1 cm).

**Figure 2.6.** UV spectra of Hb-PAA-Eth (red), Hb-PAA-1-prop (black), Hb-PAA (green) and Hb (blue) in buffer. Inside zoomed spectra is in 500 -625 nm range showing met-hemoglobin state of Hb in all the conjugates and Hb itself. It has peak at  $\sim 540\text{ nm}$  and shoulder at  $\sim 580\text{ nm}$ .

**Figure 2.7.** a) Soret band positions for Hb conjugates in PB (10 mM, pH 7.4) and organic solvents. b) The extent of structure retention for Hb conjugates in organic

solvents, estimated from the UV CD spectra. Solvent compositions were 60% v/v for EtOH, MeOH, ACN and 20% v/v for DMF, where the conjugates showed highest activities (solvents organized by increasing log P values from DMF to EtOH).

**Figure 2.8.** Absorbance spectra of Hb, Hb-PAA, Hb-PAA-Eth and Hb-PAA-1-prop in a) 60% v/v EtOH b) 20% v/v DMF c) 60% v/v MeOH d) 60% v/v ACN. All spectra are corrected for Hb concentration (1  $\mu$ M).

**Figure 2.9.** CD spectra of Hb, Hb-PAA, Hb-PAA-Eth and Hb-PAA-1-prop in a) 60% v/v EtOH b) 20% v/v DMF c) 60% v/v MeOH d) 60% v/v ACN. All spectra are corrected for Hb concentration (1  $\mu$ M).

**Figure 2.10.** Peroxidase-like activities of Hb conjugates and product formation as monitored at 470 nm, in 2.5% v/v MeOH in PB (10 mM, pH 7.4, 2.5 mM o-methoxyphenol, 1 mM H<sub>2</sub>O<sub>2</sub>).

**Figure 2.11.** Specific activities of Hb-PAA-Eth (red), Hb-PAA-1-prop (black), Hb-PAA (green) and Hb (blue) with respect to that of Hb in PB (10 mM, pH 7.4) (100%), as a function of increasing concentrations of (a) MeOH, and (b) ACN (c) EtOH and (d) DMF.

**Figure 2.12.** Averages of the specific activities of Hb-PAA-Eth (red), Hb-PAA-1-prop (black), Hb-PAA (green) and Hb (blue) bar in DMF, MeOH, ACN and EtOH. Solvents are arranged in increasing log P values from DMF to EtOH.

**Figure 2.13.** a) Activity studies of heme (1 $\mu$ M) in different organic solvents (2.5 mM o-methoxyphenol (substrate), 1 mM H<sub>2</sub>O<sub>2</sub>(oxidant)). Blue bar lines are for activity of heme in EtOH, red bar is for DMF, green bar is for ACN and purple is in

MeOH. b) Hb-PAAmix activity study in various organic solvents. Hb-PAAmix is made by mixing Hb and PAA without addition of EDC-coupling agent. Blue bar lines represent the activity of Hb-PAAmix in EtOH, red in DMF, green in ACN and purple in MeOH. Heme shows better activities above 40%v/v of organic solvents. Hb-PAAmix shows low activities above 40% v/v of organic solvents.

**Figure 2.14.** a) Activity studies of Hb-EtOH (1 $\mu$ M) in different organic solvents (2.5 mM o-methoxyphenol (substrate), 1 mM H<sub>2</sub>O<sub>2</sub>(oxidant)). Red bar lines are for activity of Hb-EtOH in DMF, purple bar is for MeOH, green bar is for ACN and blue is in EtOH. b) Hb-prop activity study in various organic solvents. Red bar lines represent the activity of Hb-prop in DMF, purple in MeOH, green in ACN and blue in EtOH. Hb-EtOH and Hb-prop was made by conjugating EtOH and 1-prop respectively to Hb using EDC chemistry to free carboxyl groups on Hb from aspartate and glutamate.

**Figure 2.15.** Lineweaver-Burk plots for Hb-PAA-Eth (red line), Hb-PAA-1-prop (black line), Hb-PAA (green line) and Hb (blue line) in, a) PB (pH 7.4, 10mM); b) DMF (20% v/v), c) ACN (60% v/v), d) MeOH (60% v/v) and e) EtOH (60% v/v) where the solvent compositions indicated highest activities.

**Figure 2.16.** Catalytic efficiencies of Hb-PAA-Eth (red), Hb-PAA-1-prop (black), Hb-PAA (green) and Hb (blue) in PB (10 mM, pH 7.4), DMF (20% v/v), MeOH (60% v/v), ACN (60% v/v) and EtOH (60% v/v). Specific solvent compositions corresponding to highest specific activities were used. Solvents are arranged in the order of increasing log (P).

**Figure 2.17.**  $1/K_M$  of Hb-PAA-Eth (red), Hb-PAA-1-prop (black), Hb-PAA (green) and Hb (blue) in PB (10 mM, pH 7.4), DMF (20% v/v), MeOH (60% v/v), ACN (60% v/v) and EtOH (60% v/v). Specific solvent compositions corresponding to highest specific activities were used. Solvents are arranged in the order of increasing log (P).

**Figure 3.1.** Activity study at pH 7.4 (phosphate buffer) for GOx-PAA/GO(1:0.1) (green), GOx-PAA/GO(1:0.25) (blue), GOx-PAA/GO(1:0.5) (brown), GOx-PAA/GO(1:1) (orange), GOx-PAA/GO (1:1.5) (yellow) and GOx-PAA/GO(1:2) (light blue), GOx-PAA (black), and GOx (red). Activity study was done at room temperature and product (dimer of o- methoxyphenol) formation was monitored at 470 nm.

**Figure 3.2.** A) Agarose gel electrophoresis with GOx-HRP-PAA loaded in lane 1, GOx-PAA in lane 2, GOx in lane 3 and HRP in lane 4. Agarose gel electrophoresis was done at pH 6.0, 40 mM Tris acetate buffer. HRP did not get stained well due to a mixture of enzymes which smeared in the lane. B) Zeta potential of GOx-HRP-PAA/GO (1:1.5) (green), GOx-HRP-PAA/GO (1:2) (red), GOx-HRP-PAA (black), GOx-PAA/GO (1:1.5) (brown) GOx-PAA/GO (1:2) (pink), GOx-PAA (grey) and GOx/HRP (blue) were done at 25°C. All measurements were performed in 10 mM sodium phosphate buffer at pH 7.0.

**Figure 3.3** (A) Agarose gel electrophoresis of GOx/HRP (lane 1), GOx/HRP/PAA (lane 2), GOx/PAA (lane 3), GOx-HRP-PAA/GO (1:2) (lane 4) and GOx-PAA/GO (1:2) (lane 5). GOx/HRP/PAA and GOx/PAA are physical mixtures, synthesized without EDC and lane 4 contains single and bienzyme conjugate hybrids. Agarose

gel was done at pH 6 in 40 mM Tris acetate buffer. (B) Zeta potential of PAA (brown), GO (maroon), GOx-HRP-PAA (black), GOx-PAA (grey) and GOx/HRP (blue). GO and PAA were used as control samples. Zeta potential was measured at pH 7.4 in 10 mM PB. For agarose gel electrophoresis and Zeta potential studies, protein equivalent of 3-4  $\mu$ M was used for analysis.

**Figure 3.4.** Comparison of the CD secondary structure retention in PB pH 7.4, 10 mM of GOx-HRP-PAA/GO(1:1.5) (green), GOx-HRP-PAA/GO(1:2) (red), GOx-HRP-PAA (black), GOx-PAA/GO(1:1.5) (orange), GOx-PAA/GO(1:2) (pink), GOx-PAA (grey), and GOx/HRP (blue). Ellipticity at 222 nm in mdeg/  $\mu$ M. cm is used to calculate % ellipticity retention and ellipticity at 222 nm of GOx/HRP is referenced at 100 nm.

**Figure 3.5.** Circular Dichroism (CD) spectra of GOx-HRP-PAA/GO(1:1.5) (green), GOx-HRP-PAA/GO(1:2) (red), GOx-HRP-PAA (black), GOx-PAA/GO(1:1.5) (orange), GOx-PAA/GO(1:2) (purple), GOx-PAA (grey), GOx-HRP (blue), buffer (maroon), GO (light blue) and PAA (dark brown). CD spectra were monitored from 190-250 nm in PB pH 7.4, 10 mM. For CD experiments protein concentration of 1  $\mu$ M, for each sample, and 0.05 cm cuvette was used.

**Figure 3.6.** Optical spectra at 403 nm for GOx (blue), HRP (red), GOx-PAA (grey) and GOx-HRP-PAA (black) to test solet environment.

**Figure 3.7.** TEM micrographs of A) GOx-HRP-PAA/GO (1:2), B) GOx-HRP-PAA and C) GOx/HRP. All samples were stained with 0.5% w/w uranyl acetate. GOx-HRP-PAA/GO (1:2) showed nanogels assembled on GO sheets, GOx-HRP-PAA showed nanogels and GOx/HRP showed aggregated particles.

**Figure 3.8.** TEM micrographs showing bare GO surface. Bare GO showed more crystalline character and hence smoother in appearance.

**Figure 3.9.** (A) Activity study as a function of increasing pH without SDS (B) Activity study at increasing pH's with 4.0 mM SDS (denaturant) – GOx-HRP-PAA/GO (1:1.5) (green), GOx-HRP-PAA/GO (1:2) (red), GOx-HRP-PAA (black) and GOx/HRP (blue). Activity of single enzyme GOx-PAA and GOx-PAA/GO (1:1.5) and (1:2) is presented in SI Figure S7. Initial activity of each sample (20-40 sec) was measured for each sample and compared to GOx/HRP which was referenced to 100%.

**Figure 3.10.** Kinetic traces of GOx-HRP-PAA/GO(1:1.5) (green), GOx-HRP-PAA/GO(1:2) (red), GOx-HRP-PAA (black), GOx-PAA/GO (1:1.5) (orange), GOx-PAA/GO (1:2) (pink), GOx-PAA (grey) and GOx/HRP (blue) in 10 mM , pH 7.4 PB. Activity was established using 1.125 mM o-methoxyphenol, 0.3 mM glucose and 1  $\mu$ M equivalent of each of GOx and HRP equivalents.

**Figure 3.11.** (A) Enzyme activities as a function of pH. (B) Enzyme activities as a function of pH, in the presence of added 4 mM SDS. GOx-PAA/GO(1:1.5) (orange), GOx-PAA/GO(1:2) (pink), GOx-PAA (grey) and GOx-HRP (blue). Activity studies were done in glycine hydrochloride buffer (pH 2.5), citrate buffer (pH 4), acetate buffer (pH 5.5) and phosphate buffer (pH 7.4).

**Figure 3.12.** Recyclability study of GOx-HRP-PAA/ GO (1:2) A) at pH 2.5 and B) at pH 7.4 in absence of SDS and at room temperature. All the % specific activities are compared to GOx/HRP at room temperature at pH 7.4 reference point (100%).



**Figure 3.13.** Activity study at 65°C for the samples of dual and single enzyme systems. % Specific activity of GOx-HRP-PAA/GO(1:1.5) (green), GOx-HRP-PAA/GO (1:2) (red), GOx-HRP-PAA (black), GOx-PAA/GO(1:1.5) (orange), GOx-PAA/GO (1:2) (pink) GOx-PAA (grey) and GOx/HRP (blue), were compared to 100% specific activity of GOx/HRP at room temperature and at pH 7.4.

**Figure 3.14.** Recyclability study of GOx-HRP-PAA/GO (1:2) at 65° C in pH 7.4. Bienzyme conjugate hybrid showed recyclability up to one cycle.

**Figure 3.15.** Lineweaver-Burk plot of GOx-HRP (blue), GOx-HRP-PAA (black), GOx-HRP-PAA/GO(1:2) (red), GOx-PAA (grey) and GOx-PAA/GO(1:2) (purple) with increasing glucose concentrations (0.075 mM- 0.6 mM), GOx and HRP concentrations were maintained at 0.5 µM and 1.125 mM o-methoxyphenol in PB pH 7.4, 10 mM. Product (dimer of o-methoxyphenol) formation was measured at 470 nm.

**Figure 3.16.** Catalytic efficiency and  $K_{cat}$  of GOx-HRP-PAA/GO(1:2) (red), GOx-HRP-PAA(black), GOx-PAA/GO(1:2) (pink), GOx-PAA (grey) and GOx/HRP (blue) in PB pH 7.4 and 10 mM with enzyme concentration of 0.5 µM, varying glucose (0.075 mM- 0.6 mM) and o-methoxyphenol (1.125 mM).

**Figure 4.1.** (A) Agarose gel electrophoresis of enzymes (Lipase, GOx, LDH, AP and HRP), 5-P and 5-S loaded in lanes 1-7 respectively. Agarose gel electrophoresis was performed in pH 7.4, 40 mM Tris acetate. (B) Zeta potential studies of 5-P (green), 5-S (black), GOx-PAA (blue) and GOx (red) done at 25 °C in pH 7.4, 10 mM PB.

**Figure 4.2.** Zeta potential of unmodified enzymes, enzyme-PAA and multienzyme complexes (MEC's), experiment was performed in pH 7.4 PB at 25 °C. Zeta potential of HRP, HRP-PAA, AP, AP-PAA, Lip, Lip-PAA, LDH, LDH-PAA, 5-P and 5-S are given in the figure.

**Figure 4.3.** Transmission electron microscopy was performed for imaging (A) 5-P, (B) 5-S and (C) GOx. Samples were diluted using pH 7.4 PB such that equivalent protein concentration was 5-10 nM and stained using 0.5 wt % uranyl acetate.

**Figure 4.4.** Circular dichroism (CD) spectra of (A) GOx (red), GOx-PAA (blue) and (B) LDH (red) and LDH-PAA (blue). CD spectra was monitored from 190-250 nm in pH 7.4 PB at room temperature (25 °C). The inset figure gives the relative ellipticity retention, when peak at 222 nm for unmodified enzyme is referenced at 100 % and relative signal intensity of enzyme-PAA is compared to that.

**Figure 4.5.** Circular dichroism (CD) spectra of (A) AP (red), AP-PAA (blue) and (B) HRP (red) HRP-PAA (blue) (C) Lip (red), Lip-PAA (blue) (D) 5-P (green) and 5-S (black). CD spectra was monitored from 190-250 nm in pH 7.4 PB at room temperature (25 °C). The inset figure gives the relative ellipticity retention, when peak at 222 or 202 nm for unmodified enzyme is referenced at 100 % and relative signal intensity of enzyme-PAA is compared to that.

**Figure 4.6.** Activity studies were carried out at room temperature (25 °C) in pH 7.4, 10 mM, PB for GOx and AP containing samples and data is presented. % specific activity is plotted on Y axis. To calculate % specific activity, initial rate of unmodified enzyme at 25 °C was referenced at 100% and all other samples were compared to that. In above figure % specific activity of GOx containing samples

(A) and AP containing samples (B) were presented 5-P, 5-S are represented as green and black. GOx, GOx-PAA, AP and AP-PAA are represented as red, blue, red and blue respectively.

**Figure 4.7.** Activity studies were carried out at room temperature (25 °C) in pH 7.4, 10 mM, PB for HRP, LDH and Lip containing samples and data is presented. % specific activity is plotted on Y axis. To calculate % specific activity, initial rate of unmodified enzyme was referenced at 100% and all other samples were compared to that. In above figure % specific activity of HRP containing samples (A), LDH containing samples (B) and Lip containing samples (C) were presented. 5-P, 5-S are represented as green and black. HRP, HRP-PAA, LDH, LDH-PAA, Lip and Lip-PAA are represented as red, blue, red, blue, red and blue respectively.

**Figure 4.8.** Activity studies were carried out at room temperature (65 °C) in pH 7.4, 10 mM, PB for GOx and AP containing samples and data is presented. % specific activity is plotted on Y axis. To calculate % specific activity, initial rate of unmodified enzyme at 25 °C was referenced at 100% and all other samples were compared to that. In above figure % specific activity of GOx containing samples (A) and AP containing samples (B) were presented 5-P, 5-S are represented as green and black. GOx, GOx-PAA, AP and AP-PAA are represented as red, blue, red and blue respectively.

**Figure 4.9.** Activity studies were carried out at room temperature (65 °C) in pH 7.4, 10 mM, PB for HRP, LDH and Lip containing samples and data is presented. % specific activity is plotted on Y axis. To calculate % specific activity, initial rate of unmodified enzyme at 25 °C was referenced at 100% and all other samples

were compared to that. In above figure % specific activity of HRP containing samples (A), LDH containing samples (B) and Lip containing samples (C) were presented. 5-P, 5-S are represented as green and black. HRP, HRP-PAA, LDH, LDH-PAA, Lip and Lip-PAA are represented as red, blue, red, blue, red and blue respectively.

**Figure 4.10.** (A) Lineweaver burk plots of GOx (red), GOx-PAA (blue), 5-P (green) and 5-S (black) with increasing glucose (0.075 – 0.45 mM). (B) Lineweaver Burk plots of AP (red), AP-PAA (blue), 5-P (green) and 5-S (black) with increasing 4-nitrophenylphosphate (2.7 – 16.2 mM). Studies were carried out in pH 7.4, 10 mM PB.'

**Figure 4.11.** (A) Lineweaver burk plots of HRP (red), HRP-PAA (blue), 5-P (green) and 5-S (black) with increasing o-methoxyphenol (0.0163 – 0.097 mM). (B) Lineweaver Burk plots of LDH (red), LDH-PAA (blue), 5-P (green) and 5-S (black) with increasing NADH (0.007 – 0.15 mM). (C) Lineweaver Burk plots of Lip (red), Lip-PAA (blue), 5-P (green) and 5-S (black) with increasing 4-nitrophenylacetate (0.008 – 0.12 mM). Studies were carried out in pH 7.4, 10 mM PB/ Tris acetate.

## **Chapter 1**

### **1.1 Introduction**

Recently use of protein-polymer nanocomposites in biocatalysis is becoming the area of interest for wide varieties of applications. Our lab focuses on development and design of the protein-polymer conjugates and then synthesizing nanocomposites using 2D nano-layered materials such as graphene oxide (GO) and graphene. These nanocomposites can be used in plethora applications such as solar cells, biofuel cells, bio-batteries and in biocatalysis for various industrial applications. The whole world is facing an energy crisis situation and we urgently need alternative to fuel source. Therefore, well thoughtful synthesis and design of protein-polymer nanocomposites are need of an hour. Preliminary part of this study is focused on production of protein-polymer conjugate and then assembly of these conjugates on GO or graphene. Then the characterization and evaluation for biocatalysis and other valuable applications.

Four major goals that form the basis of this thesis are- 1. Synthesis and characterization of the enzyme-polymer nanocomposites using simple and green method using biocompatible materials to stabilize enzymes. 2. Synthesize enzyme-polymer conjugates for biocatalysis in organic media. 3. Synthesis of bienzyme-polymer conjugates and nanocomposites for biocatalysis at low pH conditions, high temperatures and in presence of denaturant such as sodium dodecyl sulfate (SDS). 4. Production of multienzyme-polymer conjugates and nanocomposites for biocatalysis and biofuel cell applications.

## 1.2 Wrapping as Strategy

While wrapping the enzyme with the polymer, the redox and electrochemical activity and catalytic activity of enzymes should be retained to a significant extent, and should allow for full diffusional transport of the substrate to the active site of the enzyme and facile release of the product into the bulk. While simple wrapping of the enzyme without any covalent conjugation can result in un-wrapping, covalent conjugation of the polymer chains onto the side chains of the enzyme via suitable linkers has been proposed as a method to stabilize 3D structures of enzymes under denaturing conditions. However, the choice of the polymer, the type and the number of linkages to be made between the polymer and the enzyme surface are important decisions, and these can have strong influence on the properties of the resulting biocatalysts. The covalent chemistry should not interfere with the active site chemistry and should leave sensitive residues untouched. Thus, there is an urgent need to design rational strategies to stabilize enzymes under ordinary laboratory conditions but with predictable properties of the enzyme-polymer conjugate. Water-soluble polymers are generally the preferred soft materials for wrapping enzymes and this is due to several important factors such as: the availability of these polymers in large quantities with different functional groups which would allow for different conjugation strategies between the enzyme and the polymer; water-soluble polymers are more likely to produce a hydration shell around the enzyme and promote the retention of native-like structure of the enzyme; and the hydrophilic groups of the polymer are more likely to interact favorably with the polar groups on the enzyme surface and stabilize it. Thus, this

strategy of wrapping enzymes with polymers allows for the combination of the biological properties of enzymes with the material properties of synthetic polymers and produce unique biocatalysts that are otherwise not possible to make either in the biological world or in the synthetic world. Such unique hybrids enjoy special status and their design can profit from progress made in both these vastly different disciplines.

Enzyme-polymer conjugates are becoming area of interest in last few decades. The synthesis, design protocol and characteristics of such conjugates are studied widely. The growing interest in this area is because one can control the synthesis by site specific modification of proteins or random modification. Site specific modification is time consuming and expensive whereas random modification is cheap and fast. Advantage of site specific modification is that one can control the protein: polymer conjugation ratio and in case of random conjugation can result in extensive crosslinking. We opted for random modification in this case. We believe that by controlling the protein: polymer weight ratio and EDC cross-linker concentration we can control the crosslinking and hence control the size and applicability of these conjugates. These conjugates will then be adsorbed on-to GO/ graphene. Applications of these conjugates span in areas of solar cells, biofuel cells, drug delivery vehicles and biobatteries.

### **1.3 Protein-polymer conjugates: synthesis and characterization.**

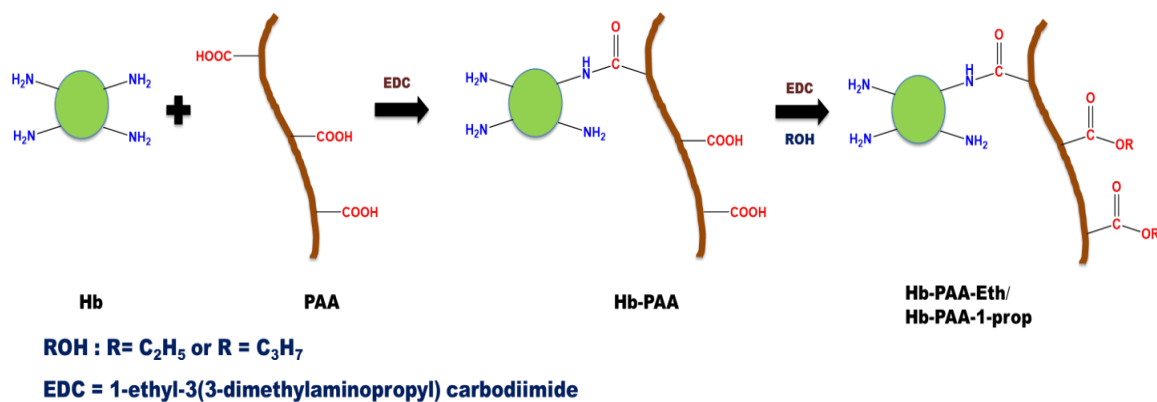
Key goal of our study is to synthesize and develop new methods to synthesize protein-polymer conjugates in random fashion using EDC chemistry. Various methods and reviews have been extensively studies for development of exciting

new and novel methods for the same. Two main protocols for synthesis of conjugates are by grafting to (mostly random conjugation) and grafting from (site specific conjugation) approach. <sup>1</sup> Many synthetic methods for use of protein-polymer conjugates are used for biomedical, <sup>2</sup> catalysis, <sup>3</sup> drug delivery, <sup>4</sup> biofuel cells <sup>5</sup> and biobattery <sup>6</sup> applications. Many studies have been carried out using grafting to as well as grafting from approach. <sup>7, 8, 9</sup> The coupling strategy selected for protein-polymer ligation has implications on many things which depend on location and placement of attachment points. In case of site specific conjugation one needs to know the exact 3D structure of proteins. Also, the attachment point of the protein to the polymer need to be decided carefully. Catalytic activity and function of the protein ultimately depends on that and on polymer characteristics. <sup>10</sup> Cysteine thiols (-SH) are generally used for site specific conjugations. <sup>11</sup> Generally with random conjugation, reduction in catalytic activity or secondary structure is noted since there can be multipoint attachment and that can have an impact too. Therefore strategic choice of polymer and its conjugation to proteins is necessary. Many characteristic methods are used to evaluate the protein-polymer conjugates such as small angle X-ray scattering (SAXS), turbidimetry, differential scanning calorimetry (DSC), infrared and UV spectrometry, etc. Electronic microscopic studies are done to evaluate the morphology of the conjugates. Zeta potential can also be employed to estimate the charge on the conjugates and composites.

As explained in scheme 1.1, protein-polymer conjugates are synthesized in our lab. A well-established EDC chemistry is used to crosslink proteins to polymers



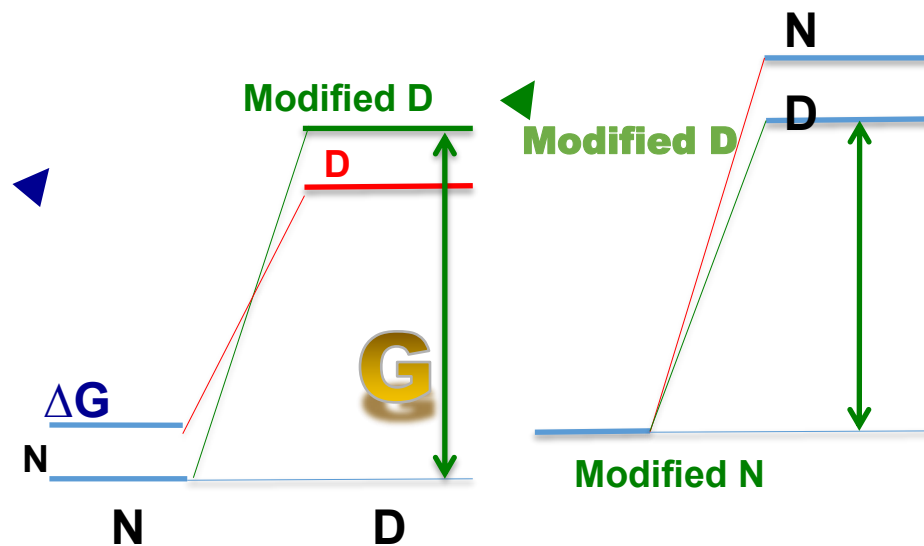
covalently. In above scheme Hb is represented as green sphere. PAA is represented as a brown string of polymer. Hb and PAA are covalently conjugated to form Hb-PAA conjugates. Hb-PAA conjugates are further modified using alcohols to form Hb-PAA-Eth/prop nanoconjugates. These nanoconjugates are then characterized using zeta potential, IR spectroscopy and circular dichroism (CD) spectroscopy before using it for further applications.



**Scheme 1.1:** Synthesis strategy for the protein-polymer conjugates. Hemoglobin (HB) will be used as model protein and PAA as a model polymer. EDC is used as a crosslinker to form Hb-PAA conjugates which is covalently conjugated to Alcohols (Ethanol/propanol) to form Hb-PAA-Eth/prop.

## 1.4 Entropy Control

Our general hypothesis is that the physical confinement of the enzyme within a polymeric shell will decrease enzyme's conformational entropy, which will directly and positively impact the retention and stability of the 3D hierarchical structure of the enzyme. This is because the confined space around the enzyme would only permit access to limited amount of space and hence, the conformational distribution is severely limited when compared to free space around the unligated enzyme. Decreased conformational entropy ( $\Delta S$ ) results in the increases of the free energy ( $\Delta G$ ) required to denature the enzyme ( $\Delta G = \Delta H - T\Delta S$ ), where the enthalpy term ( $\Delta H$ ) is essentially fixed by the primary sequence of the enzyme. Therefore, a decrease in  $\Delta S$  produces an increase in the  $\Delta G$  term and more vigorous conditions are required to denature the enzyme under these modified conditions. At room temperature,  $\Delta G$  for enzyme denaturation is large and positive, and at the denaturation temperature the native and denatured states are at equilibrium, and  $\Delta G$  equals zero. This simple strategy of entropy control of the enzyme denaturation process has been widely used in our laboratory to control the thermodynamic stabilities of enzymes by a variety of different approaches. For example, when the enzyme surface is wrapped with a synthetic polymer such that  $\Delta H$  is unchanged, the decreased conformational entropy of the enzyme is expected to increase the  $\Delta G$  needed to denature the enzyme, and hence, should enhance enzyme stability. This concept is schematically illustrated in Scheme 1.2.



**Scheme 1.2:** Stabilization of the native state (N) and destabilization of the denatured state (D) would enhance the thermodynamic stability of the enzyme (Left). When the conformational entropy of the enzyme is lowered by confinement of the enzyme with a thin polymer shell (right), there will be a corresponding increase in  $\Delta G$ , when  $\Delta H$  is kept constant. The latter is thought to depend on the primary sequence of the enzyme and hence, unaltered in this scheme. The net result is an increase in the thermodynamic stability of the polymer-encased enzyme.

### **1.5 Protein-polymer nanocomposites for biocatalysis and other applications:**

Over last few decades biocatalysis has pulled the attention of the organic chemists and biochemists since it gives high product conversion and selectivity such as, chemo, regio and stereo-selectivity. Many enzymes such as lipase, peptidase, esterase, amylase, hydrolase, etc have found its use in industrial applications for biocatalysis. Despite so much of advantages enzymes have few shortcomings as well. Enzymes tend to get denatured at extremes of pH, high temperatures and hence are deactivated. Therefore, polymers are used as supports, they give the stability at such stringent conditions and also helps in enhancing specificity of products. In last few decades protein mediated biocatalysis using polymer as a support has attracted the attention worldwide. The polymeric support backbone that can be natural or synthetic can be used to enhance specificity, stability, activity and in some cases recovery of the proteins. Various forces can be used to attach the proteins and polymers such as ionic, covalent or physical (adsorption). Covalent binding has shown to increase the stability and activity compared to all other cases. Smart polymers or stimuli responsive polymers have shown to increase the proficiency of enzymes in the stressful environment such as extremes of pH, high temperature and in organic solvents. <sup>12</sup>

Apart from biocatalysis protein-polymer conjugates are widely used in other applications as well. There has been a lot of progress in protein-PEG (polyethylene glycol) conjugates for use in medicine. Currently there are 10 PEGylated proteins which are used clinically to treat diseases and lots more under investigation. <sup>13</sup>

PEGylated proteins show increased plasma half-life due to increased solubility and permeability caused by use of the polymer. Also, stimuli responsive polymers are used in selectively precipitating/ solubilizing proteins which is used in protein purification and its stress-free recovery from the mixture. Also, use of PEGylated proteins in organic solvents is increasing as it can be used in bioreactors and biosensors. <sup>14</sup> Polymerosomes are new class of materials which are used in applications such as drug delivery and cell organelle mimics. <sup>15</sup>

## **1.6 Overview of Thesis**

The aim of this thesis was to gain knowledge of protein polymer conjugate and its various application in biocatalysis and energy applications. Next chapters discusses the detailed synthesis of protein polymer conjugates, various characterization techniques used for confirmation of the same and various applications were demonstrated. The brief overview of the thesis is presented below.

Second chapter of this thesis discusses the biocatalysis of enzyme in organic solvent using Hb as a model enzyme and PAA as a model polymer. For synthesis, EDC coupling chemistry was used to synthesize the conjugates and various characterization methods were used confirm the synthesis. Characterization methods included- zeta potential, infrared (IR) spectroscopy and dynamic light scattering (DLS). The biocatalysis applications of Hb-PAA conjugates were tested in four different organic solvents such as methanol, ethanol, dimethylformamide (DMF) and acetonitrile (ACN). Circular dichroism studies were then used to determine the structural retention of the enzyme in different solvents. These

studies showed maximum activity retention for Hb-PAA conjugates in organic solvents compared to Hb. Kinetic studies were carried out to extract the kinetic parameters such as  $K_M$  and  $V_{max}$  of all the samples in different solvents. This study showed the strategy to stabilize a single enzyme in organic solvents. Next, two enzymes were stabilized at high temperature and various pH conditions.

Third chapter focuses on stabilization of two enzymes- glucose oxidase (GOx) and horseradish peroxidase (HRP) at high temperature, in presence of denaturant and at various pH's. In this study GOx and HRP were stabilized using covalent attachment with PAA and subsequent physical adsorption onto graphene oxide (GO). The protection of bienzyme using PAA and GO resulted in increase in stability of enzymes at high temperature, in presence of denaturant and various pH's. Synthesis of enzyme polymer conjugate and enzyme conjugate hybrids were confirmed using agarose gel electrophoresis, zeta potential studies. Transmission electron microscopy (TEM) was used to elucidate the morphology of enzyme conjugate hybrids and enzyme polymer conjugates. Also CD studies were employed for structural confirmation and biocatalysis applications were tested at high temperatures and various pH's in presence of denaturant. Also, Kinetic parameters were gathered using Lineweaver Burk plots. Further, more than two enzymes were stabilized using polymer conjugate synthesis and the details of that are discussed in chapter four.

Biofuel cell application is desired using polymer encapsulation of the enzymes. To derive energy from the simple sugars upwards of thirteen enzymes are used in cascading manner. For that purpose stabilization of multiple enzymes is

necessary. Also, high energy output can be expected from the biofuel cell if the enzymes can be made stable at that temperature. Fourth chapter details the stabilization of five model enzymes such as- GOx, HRP, acid phosphatase (AP), lactate dehydrogenase (LDH) and lipase (Lip) using PAA matrix. Different routes were used for synthesis of multienzyme complex (MEC) and synthesis was confirmed using agarose gel electrophoresis, zeta potential, DLS. Structural elucidation and morphology was tested using CD and TEM studies respectively. multienzyme activity studies were explored at room and high temperature and kinetic parameters were computed. This multi-enzymatic stabilization will prove to be the promising for biofuel cell applications in future. Subsequently, future proposed work will be stabilize thirteen enzymes that catalyzes sugars to energy in cascading fashion. These future plan of the research is discussed in chapter five.

## 1.7 References

- 
1. Zhao, W.; Liu, F.; Chen, Y.; Bai, J.; Gao, W., *Polymer* **2015**, 66, A1-A10.
  2. Qi, Y.; Chilkoti, A. *Polym. Chem.* **2013**, 5, 266-276.
  3. Zore, O. V.; Pattammattel, A.; Gnanaguru, S.; Kumar, C. V.; Kasi, R. M., *ACS Catal.* **2015**, 5, 4979-4988.
  4. Ge, J.; Neofytou, E.; Lei, J.; Beygui, R. E.; Zare, R. N., *Small* **2012**, 8 , 3573-3578.



- 
5. Minteer, S. D.; Liaw, B. Y.; Cooney, M. J., *Curr. Opin. Biotechnol.* **2007**, *18*, 228-234.
6. Zhu, Z.; Kin Tam, T.; Sun, F.; You, C.; Percival Zhang, Y. H., *Nature Comm.* **2014**, *5*, 3026.
7. Hoffman, A. S.; Stayton, P. S.; Bulmus, V.; Chen, G.; Chen, J.; Cheung, C.; Chilkoti, A.; Ding, Z.; Dong, L.; Fong, R., *J. Biomed. Mater. Res.* **2000**, *52*, 577-586.
8. Chilkoti, A.; Chen, G.; Stayton, P. S.; Hoffman, A. S., *Bioconjugate Chem.* **1994**, *5*, 504-507.
9. Zore, O. V.; Lenehan, P. J.; Kumar, C. V.; Kasi, R. M., *Langmuir* **2014**, *30*, 5176-5184.
10. Gauthier, M. A.; Klok, H.-A., *Polym. Chem.* **2010**, *1*, 1352-1373.
11. Hoffman, A. S.; Stayton, P. S.; Bulmus, V.; Chen, G.; Chen, J.; Cheung, C.; Chilkoti, A.; Ding, Z.; Dong, L.; Fong, R.; Lackey, C. A.; Long, C. J.; Miura, M.; Morris, J. E.; Murthy, N.; Nabeshima, Y.; Park, T. G.; Press, O. W.; Shimoboji, T.; Shoemaker, S.; Yang, H. J.; Monji, N.; Nowinski, R. C.; Cole, C. A.; Priest, J. H.; Harris, J. M.; Nakamae, K.; Nishino, T.; Miyata, T., *J. Biomed. Mater. Res.* **2000**, *52*, 577-586.
12. Basak, S.; Punetha, V. D.; Bisht, G.; Bisht, S. S.; Sahoo, N. G.; Cho, J. W., *Polym. Rev.* **2015**, *55*, 163-198.
13. Pelegri-O'Day, E. M.; Lin, E. W.; Maynard, H. D., *J. Am. Chem. Soc.* **2014**, *136*, 14323- 14332.

---

14. Thordarson, P.; Droumaguet, B.; Velonia, K., *Appl. Microbiol. Biotechnol.* **2006**, 73, 243-254.

15. Grover, G. N.; Maynard. H. D.; *Curr. Opin. Chem. Biol.* **2010**, 14, 818-827

## Chapter 2

### 2. Efficient Biocatalysts in Organic Media with Hemoglobin and Poly (Acrylic Acid) Nanogels

#### 2.1 Abstract

We previously reported that stability and aqueous catalytic activity of met-hemoglobin (Hb) was improved when covalently conjugated with poly(acrylic) acid (PAA). In the current study, the Hb-PAA-water interface was modified to improve Hb catalytic efficiency in organic solvents (0-80% v/v organic solvent, remaining is the conjugate, the substrate, and water). The protein-polymer-solvent interface modification was achieved by esterifying the carboxylic acid groups of Hb-PAA with ethanol (EtOH) or 1-propanol (1-prop) after activation with carbodiimide. The resulting esters (Hb-PAA-Eth and Hb-PAA-1-prop, respectively) showed high peroxidase-like catalytic activities in acetonitrile (ACN), dimethyl formamide (DMF), EtOH and methanol (MeOH). Catalytic activities depended on the log(P) values of the solvents, which is a measure of solvent lipophilicity. The highest weighted average activities were noted in MeOH for all three conjugates and the lowest average activities were noted in DMF for two of the conjugates. Interestingly, the average activities of the conjugates were higher than that of Hb, in all solvents, except in ACN. The ratio of catalytic rate constant ( $k_{cat}$ ) to Michaelis constant ( $K_M$ ), the catalytic efficiency, for Hb-PAA-Eth in MeOH was the highest noted and it is ~ 3-fold higher than that of Hb in buffer, and conjugates offered higher efficiencies than Hb at most solvent compositions. This is the very first general, versatile, modular strategy of coupling the enhanced stability of Hb with

improved activity in organic solvents via the chemical manipulation of the polymer shell around Hb and provides a robust approach for efficient biocatalysis in organic solvents.

## 2.2 Introduction

A general but powerful approach for the design of enzyme-polymer conjugates for use in organic enzymology is reported here, for the first time. Enzymes are widely used in biocatalysis, diagnostics, in the manufacture of fine chemicals, and in the food industry.<sup>1</sup> They are very effective chiral catalysts and they can increase the rates of reactions by factors of  $10^{20}$  or more when compared to uncatalyzed reactions, with very high stereospecificity.<sup>2</sup> Despite these advantages, the use of enzymes in several applications are mired under non-physiological conditions such as high temperature, extreme pH's and organic solvents due to loss of their 3D structure, denaturation and consequent loss of catalytic activities.<sup>3, 4</sup> These issues have been overcome, to some extent, by (i) embedding enzymes within layered inorganic nanosheets,<sup>5, 6, 7, 8</sup> (ii) linking and confining enzymes to surfaces,<sup>9, 10</sup> (iii) crosslinking as enzyme crystals,<sup>11, 12</sup> (iv) covalent binding enzymes to polymers,<sup>13</sup> (v) modification of enzymes with hydrophilic molecules<sup>14</sup> and subsequent use in multi-phase systems.<sup>15</sup>

However, the challenging proposition that remains is that enzyme catalysis is still mostly limited to aqueous media, since most organic solvents denature enzymes and controlling enzyme-water interface is critical here. For example, Penicillin G acylase deactivated in less than 3 minutes in 95% dioxane.<sup>16</sup> Alcohol

dehydrogenase<sup>17</sup> was used in dimethyl sulfoxide (DMSO), acetonitrile (ACN) and methanol (MeOH) under different pH conditions and salt concentrations up to only 10% v/v of organic solvents and the enzyme retained only a maximum of 40% of its activity. But, organic solvents offer many advantages as reaction media in that, (i) many organic substrates are insoluble in water but soluble in organic solvents; (ii) enzyme degradation by microbes is inhibited in organic media as it does not support their growth or survival; (iii) substrates/products that are sensitive to aqueous media can be protected by carrying out the catalysis in organic solvents, and (iv) in some cases, organic media could provide better control of specificity, chemo-, regio- and/or enantio- selectivities.<sup>18, 19</sup> The field of organic enzymology is also important for the production of enantiopure alcohols and amines, semisynthetic penicillins and cephalosporins, insecticides and anti-tuberculosis drugs.<sup>20</sup> Thus, it is imperative to devise modular methods to protect the 3D structure and catalytic activity of enzymes such that they may function in organic solvents. This goal is achieved here by controlling the solvent-enzyme interface with a polymer which is further modified to control the polarity of this interface.

The protein used here, met-hemoglobin (Hb), is not an enzyme in natural systems. However, Hb catalyzes hydroxylation, dealkylation reactions,<sup>21</sup> acts as nitrite reductase,<sup>22</sup> shows monooxygenase activity,<sup>23</sup> and functions as a peroxidase in the oxidation of polycyclic aromatic hydrocarbons (PAH's).<sup>24</sup> Also, Hb is important for sensing of various biomolecules.<sup>25, 26</sup> Recently, Hb was stabilized with graphene oxide (GO),<sup>27</sup> which showed higher peroxidase-like activities with pyrogallol than Hb. In another example, Hb was immobilized in

layered Zr(IV)phosphate for high thermal stability or in titanate for stability against organic solvents,<sup>28</sup> and the latter showed only 33% of activity in ACN. Thus, numerous attempts were made to use Hb as a biocatalyst in organic solvents with very limited success.

The approach used here is to systematically alter the Hb-solvent interface by covalent conjugation of a hydrophilic polymer and then use this polymer as a scaffold to further manipulate the microenvironment of Hb. For example, thermal stability of Hb was increased by covalent conjugation with a water-soluble polymer, poly(acrylic acid) (PAA) and enhanced stability was attributed to the presence of a nanolayer of polymer shell around the protein.<sup>29</sup> We hypothesize that the Hb-PAA conjugate could be further modified with small organic molecules such that Hb-PAA is soluble both in water and in organic solvents, while the polymer shell protects Hb from denaturation on exposure to organic solvents. Thus, the modification of PAA in the Hb-PAA conjugates could confer some benefits for solubility in organic media and provide a systematic handle to control the Hb-solvent interface in a predictable manner. A simple strategy would be to increase the solubility of the polymer shell in organic solvents by the esterification of the carboxyl groups (COOH) of PAA with alcohols to yield the corresponding ester derivatives of Hb-PAA, Scheme 2.1. Other advantages of using PAA for protein conjugation include (i) ability to bind to magnetic particles for separation and recycling of the biocatalyst and (ii) possibility of sterilization of the Hb-PAA at low pH due to pH reversible nature of PAA. These randomly formed conjugates give

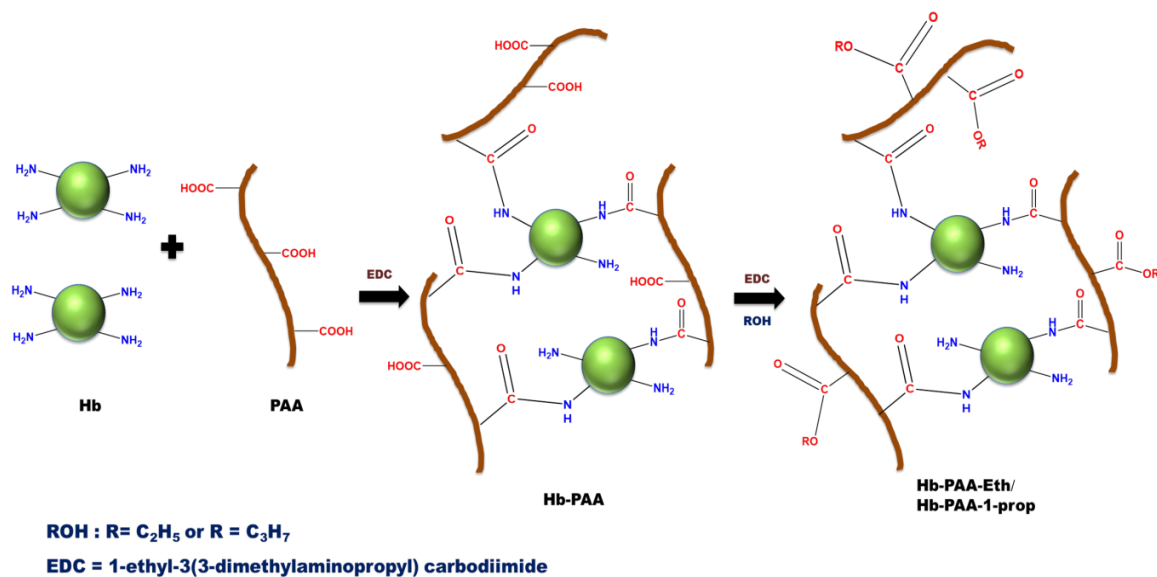
an edge over site-specific conjugation between protein and polymer in that they are modular, easy to produce and scalable for practical applications.

In this paper, the synthesis of new Hb-PAA-ester conjugates is demonstrated. In Scheme 2.1, Hb is represented as a green circle, PAA chain as a brown line, and ROH represents EtOH/1-propanol. In the first step, –COOH groups in PAA were activated using 1-ethyl-3(3-dimethylaminopropyl) carbodiimide (EDC) and coupled with amino groups of lysine side chains on Hb to produce Hb-PAA. Typically mammalian Hb have nearly 44 lysine residues.<sup>30, 31</sup> In the second step, the Hb-PAA conjugates were reacted with EtOH or 1-propanol to form the corresponding Hb-PAA-Eth and Hb-PAA-1-prop, respectively.

The Hb-PAA-ester conjugates are suitable to carry out biocatalysis in organic solvents such as DMF, MeOH, ACN and EtOH. These solvents are selected because of their use in various scale-up applications. For example, ACN is an important solvent for the synthesis of pharmaceuticals,<sup>32</sup> while EtOH and MeOH play a crucial role in fuel cell applications of enzymes.<sup>33</sup> These solvents also represent a range of Log P (logarithm of organic solvent/water partition coefficient) values that are in the order, DMF > MeOH > ACN > EtOH, where DMF is the most hydrophilic and EtOH, the least. The retention of Hb structure in Hb-PAA-ester conjugates dissolved in organic media was confirmed by Circular Dichroism (CD) spectroscopy. The peroxidase-like activities of the modified Hb-PAA in organic solvent-water mixtures showed higher catalytic activities, under specific reaction conditions, but activities and catalytic efficiencies depended on the polarity of the solvent as well as the conjugate. Thus, this post-functionalization strategy opened

up a plethora of new opportunities for biocatalysis in organic solvents with catalytic efficiencies that are nearly 4-fold larger than in buffer. These details are given below.





**Scheme 2.1:** Synthesis of Hb-PAA nanogel by  $-\text{COOH}$  activation with EDC followed by the esterification of Hb-PAA.

## 2.3 Experimental

**2.3.1 Materials.** Poly(acrylic acid) (MW 450,000 g/mol) [MW is in terms of viscosity average molecular weight ( $M_v$ )] , 1-ethyl-3(3-dimethylaminopropyl) carbodiimide (EDC), o-methoxyphenol, 1-prop and hydrogen peroxide ( $H_2O_2$ ) were purchased from Sigma-Aldrich (St. Louis, MO). Bovine hemoglobin was obtained from MP Biomedicals (Solon, OH). Solvents, DMF, ACN and MeOH were purchased from J.T. Baker chemicals (Phillipsburg, NJ); EtOH was purchased from Pharmaco-Aaper (Brookfield, CT).

**2.3.2 Synthesis of Hb-PAA conjugates.** Stock solution of Hb (26 mg/ml) was prepared by dissolving in 10 mM phosphate buffer (PB, pH 7.4). Stock PAA solution of 2 wt % was prepared by dissolving in deionized water (DI) and the pH was adjusted to 7.4. PAA solution (2.8 mL) mixed with PB (10 mM, pH 7.4) (15.1 mL) and EDC (1.7 mL of 130 mg/mL solution in PB) was added such that mole ratio of EDC:COOH was 1.5:1, and the mixture was stirred for 10 minutes and Hb solution (0.4 mL) added slowly over a period of 5 minutes. After six hours of stirring, the samples were quenched by refrigerating and purified to remove any unreacted EDC by dialysis using 8 kD membrane or reacted further with alcohols. The resultant conjugate produced from a Hb:PAA mole ratio of 1.3:1 is referred to as Hb-PAA.

**2.3.3 Synthesis of Hb-PAA ester conjugates.** To Hb-PAA conjugates, EDC was added in such a way that proportion of EDC: COOH was 1.5:1 as in the synthesis of Hb-PAA. The reaction mixture was stirred for 10 minutes, 30% v/v of EtOH was added and stirred for six hours (3 mL of EtOH used for 10 mL of Hb-

PAA for synthesis of Hb-PAA-Eth). The mole ratio of EtOH: COOH was maintained at 132:1. Thus, the formation of Hb-PAA ester is a two-step synthesis and labeled as Hb-PAA-Eth. Similar reaction protocol was followed for 1-prop modified Hb-PAA where in the mole ratio of 1-prop: COOH was maintained as 50:1 (1.45 mL of 1-propanol used for 10 mL of Hb-PAA for synthesis of Hb-PAA-1-prop). This conjugate was labeled as Hb-PAA-1-prop. A sample synthesis is illustrated in Scheme 2.1.

**2.3.4 Circular dichroism (CD) studies.** Secondary structure of Hb in the conjugates was examined by heme CD spectra while the heme environment was probed by the Soret CD band using a Jasco 710 spectropolarimeter. Step resolution was maintained at 0.2 nm/data point and bandwidth and sensitivity were 1 nm and 20 millidegrees, respectively. When collecting Soret CD spectra each sample from 350 nm to 450 nm recorded at a scan speed of 50 nm/minute in a 1 cm cuvette. Eight scans were averaged.

**2.3.5 Activity studies.** Peroxidase-like activities of ester conjugates (Hb-PAA-Eth and Hb-PAA-1-prop), conjugates (Hb-PAA) and Hb were evaluated by measuring the peroxidase activity by reported methods.<sup>1</sup> The substrate used was o-methoxyphenol (2.5 mM) and the oxidant, H<sub>2</sub>O<sub>2</sub> (1 mM) were added to the solution containing 1  $\mu$ M Hb in PB (10 mM, pH 7.4) or appropriate organic solvent.<sup>34, 35</sup> Activity studies were performed on FlexStation 3 multi-mode microplate reader (Molecular Devices, Sunnyvale, CA). The instrument consists of source plate (carrying solvent, Hb/Hb-PAA/Hb-PAA-ester and o-methoxyphenol) and a transfer plate (carrying H<sub>2</sub>O<sub>2</sub> and solvent) and pipette tips to transfer the

appropriate amount of oxidant. The organic solvent and PB volume was adjusted in source plate and transfer plate to get the required concentration of organic solvent eventually. It is vital to note that the Hb-PAA-Eth and Hb-PAA-1-prop already carried 30% and 14.5% v/v of corresponding alcohol that was added at the time of synthesis.

**2.3.6 Calculating  $K_M$  and  $V_{max}$  values.**  $K_M$  and  $V_{max}$  values for ester conjugates, conjugates and Hb by evaluating the peroxidase activity of Hb at varying concentrations of o-methoxyphenol (0.5 mM to 3 mM) using the FlexStation 3 benchtop multi-mode microplate reader. Then Lineweaver-Burk plots were constructed. Inverse of initial rate of activity vs. inverse of substrate (o-methoxyphenol) was plotted. Using these graphs the  $K_M$  (Michaelis constant) and the  $V_{max}$  (maximum velocity) were obtained. The Hb concentration was maintained at 1  $\mu$ M and  $H_2O_2$  concentration was maintained at 1 mM.

**2.3.7 Dynamic light scattering (DLS).** Hydrodynamic radius of ester conjugates, conjugates and Hb were determined using CoolBatch+ dynamic light scattering apparatus with Precision Detectors (PD2074 N) (Varian Inc.,) were used in conjunction with a 0.5 x 0.5 cm<sup>2</sup> square cuvette and 658 nm excitation laser source at 90° geometry. Samples corresponding to 0.5 nM Hb concentration in PB (10 mM, pH 7.4) were filtered with 0.2-micron filter (PVDF, 13 mm, Fisher Scientific) before all the measurements were performed. All the samples were equilibrated for 300 s at 26 °C; 5 repetitions with 60 accumulations were recorded at the same temperature. The software, Precision Elucidate Version 1.1.0.9 was

used to run the experiment and Deconvolve Version 5.5 was used to process the data.

**2.3.8 Transmission Electron Microscopy (TEM).** The morphology of ester conjugates and conjugates were evaluated using TEM. Tecnai T12 instrument operating at an accelerating voltage of 120 kV was used to obtain the TEM images. Samples were prepared using Hb concentration of 0.026 mg/ml and PAA concentration of 0.007 mg/ml. The solution was drop casted onto a copper grid covered with formvar film. Then excess solution was blotted using a filter paper to leave a thin layer of the sample on the film and dried for 20 minutes, stained with uranyl acetate for 30 minutes before recording images.

**2.3.9 Infrared spectroscopy.** Infrared spectroscopy was carried out by using Bruker alpha FT-IR instrument (Billerica MA). The spectra were analyzed using opus 7.2 software and QuickSnap™ sampling modules. The ester conjugates and conjugates were first freeze-dried to remove water. Approximately, ~10 mg of sample was used for FR-IR analyses. The data was processed using Opus 7.2 (Bruker, version 7.2, Billerica, MA).

**2.3.10 Zeta potential studies.** Brookhaven zeta plus zeta potential analyzer (Brookhaven Instruments Corporation, Holtsville, NY) was used to determine the amount of charge on a sample using Laser doppler velocimetry. Sample with Hb concentration ~0.1 mM and volume of 1.5 mL was used for each conjugate or Hb itself. Polystyrene cuvettes (4 mL) were used to hold the sample. Zeta potential values were acquired by Smoluchowski fit by the software supplied by the

manufacturer, and zeta potential values were calculated by using matching electrophoretic mobility of the sample.

## **2.4 Result and Discussion**

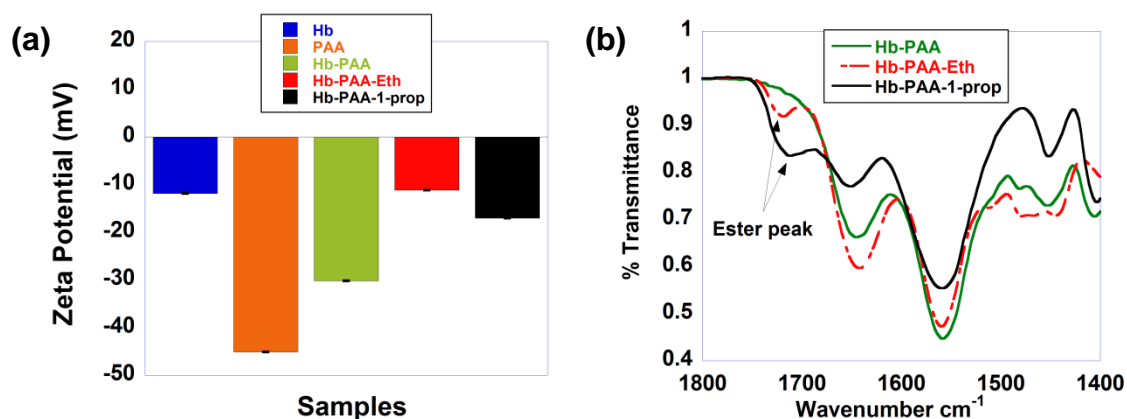
Enzyme-water interface was hypothesized to influence the structure, stability and activity of enzymes and a general, facile but powerful approach is described here to alter this interface in Hb systematically. The data presented here support the above hypothesis, and Hb-PAA conjugates often indicated higher activities and catalytic efficiencies in organic solvents when compared to those of Hb in aqueous solutions. At highest organic solvent concentration (e.g. 80% v/v), the majority phase is organic while remaining minority phase comprised conjugate or Hb, o-methoxyphenol and H<sub>2</sub>O<sub>2</sub>. Our investigations are described in the following sections.

**2.4.1 Synthesis.** The Hb-PAA conjugates were produced from a 1.3:1 ratio of Hb to PAA (MW 450, 000 g/mol) and the COOH groups of the conjugates were coupled to either EtOH or 1-prop (132:1 or 50:1 alcohol to COOH) for six hours (Scheme 2.1). These conjugates were labeled as Hb-PAA-Eth or Hb-PAA-1-prop for the corresponding ethyl or 1-propyl esters, respectively. The Hb-PAA-ester conjugates were purified by dialysis and characterized by zeta potential, circular dichroism, IR, and TEM, as described below.

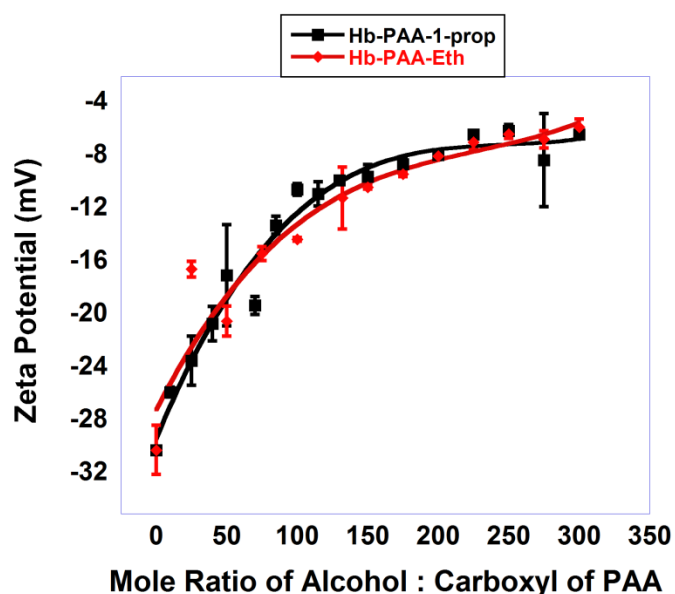
**2.4.2 Zeta Potential Studies.** Esterification of the COOH groups of Hb-PAA with alcohols altered its charge, which was followed by zeta potential studies (Figure 2.1a). For example, Hb-PAA had a net negative charge of -30 at pH 7.4 in PB (10 mM) while PAA had net negative charge of -45. Conversion of the carboxyl

groups into the corresponding esters decreased the negative charge on the conjugate, and the charge on Hb-PAA-Eth was -11. The charge on Hb-PAA-1-prop was reduced to -17. Both the ester conjugates, however, are negatively charged but the decreased charge clearly supported esterification of the COOH groups. Thus, greater numbers of COOH groups were esterified by ethanol than 1-propanol (132 equivalents of ethanol vs. 50 of 1-propanol for each COOH of PAA), and the corresponding relative values of charge reduction on esterification were 60 and 40%, respectively.

Furthermore, zeta potential measurements were carried out as a function of increasing amounts of esterification, and charge reduction saturated at approximately 225 equivalents of alcohol added (Figure 2.2). From the net charge of each of the conjugates obtained in our synthesis and the above zeta titration plot, the degrees of esterification for the conjugates were estimated to be ~ 60% and ~ 25% for ethyl and propyl esters, respectively. Considering the higher carbon content of 1-prop when compared to that of EtOH, lower concentration of 1-prop was used. We also intended to keep some COOH groups unmodified to keep conjugates soluble in a wide range of solvents.



**Figure 2.1.** (a) Zeta potentials of Hb-PAA conjugates, (b) IR spectra of Hb-PAA (green line), Hb-PAA-Eth (red broken line) and Hb-PAA-1-prop (black line), and the esters showed the characteristic carbonyl stretch at  $1720\text{ cm}^{-1}$  and  $1710\text{ cm}^{-1}$ , respectively, while the acid carbonyl of PAA indicated a strong band at  $1699\text{ cm}^{-1}$ .

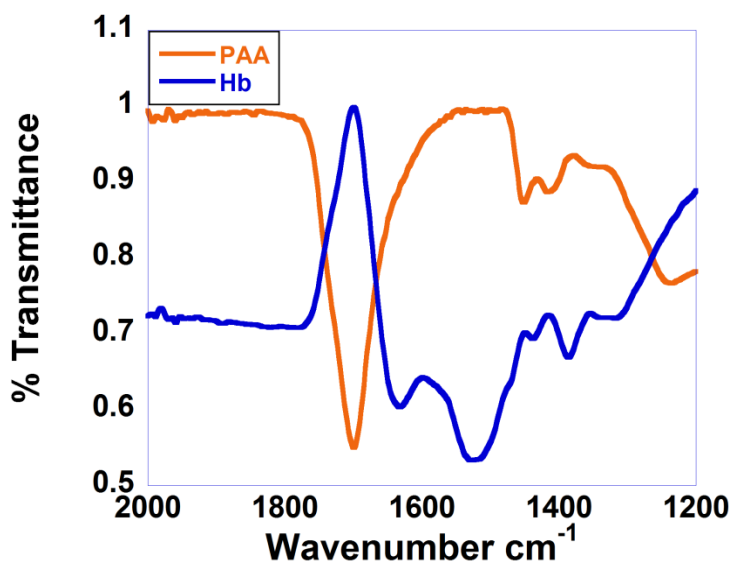


**Figure 2.2.** Zeta potential saturation plot for Hb-PAA-Eth (red line) and Hb-PAA-1-prop (black line).



**2.4.3 Infrared Spectroscopy (IR).** The IR absorption bands of the ester carbonyls are clearly noted (Figure 2.1b) at 1710-1720  $\text{cm}^{-1}$  (Hb-PAA green curve, Hb-PAA-Eth, red broken line and Hb-PAA-1-prop, black line), which are at higher frequencies than the C=O stretch of PAA (1699  $\text{cm}^{-1}$ , Figure 2.3). The appearance of this new band ( $\sim 1710 \text{ cm}^{-1}$ ) is in direct support of the ester formation. Thus, IR studies in conjunction with Zeta Potential studies confirm the esterification of the Hb-PAA. A contradiction was noted between IR and Zeta Potential data for the % functionalization of Hb-PAA by EtOH and 1-prop. But, the Zeta Potential data are probably more reliable as an entire titration was carried out and they are also consistent with the underlying chemistry. The contradiction with the IR is important but not necessarily quantitative as the peak heights might also depend on the background and the baseline of the instrument. Thus, IR data are taken only as a qualitative evidence for esterification while the Zeta Potential data are quantitative.

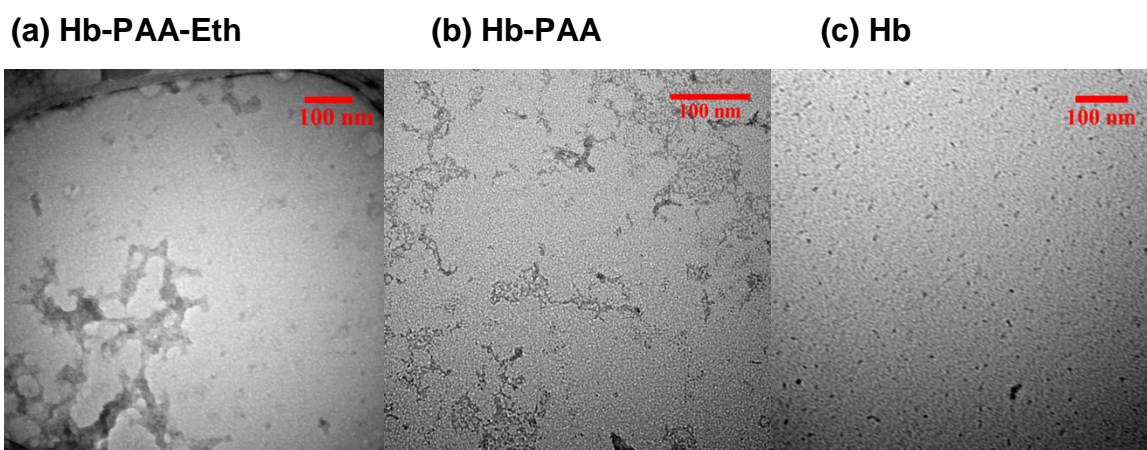
**2.4.4 TEM and DLS.** The morphology and size of protein-polymer conjugates were examined by TEM and DLS, respectively. Extensive network structures were noted for Hb-PAA-Eth and Hb-PAA. These are referred to as nano-gels, since these are soluble under all our conditions, they did not pass the inversion test, and much smaller in size compared to 3D gels. The average size of the aggregates was estimated from TEM to be 100-200 nm by examining multiple regions of the micrographs. This size estimation was consistent with DLS data (100-200 nm, Table 2.1). In contrast, TEM image of Hb showed large spherical aggregates as well as smaller particles, as reported previously.<sup>31</sup>



**Figure 2.3.** IR spectra for Hb (blue line) and PAA (brown line). PAA showed C=O stretch at 1699 cm<sup>-1</sup> whereas Hb shows no peak in same region.

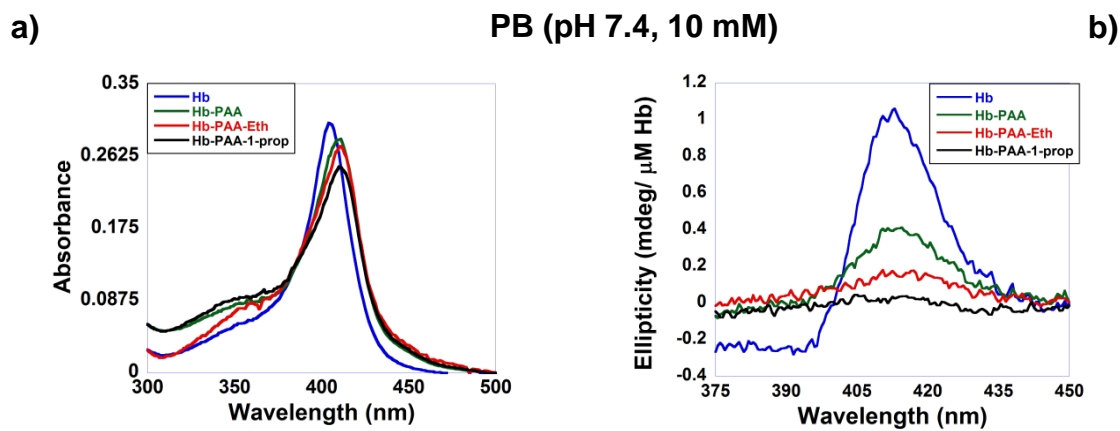
**Table 2.1.** Size (hydrodynamic diameter) of conjugates and Hb using Dynamic Light Scattering in PB (10 mM. pH 7.4) at room temperature.

Sample	Size (D <sub>h</sub> )
Hb	75.2 nm (58%)
Hb-PAA	80 nm (93%)
Hb-PAA-Eth	113 nm (99%)
Hb-PAA-1-prop	143.8 nm (98%)

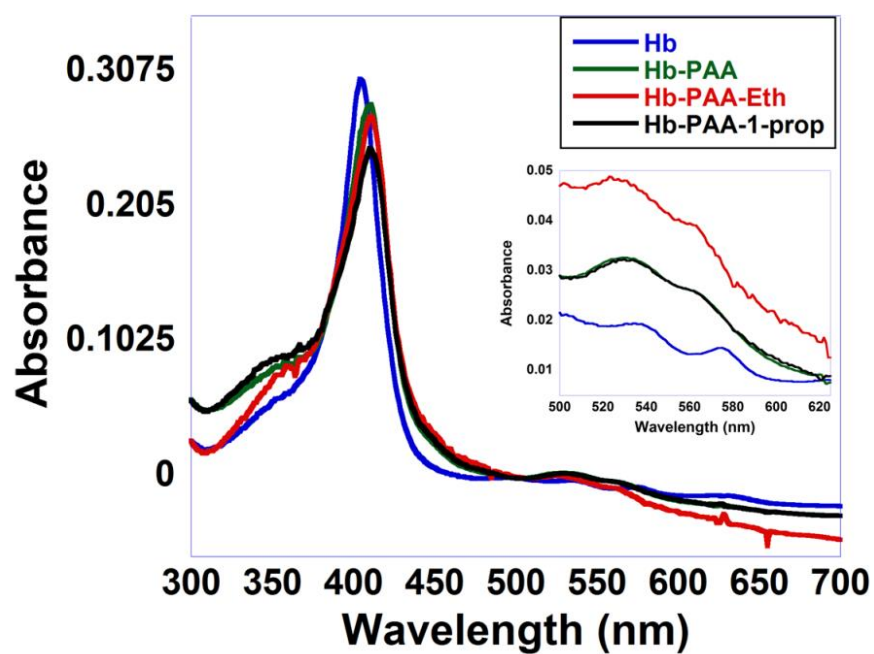


**Figure 2.4.** TEM images of (a) Hb-PAA-Eth (b) Hb-PAA (c) Hb. All samples were stained with uranyl acetate. Hb-PAA and Hb-PAA-Eth formed nanogels while Hb showed discrete particles.

**2.4.5 Protein Structure in the Conjugates.** One advantage with Hb is that changes in its secondary structure are reflected by the changes in its Soret absorption and Soret circular dichroism bands. Soret bands of the conjugates (Figure 2.5a, recorded in PB 10 mM, pH 7.4) were slightly red shifted from that of Hb (409 nm) and these indicated nearly unperturbed micro-environment around the heme unit. If heme was released from its binding pocket during or after the conjugation/modification, this band would have been blue shifted and broadened considerably.<sup>36</sup> The minor shift in the Soret band confirmed that the chemical modification with PAA or alcohols did not significantly alter the heme environment but the CD data show considerable distortions of the heme environment.<sup>37</sup> This aspect is important as changes in the heme environment could adversely affect its biochemical functions. Absorbance spectra recorded from 450 to 700 nm showed that Hb and all the conjugates are in met-hemoglobin state in PB. It showed peak at ~540 nm and shoulder at ~580 nm.<sup>38</sup> (Figure 2.6).



**Figure 2.5.** a) Soret absorption bands of Hb, Hb-PAA, Hb-PAA-Eth and Hb-PAA-1-prop in PB (pH 7.4, 10 mM). b) Soret CD bands of Hb, Hb-PAA, Hb-PAA-Eth and Hb-PAA-1-prop in PB (pH 7.4, 10 mM). All spectra were normalized with respect to their corresponding protein concentrations (1  $\mu$ M) and path lengths (1 cm).



**Figure 2.6.** UV spectra of Hb-PAA-Eth (red), Hb-PAA-1-prop (black), Hb-PAA (green) and Hb (blue) in buffer. Inside zoomed spectra is in 500 -625 nm range showing met-hemoglobin state of Hb in all the conjugates and Hb itself. It has peak at ~540 nm and shoulder at ~580 nm.

The heme environment was further examined by Soret CD spectra (Figure 2.5b, recorded in PB 10 mM, pH 7.4) and showed decreased intensities of the conjugates when compared to that of Hb. Though the Soret absorption band positions were not significantly altered, the CD band intensities decreased rather drastically, and the band intensities were used to estimate the extent of retention of chirality of the prosthetic group.<sup>39</sup> The intensities followed the order Hb>Hb-PAA>Hb-PAA-Eth>Hb-PAA-1-prop and the chiral nature of the environment was perturbed to a significant extent in the conjugates, even though the chemical environment of the heme appeared to be nearly unchanged. Thus, the absorption and CD spectra provided different aspects of the heme environment.

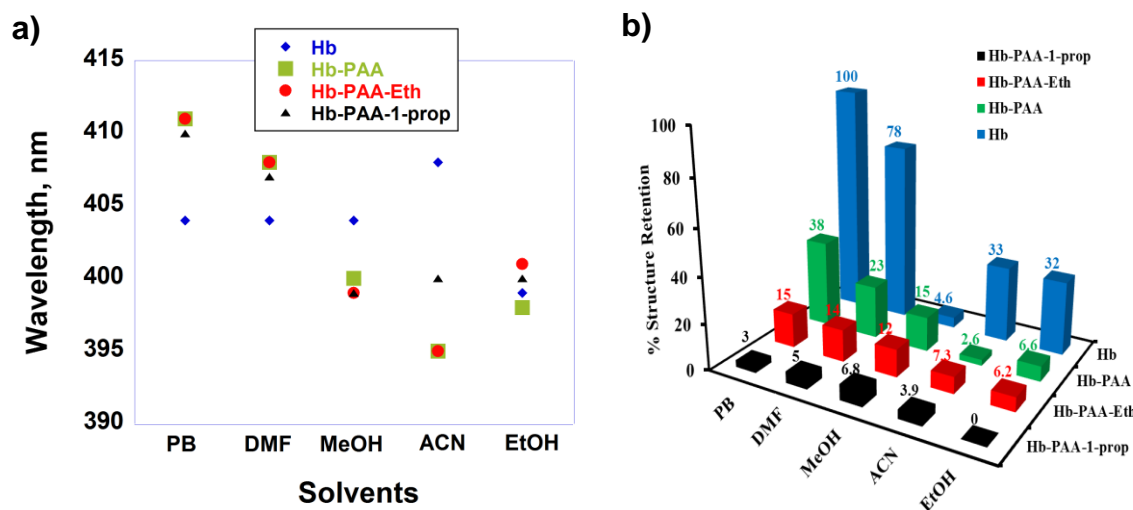
Next, we examined the absorption and CD spectra of the conjugates in organic solvents where the organic component is DMF, MeOH, ACN or EtOH. The Log P (logarithm of octanol/water partition coefficient) values are in the order, DMF> MeOH> ACN> EtOH, where DMF is most hydrophilic and EtOH is the least, in the order of increasing log(P) values.

Soret absorption band positions and Soret CD band intensities of the conjugates were evaluated in organic solvents and compared in Figure 2.7a. When absorbance spectra overlapped well in any given solvent and the peak positions were minimally shifted, a well-preserved heme environment is expected which was noted in the case of EtOH as a solvent for the ester conjugates, conjugate and Hb (Figure 2.7a). Soret maximum of the conjugates gradually shifted to shorter wavelengths with decrease in solvent polarity, and followed the trend PB>DMF>MeOH>ACN>EtOH. The blue shift in the Soret band is indicative of

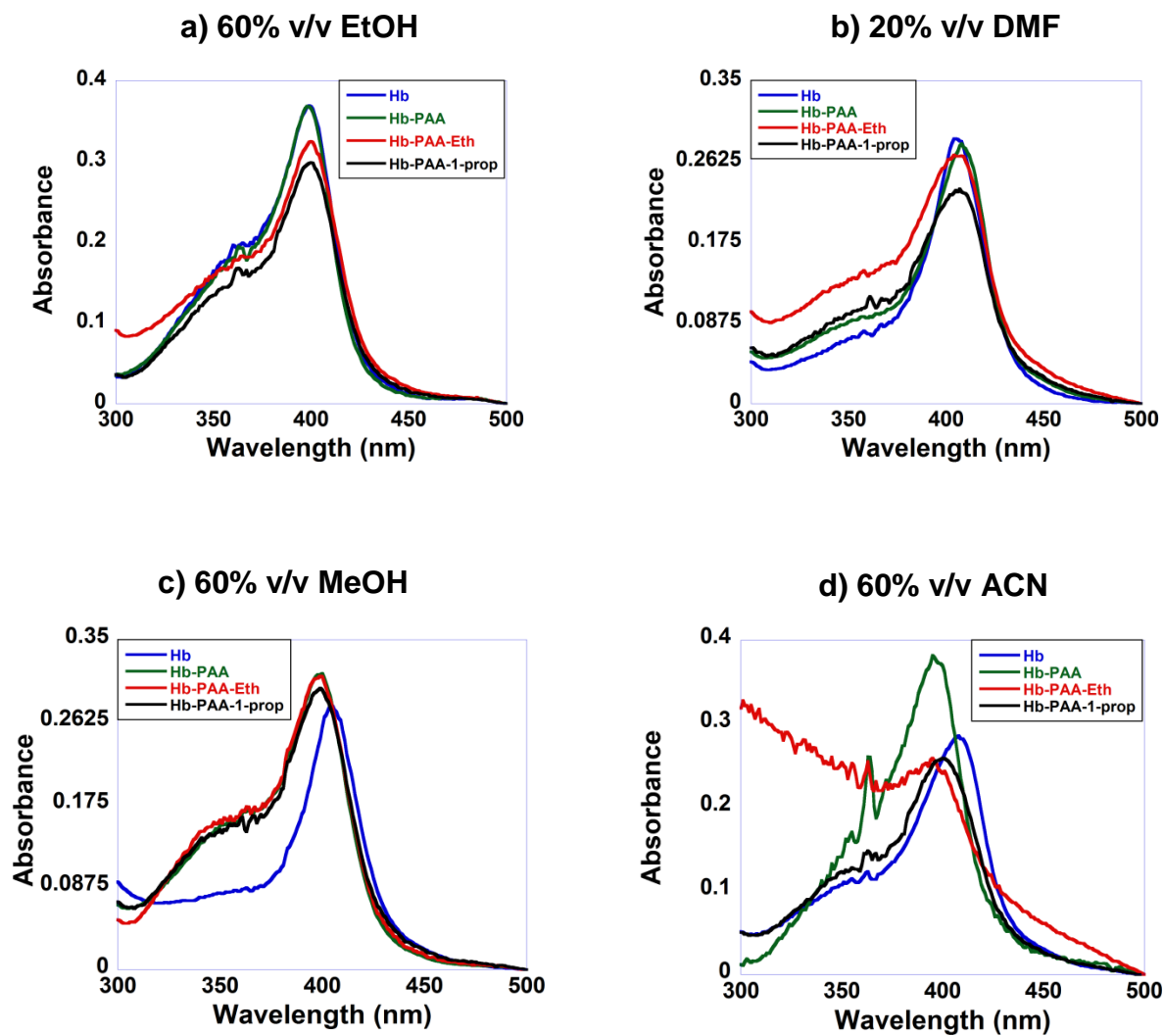
increased solvent exposure of the heme group, and this interpretation is supported by the heme CD band intensities of the conjugates (Figures 2.8 and 2.9). The CD band intensities in any given solvent were lower for the conjugates than that of Hb in the same solvent.

The extent of structure retention was calculated by comparing the CD spectra of the sample with that of Hb in PB, and the extent of structure retention was plotted as a function of solvent polarity or increasing log(P) values (Figure 2.7b). The structure retention followed the trend Hb>Hb-PAA>Hb-PAA-Eth>Hb-PAA-1-prop with respect to the conjugate while the solvent dependence was PB>DMF>MeOH>ACN>EtOH. Specifically, Hb in PB showed the highest structure retention (taken as 100%) and Hb-PAA-1-prop in EtOH (60% v/v) indicated the lowest retention of secondary structure (3%). In 20% v/v of DMF, the CD spectra for Hb-PAA-1-prop, Hb-PAA-Eth, Hb-PAA and Hb showed 14, 5, 23 and 78% structure retention, respectively. In MeOH (60% v/v), the CD spectra demonstrated 12, 6.8, 15 and 4.6% structure retention for these conjugates. All the conjugates retained the secondary structure better than Hb in MeOH. UV and CD spectra of Hb in MeOH are remarkably similar to those in water (Figure 2.8 and 2.9) and this is probably due to the formation of Hb nanoparticles in MeOH, reported previously.<sup>40</sup> In ACN (60% v/v), the CD spectra showed 7.3, 3.9, 2.6 and 33% structure retention in Hb-PAA-1-prop, Hb-PAA-Eth, Hb-PAA and Hb, respectively. While in EtOH (60% v/v), corresponding CD spectra indicated 6.2, 0, 6.6 and 32% structure retention in Hb-PAA-1-prop, Hb-PAA-Eth, Hb-PAA and Hb, respectively.

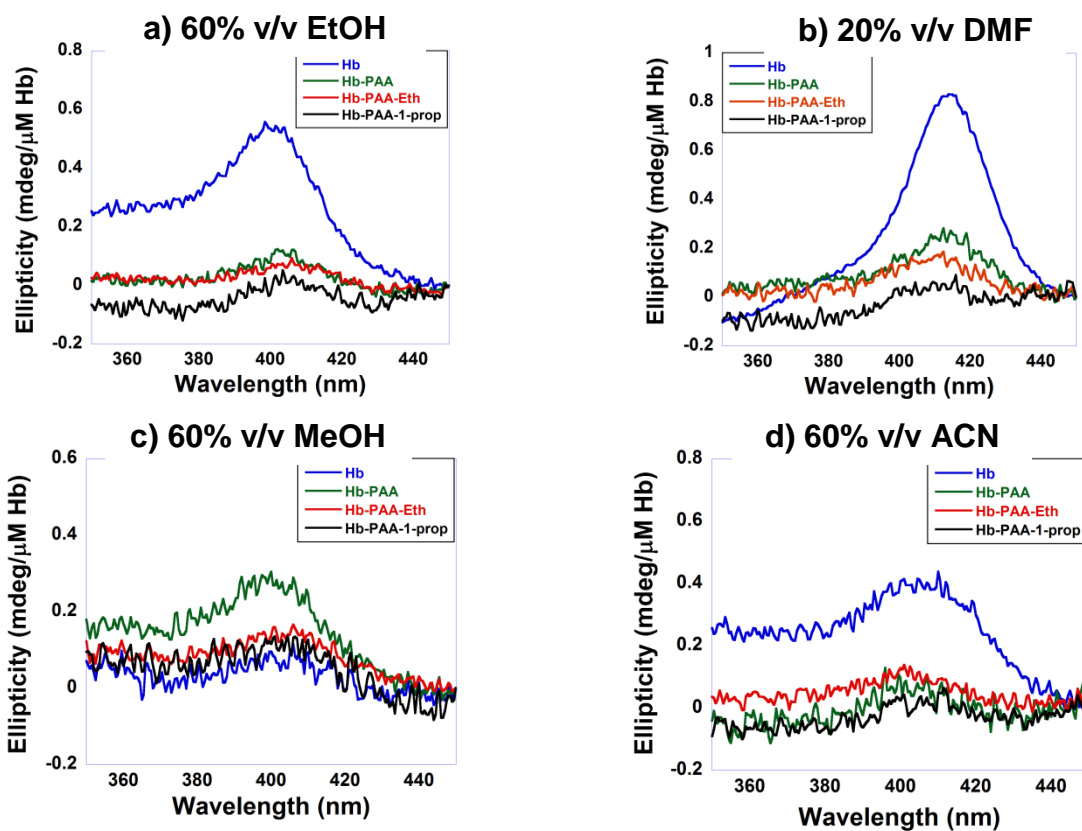




**Figure 2.7.** a) Soret band positions for Hb conjugates in PB (10 mM, pH 7.4) and organic solvents. b) The extent of structure retention for Hb conjugates in organic solvents, estimated from the UV CD spectra. Solvent compositions were 60% v/v for EtOH, MeOH, ACN and 20% v/v for DMF, where the conjugates showed highest activities (solvents organized by increasing log P values from DMF to EtOH).



**Figure 2.8.** Absorbance spectra of Hb, Hb-PAA, Hb-PAA-Eth and Hb-PAA-1-prop in a) 60% v/v EtOH b) 20% v/v DMF c) 60% v/v MeOH d) 60% v/v ACN. All spectra are corrected for Hb concentration (1  $\mu$ M).



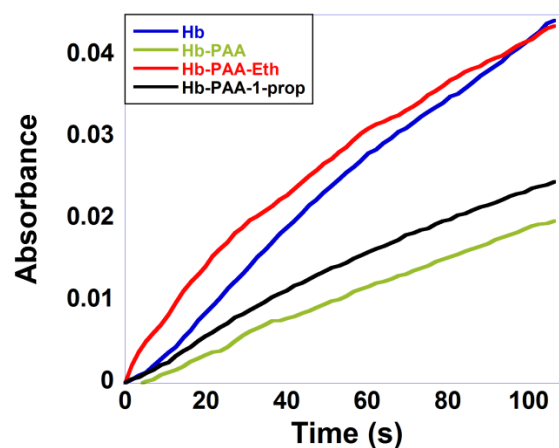
**Figure 2.9.** CD spectra of Hb, Hb-PAA, Hb-PAA-Eth and Hb-PAA-1-prop in a) 60% v/v EtOH b) 20% v/v DMF c) 60% v/v MeOH d) 60% v/v ACN. All spectra are corrected for Hb concentration (1 μM).

Our previous work demonstrated high thermal stability of Hb-PAA conjugates, even against steam-sterilization conditions of 120 °C.<sup>29</sup> We took advantage of this observation and modified the polymer side chains to enhance their compatibility and catalytic activities in organic solvents. CD study helped to estimate the integrity of Hb secondary structure in the ester conjugates. The reduction in % retention of structure of the ester conjugates, Hb-PAA and Hb in organic solvents could be related to the solubility of polymer in the organic solvents and the loss of structurally important water from the protein surface. The chirality retention increased with increased solvent polarity as well as the hydrophilicity of the Hb-solvent interface. In summary, modification of Hb-PAA with alcohols can be used as a modular method to control their compatibility with organic solvents for the retention of catalytic activities, even at the expense of some structure loss in the heme environment, and this goal is achieved. Since Hb structure influences its biological activity, we next examined the peroxidase-like activities of the conjugates in organic-water solvent mixtures.

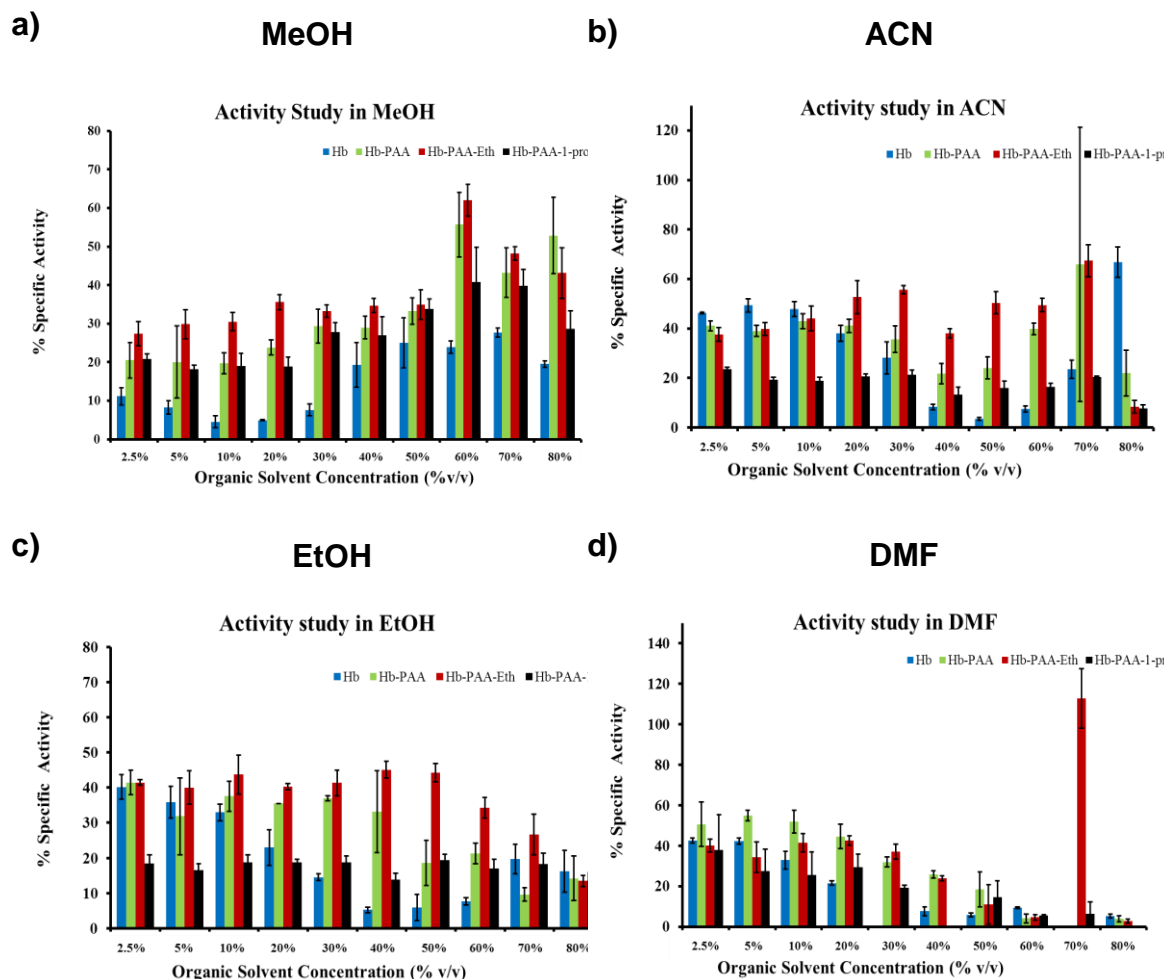
**2.4.6 Activity Studies.** While Hb does not function as an enzyme in biological systems, its peroxidase-like activity is well known, and it is being used commercially in biosensor applications and in the oxidation of polycyclic aromatic hydrocarbons.<sup>24, 26</sup> Here, the oxidation of 2-methoxyphenol by hydrogen peroxide is catalyzed by Hb,<sup>31, 41</sup> and the corresponding oxidation product which absorbs at 470 nm, was monitored as a function of reaction time. The kinetic traces of Hb-PAA-Eth, Hb-PAA-1-prop, Hb-PAA and Hb in 2.5% v/v MeOH (2.5 mM o-methoxyphenol, 1 mM H<sub>2</sub>O<sub>2</sub>) are shown in Figure 2.10. At 80% v/v of organic

solvent concentration, the majority phase remains organic while the minority phase consisted of the conjugate or Hb, o-methoxyphenol and  $\text{H}_2\text{O}_2$ . The initial rates were used to calculate specific activities and compared with that of Hb in PB, as a reference (Figure 2.10 and 2.11). In all the plots, Hb-PAA-Eth, Hb-PAA-1-prop, Hb-PAA and Hb are represented as red, black, green and blue bars, respectively.

The highest activities were noted for all conjugates at 60% v/v MeOH: Hb-PAA-Eth, Hb-PAA-1-prop and Hb-PAA had activities of 62%, 40% and 55%, respectively, while Hb had the lowest activity (Figure 2.11a). In ACN, a clear trend of activities based on the catalyst and solvent mixture could not be discerned (Figure 2.11b). For example, Hb-PAA-Eth showed high activities (40-60%) when scanned over concentrations of 2.5-80% v/v of ACN, while, Hb-PAA-1-prop showed activity of 10-25% under similar solvent compositions. Hb-PAA showed highest activity at 70% v/v while Hb in ACN showed decrease in activity from 2.5 to 50% v/v ACN. Surprisingly, the activity increased upon further addition of ACN, while Hb showed the highest activity in 80% v/v ACN (Figure 2.11b).



**Figure 2.10.** Peroxidase-like activities of Hb conjugates and product formation as monitored at 470 nm, in 2.5% v/v MeOH in PB (10 mM, pH 7.4, 2.5 mM o-methoxyphenol, 1 mM H<sub>2</sub>O<sub>2</sub>).



**Figure 2.11.** Specific activities of Hb-PAA-Eth (red), Hb-PAA-1-prop (black), Hb-PAA (green) and Hb (blue) with respect to that of Hb in PB (10 mM, pH 7.4) (100%), as a function of increasing concentrations of (a) MeOH, and (b) ACN (c) EtOH and (d) DMF.

In DMF, Hb-PAA-Eth showed >100% at 70% v/v DMF, Hb-PAA-1-prop showed 30%-40% activities at lower concentrations of DMF and very low activities (~0%) at higher concentrations (80% v/v, Figure 2.11d). In EtOH, Hb-PAA-Eth showed very high activities at all solvent concentrations examined here, while Hb-PAA-1-prop showed lower activity of 15-20% (Figure 2.11c). In contrast, Hb-PAA showed slight decrease in activities when the concentration of EtOH was increased above 40% v/v, while, Hb showed gradual decrease in activity when EtOH content was raised from 2.5 to 40% v/v, then activities increased.

The above trends in activities in the organic solvents were examined in the context of solvent log P values, a measure of lipophilicity of the solvent. Log P values of these solvents are: DMF (−1.01), MeOH (−0.77), ACN (−0.34), and EtOH (−0.30),<sup>42</sup> and polarity decreased or hydrophobicity increased from DMF to EtOH in this order. To simplify the complexity of the above trends, we calculated average activities of each conjugate in a particular solvent and compared these with that of Hb in PB. The average activity of a conjugate in the organic solvent was calculated using the formula:

$$\% \text{ weighted average activity} = \frac{\sum(\% \text{ organic solvent} \times \% \text{ activity})}{100}$$

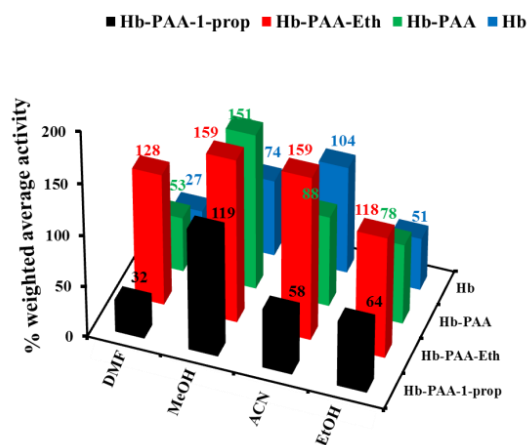
Where the percent of organic solvent in the solvent mixture and the relative activity of the sample in that mixture with respect to that of Hb in PB is used. This analysis assumes that activities of a given conjugate follow a smooth function of solvent composition and that the weighted average can be compared among different solvents. The resulting activity data plots are shown in Figure 2.12.



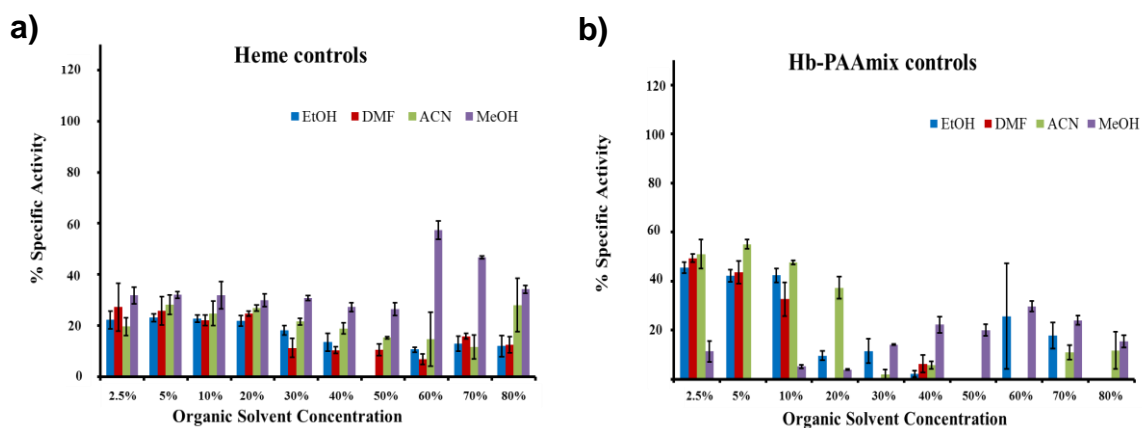
Conjugation of PAA to Hb and esterification improved activities in organic solvents. Out of 20 activity measurements in 5 different solvents, the conjugates outperformed Hb where 18 of the measurements with conjugates exceeded that of Hb, under the same solvent conditions (Figure 2.12). The two underperformers were in ACN, where Hb has unusually high activity or nearly the same as in PB and there has been no precedence for this behavior.

Hb-PAA-Eth showed higher catalytic activities than both Hb-PAA and Hb. However, further increased hydrophobicity of Hb-PAA-1-prop reduced the activity, which is likely due to a mismatch in the polarity of the solvent and the polymer shell around the protein. Thus, the balance of lipophilicity of the conjugates and the solvent appears to play an important role in controlling the catalytic activities of the conjugates and serves as general guideline in the design of Hb-PAA-ester conjugates.

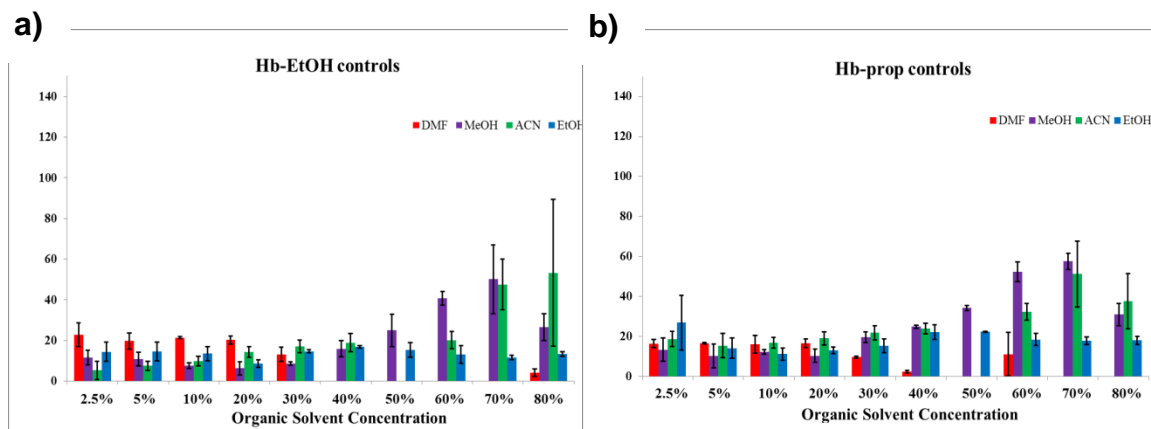
During catalytic reactions in organic solvents, heme may leach out and control experiments were carried out with only heme and with physical mixtures of Hb and PAA (Hb-PAAmix, Figure 2.13) to test this possibility and heme showed less activity compared to Hb-PAA and ester conjugates. Another control was to test if the COOH groups of Hb are modified in the above reactions, and the corresponding EtOH and 1-propanol modified samples, Hb-EtOH and Hb-prop, respectively, which resulted in the precipitation of the sample. These samples showed poor catalytic activities (Figure 2.14).



**Figure 2.12.** Averages of the specific activities of Hb-PAA-Eth (red), Hb-PAA-1-prop (black), Hb-PAA (green) and Hb (blue) bar in DMF, MeOH, ACN and EtOH. Solvents are arranged in increasing log P values from DMF to EtOH.



**Figure 2.13.** a) Activity studies of heme (1  $\mu$ M) in different organic solvents (2.5 mM o-methoxyphenol (substrate), 1 mM  $\text{H}_2\text{O}_2$ (oxidant)). Blue bar lines are for activity of heme in EtOH, red bar is for DMF, green bar is for ACN and purple is in MeOH. b) Hb-PAAmix activity study in various organic solvents. Hb-PAAmix is made by mixing Hb and PAA without addition of EDC-coupling agent. Blue bar lines represent the activity of Hb-PAAmix in EtOH, red in DMF, green in ACN and purple in MeOH. Heme shows better activities above 40%v/v of organic solvents. Hb-PAAmix shows low activities above 40% v/v of organic solvents.



**Figure 2.14.** a) Activity studies of Hb-EtOH (1 $\mu$ M) in different organic solvents (2.5 mM o-methoxyphenol (substrate), 1 mM H<sub>2</sub>O<sub>2</sub>(oxidant)). Red bar lines are for activity of Hb-EtOH in DMF, purple bar is for MeOH, green bar is for ACN and blue is in EtOH. b) Hb-prop activity study in various organic solvents. Red bar lines represent the activity of Hb-prop in DMF, purple in MeOH, green in ACN and blue in EtOH. Hb-EtOH and Hb-prop was made by conjugating EtOH and 1-prop respectively to Hb using EDC chemistry to free carboxyl groups on Hb from aspartate and glutamate.

**2.4.7  $K_M$  and  $V_{max}$  Studies.** The enzymatic activities depend on the rates of several steps in the catalytic cycle and insight into these steps was gained by measuring the Michaelis constant ( $K_M$ ) and maximum initial velocity ( $V_{max}$ ). Using the initial rates determined with increasing substrate concentrations, Lineweaver-Burk plots (plot of inverse of initial rate vs. inverse of substrate concentration) and Michaelis-Menton plots were constructed using the equation,

$$\frac{1}{V} = \frac{K_M}{V_{max}} \cdot \frac{1}{[S]} + \frac{1}{V_{max}}, \text{ Where } [S] = \text{substrate concentration, } V = \text{initial reaction rate,}$$

$K_M$  = Michaelis constant and  $V_{max}$  = maximum initial velocity.

The Lineweaver-Burk plots for Hb-PAA-Eth (red line), Hb-PAA-1-prop (black line), Hb-PAA (green line) and Hb (blue line), obtained under five different conditions (a) in PB 10 mM in pH 7.4, (b) DMF (20% v/v) and (c) ACN (60% v/v), (d) MeOH (60% v/v) and (e) EtOH (60% v/v) are shown in Figure 2.15. Specific concentrations of solvents were used since all the conjugates showed optimum catalytic activities under these conditions. The corresponding  $K_M$ ,  $V_{max}$ ,  $k_{cat}$  and  $k_{cat}/K_M$  extracted from these data are collected in Table S2, Supporting Information. Lower  $K_M$  values indicate increased affinity of the substrate for the enzyme active site, and  $k_{cat}$  is the turnover number, i.e. the number of moles of substrate molecules converted to the product molecules per unit time, while  $k_{cat}/K_M$  is the catalytic efficiency. Highest catalytic efficiency is the most desired.

Hb-PAA-Eth indicated higher affinity for substrate in MeOH and varied substantially with polarity, while Hb-PAA-1-prop showed higher affinity for the same substrate in DMF but it varied very little with solvent polarity. In comparison, Hb-PAA and Hb showed preferred affinity for PB (10 mM, pH 7.4) and EtOH, respectively, and Hb-PAA indicated highest sensitivity to solvent polarity. Also, from Table 2.2 it is clear that Hb-PAA-Eth and

Hb-PAA-1-prop showed highest  $V_{\max}$  and  $k_{\text{cat}}$  in EtOH and PB (10 mM, pH 7.4), respectively, while, Hb-PAA and Hb showed highest  $V_{\max}$  and  $k_{\text{cat}}$  in ACN and PB (10 mM, pH 7.4), respectively.

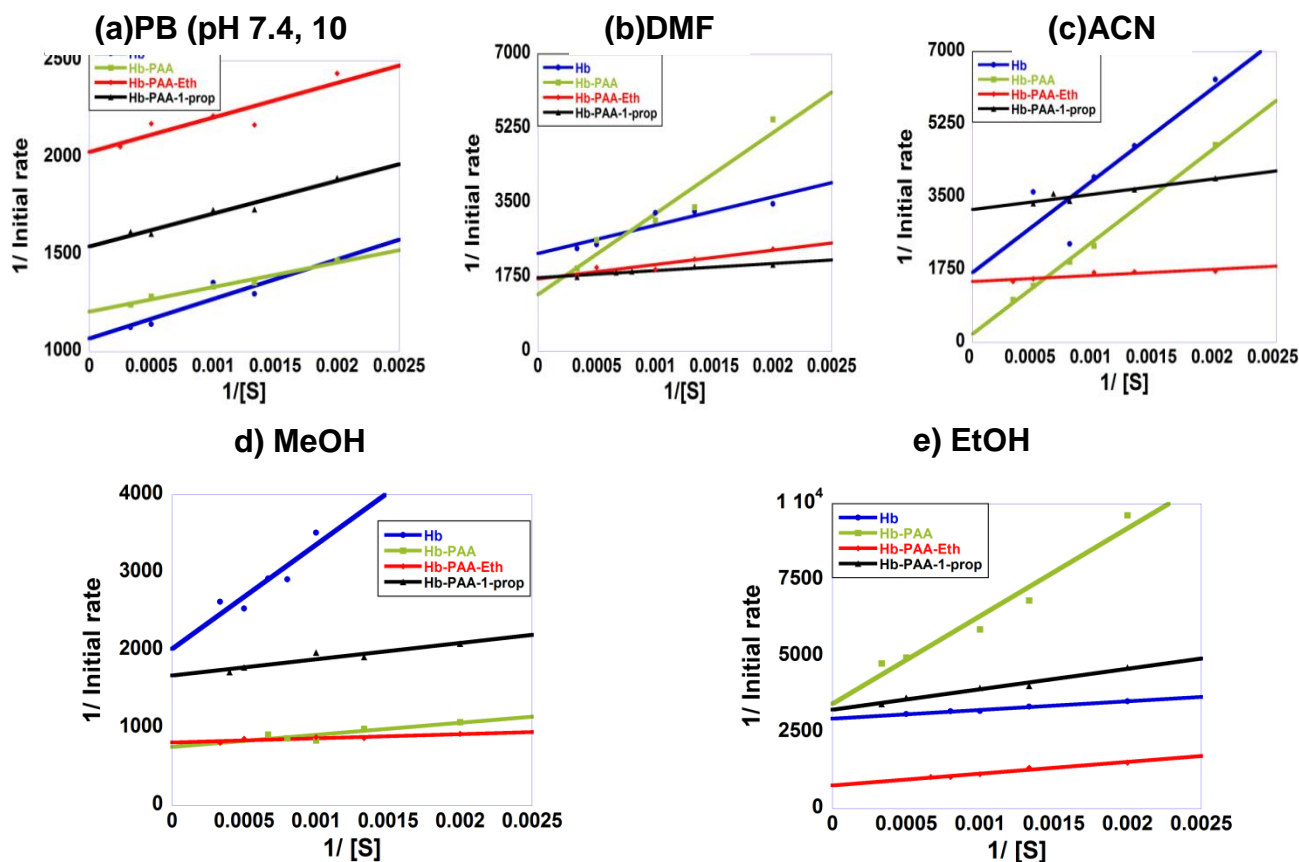
Hb-PAA-Eth and Hb-PAA-1-prop showed highest catalytic efficiency in MeOH and DMF, while Hb-PAA and Hb showed highest catalytic efficiency in PB (10 mM, pH 7.4). Hb-PAA-Eth and Hb-PAA-1-prop had increased affinity for the substrate in MeOH and DMF, respectively. Also, due to the unmodified COOH groups, Hb-PAA is more hydrophilic than the ester conjugates, and showed increased affinity for substrate in PB (10 mM, pH 7.4) and not in organic solvents. There were no specific trends in  $K_M$  as a function of solvent polarity for a given biocatalyst or the polarity of the polymer shell around the protein while MeOH showed the lowest average  $K_M$  values.

Hb and Hb-PAA-1-prop showed high  $V_{\max}$  values in PB (10 mM, pH 7.4), which suggested that substrate replenishment for reaction is faster in this solvent for these two samples. In contrast, Hb-PAA and Hb-PAA-Eth showed high  $V_{\max}$  in ACN and EtOH, respectively, which implied that the PAA sheath around Hb helped in faster entry of substrate and exit of product and resulted in faster reaction velocity. All conjugates showed higher  $V_{\max}$  values in all the four organic solvents tested here, than Hb, with only one significant exception. Thus, conjugates, by and large excelled when compared to Hb in the same solvent.

The catalytic efficiencies ( $k_{\text{cat}}/K_M$ ) are plotted (Figure 2.16) to gain further insight into how the solvent influenced the overall catalytic efficiency of the modified biocatalyst. 3D plots of  $1/K_M$  are shown in, Figure 2.17. The catalytic efficiencies, surprisingly, showed a systematic relationship with solvent polarity, and the efficiencies peaked smoothly with

polarity, for Hb-PAA-1-prop. While, Hb showed highest efficiency in PB, two of the conjugates (Hb-PAA and Hb-PAA-1-prop) showed higher efficiencies in PB than Hb itself. Two of the conjugates (Hb-PAA-Eth and Hb-PAA-1-prop) showed higher efficiencies than Hb in DMF, MeOH and ACN, while Hb showed the highest efficiency in EtOH.

Hb-PAA-Eth showed highest catalytic efficiencies in MeOH, ACN and higher than Hb in PB, while Hb-PAA-1-prop showed the highest efficiency in DMF, higher than Hb in PB. Therefore, ester modified conjugate, Hb-PAA-Eth worked as a superior catalyst compared to Hb-PAA or Hb in hydrophobic solvents. Hb-PAA-Eth showed more than three times catalytic efficiency in MeOH compared to Hb in PB (10 mM, pH 7.4). Hb-PAA, on the other hand, showed the highest efficiency in PB, higher than Hb in PB, and therefore, conjugates can be tailored based on the log P value of reaction medium to achieve the highest catalytic efficiency. The data clearly show that the conjugates can enhance the catalytic efficiencies many-fold higher in organic solvents than the natural system in PB. Based on catalytic efficiency and kinetic data we may be able to predict which enzyme conjugate will show maximum efficiency in a particular solvent, but further studies are required to map out the complex relationships between the solvent, the interface, the substrate, the product and the solvent.

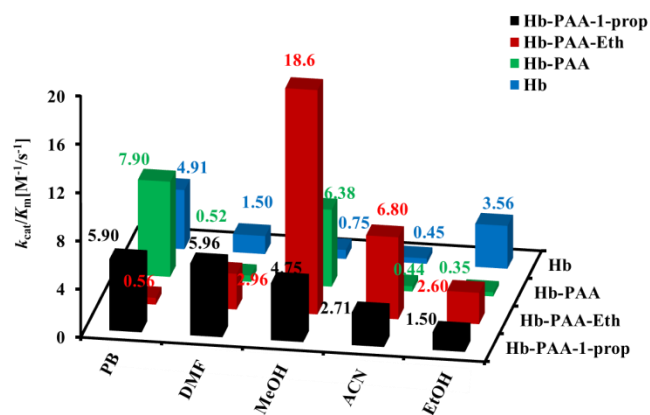


**Figure 2.15.** Lineweaver-Burk plots for Hb-PAA-Eth (red line), Hb-PAA-1-prop (black line), Hb-PAA (green line) and Hb (blue line) in, a) PB (pH 7.4, 10mM); b) DMF (20% v/v), c) ACN (60% v/v), d) MeOH (60% v/v) and e) EtOH (60% v/v) where the solvent compositions indicated highest activities.

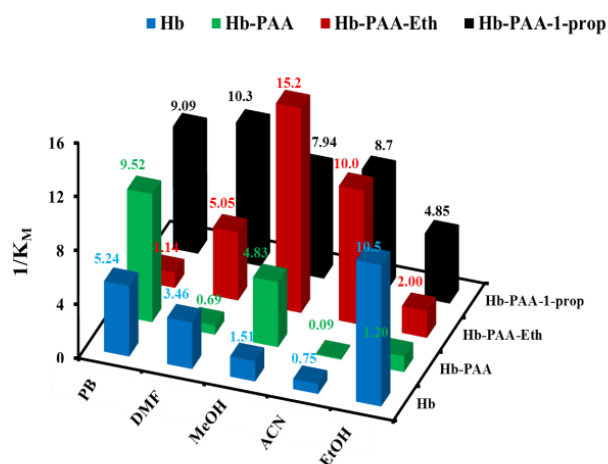


**Table 2.2.** Determination of  $K_M$ ,  $V_{max}$ ,  $k_{cat}$  and  $k_{cat}/K_M$ 

Conditions	Sample	$K_M$ [mM]	$V_{max}$ [ $\mu$ M/s]	$k_{cat}$ [s <sup>-1</sup> ]	$k_{cat}/K_M$ [M <sup>-1</sup> /s <sup>-1</sup> ]
<u>PB (10 mM)</u> <u>pH 7.4</u>	Hb	0.191	$9.37 \times 10^{-4}$	$9.37 \times 10^{-4}$	4.91
	Hb-PAA	0.105	$8.29 \times 10^{-4}$	$8.29 \times 10^{-4}$	7.90
	Hb-PAA-Eth	0.878	$4.93 \times 10^{-4}$	$4.93 \times 10^{-4}$	0.56
	Hb-PAA-1-prop	0.110	$6.49 \times 10^{-4}$	$6.49 \times 10^{-4}$	5.90
<u>20% v/v</u> <u>DMF</u>	Hb	0.289	$4.34 \times 10^{-4}$	$4.34 \times 10^{-4}$	1.50
	Hb-PAA	1.430	$7.50 \times 10^{-4}$	$7.50 \times 10^{-4}$	0.52
	Hb-PAA-Eth	0.198	$5.86 \times 10^{-4}$	$5.86 \times 10^{-4}$	2.96
	Hb-PAA-1-prop	0.097	$5.78 \times 10^{-4}$	$5.78 \times 10^{-4}$	5.96
<u>60% v/v</u> <u>ACN</u>	Hb	1.325	$5.92 \times 10^{-4}$	$5.92 \times 10^{-4}$	0.45
	Hb-PAA	10.959	$48.7 \times 10^{-4}$	$48.7 \times 10^{-4}$	0.44
	Hb-PAA-Eth	0.100	$6.80 \times 10^{-4}$	$6.80 \times 10^{-4}$	6.80
	Hb-PAA-1-prop	0.115	$3.12 \times 10^{-4}$	$3.12 \times 10^{-4}$	2.71
<u>60%v/v</u> <u>EtOH</u>	Hb	0.095	$3.38 \times 10^{-4}$	$3.38 \times 10^{-4}$	3.56
	Hb-PAA	0.835	$2.90 \times 10^{-4}$	$2.90 \times 10^{-4}$	0.35
	Hb-PAA-Eth	0.500	$13.0 \times 10^{-4}$	$13.0 \times 10^{-4}$	2.60
	Hb-PAA-1-prop	0.206	$3.08 \times 10^{-4}$	$3.08 \times 10^{-4}$	1.5
<u>60%v/v</u> <u>MeOH</u>	Hb	0.664	$4.96 \times 10^{-4}$	$4.96 \times 10^{-4}$	0.75
	Hb-PAA	0.207	$13.2 \times 10^{-4}$	$13.2 \times 10^{-4}$	6.38
	Hb-PAA-Eth	0.066	$12.3 \times 10^{-4}$	$12.3 \times 10^{-4}$	18.6
	Hb-PAA-1-prop	0.126	$5.98 \times 10^{-4}$	$5.98 \times 10^{-4}$	4.75



**Figure 2.16.** Catalytic efficiencies of Hb-PAA-Eth (red), Hb-PAA-1-prop (black), Hb-PAA (green) and Hb (blue) in PB (10 mM, pH 7.4), DMF (20% v/v), MeOH (60% v/v), ACN (60% v/v) and EtOH (60% v/v). Specific solvent compositions corresponding to highest specific activities were used. Solvents are arranged in the order of increasing log (P).



**Figure 2.17.**  $1/K_M$  of Hb-PAA-Eth (red), Hb-PAA-1-prop (black), Hb-PAA (green) and Hb (blue) in PB (10 mM, pH 7.4), DMF (20% v/v), MeOH (60% v/v), ACN (60% v/v) and EtOH (60% v/v). Specific solvent compositions corresponding to highest specific activities were used. Solvents are arranged in the order of increasing log (P).

## 2.5 Conclusions

We have demonstrated the design, synthesis and characterization of Hb-PAA conjugates and their ester derivatives for use as catalysts in organic solvents. Our strategy to maximize the activities in organic solvents was to manipulate the Hb-PAA-solvent interface in a systematic manner by functionalizing the polymer shell around the protein and examining the influence of the interface polarity on activities and catalytic efficiencies. Enhanced catalytic efficiencies noted for the conjugates in organic solvents is unexpected but consistent with studies reported by other research groups, which used different approaches for organic biocatalysis than the approach described here.

The catalytic efficiencies of the conjugates were higher than that of Hb in each organic solvent, except in EtOH, where Hb outperformed the conjugates. In all other solvents the conjugates outperformed Hb, and successful conversion of carboxyl groups was confirmed by IR studies and independently verified by zeta potential. The systematic increase in catalytic efficiency of the modified conjugates in various organic solvents showed promising results.

The Hb-PAA ester conjugates are the first examples of biocatalysts used in these particular organic solvents: DMF, MeOH, ACN and EtOH. Higher weighted % catalytic activities were noted in DMF, EtOH and MeOH, than the corresponding activities of Hb in the respective solvents, and catalytic activities depended on solvent log(P) values and followed the trend  $Hb < Hb-PAA-1-prop < Hb-PAA < Hb-PAA-Eth$ , irrespective of the organic solvent, and highest activities followed the order  $DMF < EtOH < ACN < MeOH$  with some exceptions, irrespective of the

conjugate. Thus, catalytic activities increased and then decreased with solvent polarity.

The catalytic efficiencies depended on solvent polarity and highest efficiencies were found for Hb-PAA in water, Hb-PAA-Eth in DMF and Hb-PAA-1-prop in ACN. Thus, highest efficiencies were noted in organic solvents but not in water! Catalytic efficiencies in organic solvents exceeded that of Hb in water by more than 3-fold, and this is the very first general, versatile, modular platform for enzyme-based biocatalysis in organic solvents. An important aspect of this study is that the polarity of the polymer shell around the protein can be tailored for maximum catalytic efficiency for a particular organic solvent. This strategy of coupling the enhanced stability of Hb reported earlier with control over the protein-solvent interface provided a rational approach to achieve efficient biocatalysis in organic solvents. This comprehensive synthesis and structure-activity study opens up plethora of options to investigate and exploit organic enzymology of Hb, which may be extended to other enzymes and other solvents in the future.

## 2.6 References.

- 
1. Aehle, W., *Enzymes in Industry*. Wiley: **2008**.
  2. Campbell, M. K.; Farrell, S. O., *Biochemistry*. BROOKS COLE Publishing Company: **2011**.
  3. Jaenicke, R.; Bohm, G., *Curr.Opin. Struct. Biol.* **1998**, 8, 738-748.
  4. Polizzi, K. M.; Bommarius, A. S.; Broering, J. M.; Chaparro-Riggers, J. F., *Curr. Opin. Chem. Biol.* **2007**, 11, 220-225.
  5. Bhambhani, A.; Kumar, C. V. *Adv. Mater.* **2006**, 18, 939-942.

- 
6. Kumar, C. V.; Chaudhari, A., *J. Am. Chem. Soc.* **2000**, 122, 830-837.
  7. Kumar, C. V.; Chaudhari, A., *Chem. Mater.* **2001**, 13, 238-240.
  8. Kumar, C. V.; Chaudhari, A., *Chem. Commun.* **2002**, 0, 2382-2383.
  9. Kim, J.; Grate, J. W., *Nano Lett.* **2003**, 3, 1219-1222.
  10. Novick, S. J.; Dordick, J. S., *Chem.Mater.* **1998**, 10, 955-958.
  11. Khalaf, N.; Govardhan, C. P.; Lalonde, J. J.; Persichetti, R. A.; Wang, Y.-F.; Margolin, A. L., *J. Am. Chem. Soc.* **1996**, 118, 5494-5495.
  12. Xu, K.; Klibanov, A. M., *J. Am. Chem. Soc.* **1996**, 118, 9815-9819.
  13. Woodward, C. A.; Kaufman, E. N., *Biotechnol. Bioeng.* **1996**, 52, 423-428.
  14. Khmelnitsky, Y. L.; Belova, A. B.; Levashov, A. V.; Mozhaev, V. V., *FEBS Lett.* **1991**, 284, 267-269.
  15. Antonini, E.; Carrea, G.; Cremonesi, P., *Enzyme Microb.Technol.* **1981**, 3, 291-296.
  16. Abian, O.; Mateo, C.; Fernández-Lorente, G.; Palomo, J. M.; Fernández-Lafuente, R.; Guisán, J. M., *Biocatal. Biotransform.* **2001**, 19, 489-503.
  17. Alsafadi, D.; Paradisi, F., *Extremophiles* **2013**, 17, 115-122.
  18. Gupta, M. N., *Methods in non-aqueous enzymology*. Birkhauser Verlag GmbH: **2000**.
  19. Koskinen, A. M. P.; Alexander, M. K., Blackie Academic & Professional: **1996**.
  20. Schmid, A.; Dordick, J. S.; Hauer, B.; Kiener, A.; Wubbolts, M.; Witholt, B., *Nature*. **2001**, 409, 258-268.
  21. Mieyal, J. J.; Starke, D. W., *Methods in Enzymology*, Johannes Everse, K. D. V. R. M. W., Ed. Academic Press: **1994**, 231, 573-598.

- 
22. Huang, Z.; Shiva, S.; Kim-Shapiro, D. B.; Patel, R. P.; Ringwood, L. A.; Irby, C. E.; Huang, K. T.; Ho, C.; Hogg, N.; Schechter, A. N.; Gladwin, M. T., *J. Clin. Invest.* **2005**, *115*, 2099-2107.
23. Starke, D. W.; Blisard, K. S.; Mieyal, J. J., *Mol. Pharmacol.* **1984**, *25*, 467-475.
24. Ortizleon, M.; Velasco, L.; Vazquezduhalt, R., *Biochem. Biophys. Res. Commun.* **1995**, *215*, 968-973.
25. Xiong, H. Y.; Chen, T.; Zhang, X. H.; Wang, S. F., *Electrochem. Commun.* **2007**, *9*, 2671-2675.
26. Briand, V. A.; Thilakarathne, V.; Kasi, R. M.; Kumar, C. V., *Talanta* **2012**, *99*, 113-118.
27. Huang, C.; Bai, H.; Li, C.; Shi, G., *Chem. Commun.* **2011**, *47*, 4962-4964.
28. Wang, Q.; Gao, Q.; Shi, J., *J. Am. Chem. Soc.* **2004**, *126*, 14346-14347.
29. Mudhivarthi, V. K.; Cole, K. S.; Novak, M. J.; Kippfuth, W.; Deshapriya, I. K.; Zhou, Y.; Kasi, R. M.; Kumar, C. V., *J. Mater. Chem.* **2012**, *22*, 20423-20433.
30. Lee, C. K.; Manning, J. M., *J. Biol. Chem.* **1973**, *248*, 5861-5865.
31. Thilakarathne, V.; Briand, V. A.; Zhou, Y.; Kasi, R. M.; Kumar, C. V., *Langmuir* **2011**, *27*, 7663-7671.
32. McConvey, I. F.; Woods, D.; Lewis, M.; Gan, Q.; Nancarrow, P., *Org. Process Res. Dev.* **2012**, *16*, 612-624.
33. Kamaruddin, M. Z. F.; Kamarudin, S. K.; Daud, W. R. W.; Masdar, M. S., *Renewable Sustainable Energy Rev.* **2013**, *24*, 557-565.
34. Thilakarathne, V.; Briand, V. A.; Zhou, Y.; Kasi, R. M.; Kumar, C. V., *Langmuir* **2011**, *27*, 7663-7671.
35. Maehly Ac Fau - Chance, B.; Chance, B., *Methods Biochem. Anal.* **1954**, *1*, 357-424

- 
- 36 . Samejima, T.; Miyahara, T.; Takeda, A.; Hachimori, A.; Hirano, K., *J. Biochem.* **1981**, 89, 1325-1332.
37. Torres, E.; Vazquez-Duhalt, R., *Biochem.Biophys. Res. Commun.* **2000**, 273, 820-823.
38. Reeder, B. J., *Antioxid. Redox Signaling* **2010**, 13, 1087-1123
39. Kelly, S. M.; Jess, T. J.; Price, N. C., *Biochim. Biophys. Acta, Proteins Proteomics* **2005**, 1751, 119-139.
40. Kumar, C. V.; Deshapriya, I. K.; Duff Jr., M. R.; Blackeley, B.; Lee-Haye, D.; *J. Nano Res.* **2010**, 12, 77-88.
41. Maehly Ac Fau - Chance, B.; Chance, B., *Methods Biochem. Anal.* **1954**, 1, 357-424
42. Sangster J. *J. Phys. Chem. Ref. Data.* **1989**, 18, 1111-1227.



## Chapter 3

### 3. Bienzyme-Polymer-Graphene Oxide Quaternary Hybrid Biocatalysts: Efficient Substrate Channeling at Chemically and Thermally Denaturing Conditions

#### 3.1 Abstract

An example of a highly stable and functional bienzyme-polymer conjugate triad assembled on a topologically orthogonal support, layered graphene oxide (GO), is reported here. Glucose oxidase (GOx) and Horseradish Peroxidase (HRP) catalytic dyad were used as the model system for cascade biocatalysis. Poly (Acrylic Acid) (PAA) was used to covalently conjugate these enzymes and then the conjugate has been subsequently adsorbed on to GO. The resultant nano-biocatalysts are represented as GOx-HRP-PAA/GO. Their morphology and structural characteristics were examined by transmission electron microscopy (TEM), agarose gel electrophoresis, circular dichroism (CD) and zeta potential. These robust conjugates remarkably functioned as active catalysts under biologically challenging conditions such as extreme pH's, high temperature (65°C) and in the presence of a chemical denaturant. In one example, GOx-HRP-PAA/GO presented doubling of the  $K_{cat}$  (TON) ( $68 \times 10^{-2} \text{ s}^{-1}$ ) at pH 7.0 and room temperature, when compared to the corresponding physical mixture of GOx/HRP ( $32 \times 10^{-2} \text{ s}^{-1}$ ) under similar conditions. In another case, at 65°C, GOx-HRP-PAA/GO displayed ~120% specific activity, whereas GOx/HRP showed only 16% of its original activity. At pH 2.0 and in the presence of 4.0 mM SDS as the denaturant, GOx-HRP-PAA/GO presented greater than 100% specific activity,

while GOx/HRP was completely deactivated under these conditions. Thus, we combined two concepts, enzyme-polymer conjugation followed by adsorption on to a 2D nanolayered material to obtain enhanced substrate channeling and excellent enzyme stability under challenging conditions. These features have never been attained by either traditional enzyme-polymer conjugates or enzyme-GO hybrids. This, general, modular and powerful approach may also be used to produce environmentally benign, biologically compatible (edible) and efficient cascade biocatalysts.

### **3.2 Introduction**

In our quest to design and stabilize enzyme cascade dyads, we demonstrated high temperature and pH stability of a new bienzyme catalytic quaternary hybrid assembly prepared by conjugation of the two enzymes with a polymer followed by adsorption onto nanoplates of graphene oxide (GO). Glucose oxidase (GOx) and Horseradish Peroxidase (HRP) were used as model enzymes and Poly (Acrylic Acid) (PAA) as the model polymer to tether the two enzymes within a network to function as an enzyme cascade dyad, Scheme 3.1, wherein hydrogen peroxide generated by GOx is used to oxidize a phenolic substrate by HRP.

GOx and HRP are industrial enzymes. GOx is used in food and baking industry. Whereas, HRP has potential uses in wastewater treatment.<sup>1,2</sup> GOx is also widely used for glucose sensing.<sup>3</sup> GOx/HRP redox couple is integrated within glucose biosensors to convert chemical signal (glucose) into an electrical signal, which can be conveniently registered.<sup>4</sup> Furthermore, HRP coupled with other enzymes and antibodies is widely used in ELISA bioassays.<sup>5</sup> However, the problem is that GOx

and HRP get destabilized at temperatures greater than 50° C and have a narrow pH range (4.5-6) for retention of catalytic activity.<sup>2,6,7,8</sup> Thus, numerous methods to stabilize GOx and HRP to keep them active at biologically challenging conditions were developed. These methods include adsorption onto enzyme-polymer nanoparticles,<sup>9</sup> use of additives,<sup>10,11</sup> by silanization,<sup>12</sup> and enzymes based stabilizers.<sup>13</sup> We recently reported that enzyme-PAA conjugates added attractive features to the enzymes such as proteases (trypsin) and inhibitor ( $\text{Cu}^{2+}$ ) resistance, which rendered them stable at 85-90 °C and improved shelf life (10 weeks). In this example, PAA also helped to protect catalase, a model enzyme, against heat, inhibitors and proteases.<sup>14</sup> Many examples in literature report single enzyme systems.<sup>15,16</sup> However, applications in biofuel cells and bioassay require multi-step enzyme cascade reactions.<sup>17</sup> Thus there is great need and substantial challenge for the stabilization of multi-enzyme nanobiocatalysts which is a currently unmet challenge. Stabilized and catalytically active multi-enzyme nanobiocatalysts will not only enhance the productivity but will also reduce the cost of enzyme-catalyzed bioprocesses.<sup>18</sup>

Polymer-graphene oxide (polymer-GO) nanocomposites are a new platform to stabilize multiple enzymes on GO sheets and thus enhance their function and biological applications.<sup>19,20</sup> For example, GO has been conjugated covalently to polyethylene glycol and then biologically-relevant enzymes were assembled and delivered successfully to cells.<sup>21</sup> In another case, these types of hybrid materials were successfully used for targeted drug delivery systems where enzymes

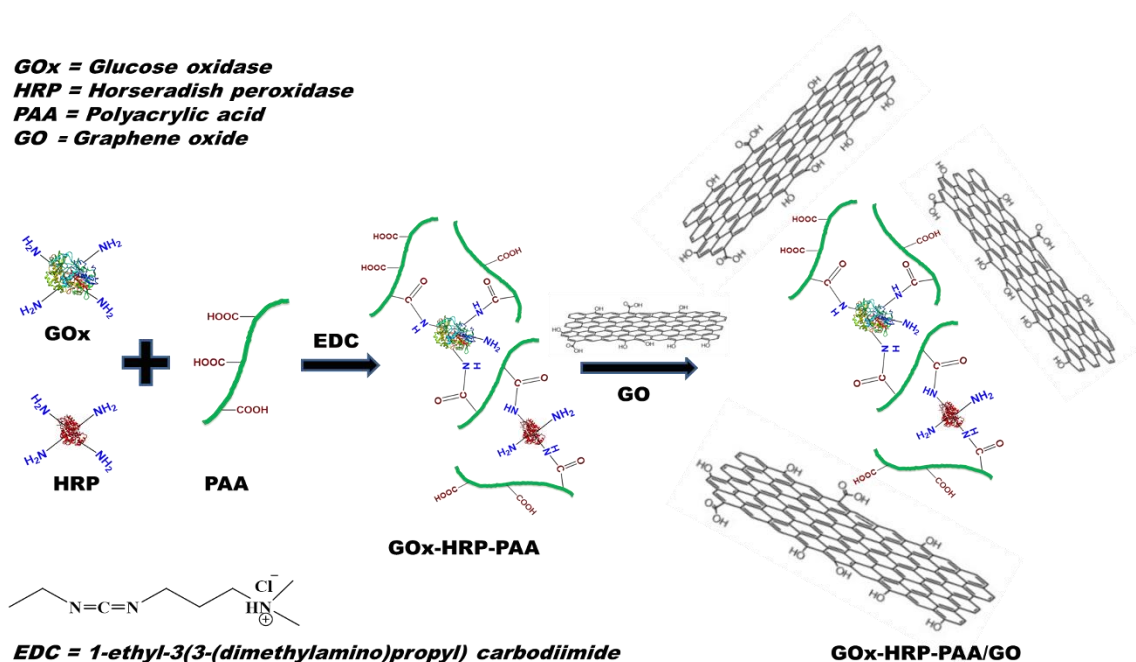
retained structure and the biocatalyst was not released at low pH in stomach but released effectively at higher pH in the intestine.<sup>22</sup>

When enzymes were non-covalently assembled on GO, structure denaturation and reduced activity was noted.<sup>23</sup> To address these issues, in our lab, an enzyme was conjugated with GO by coating its surface with sticky enzyme glues and the enzyme activity was retained.<sup>24</sup> Similarly, stabilization of enzymes at high temperatures and in organic solvents was attained by intercalating enzymes between the layers of zirconium phosphate,<sup>25</sup> biophilized GO or by covalent attachment to PAA.<sup>26</sup> However, the synergetic effect of conjugation and assembly, whereby the enzyme-polymer conjugate is further protected by GO nanosheets, is expected to further enhance the protective effects of both the host materials, and this concept has never been tested. In this report, bienzyme protection using topologically distinct host materials is tested for the first time. These unique bienzyme dual-hybrid materials could be more functional than single enzyme protected by a single host material. PAA shielded the enzymes from denaturation-induced aggregation due to charge repulsion between the polymer chains.<sup>14</sup> Subsequent assembly of the polymer-enzyme conjugate on GO sheets could further reduce the conformational entropy of the enzyme denatured state and thereby providing improved thermodynamic stability.<sup>27</sup> Note that GO can also protect the encased enzymes from inhibitors and proteases.

Bienzyme catalytic cascades are used in biosensors<sup>28</sup> and biocatalysis.<sup>29</sup> However, stability and activity of the enzyme cascade system has been a major concern. For example, GOx and HRP were immobilized within macroporous silica

foam, however, stability of the conjugate at lower pH's (<5.5) and at high temperatures have not been addressed.<sup>30</sup> To use GOx and HRP in cascade reactions for biofuel cell applications, the enzymes need to be stabilized to perform under a variety of pH's and temperatures. Thus, in the current work, we designed and stabilized bienzyme hybrid materials, for the first time, with topologically distinct host materials and achieved remarkable pH, chemical denaturant as well as high temperature stability of the enzymes. The bienzyme conjugate and the dual-hybrid system are presented in Scheme 3.1, where GOx and HRP are shown and green line is represented as PAA. GOx and HRP are conjugated to PAA by EDC chemistry to form GOx-HRP-PAA conjugate which then is assembled onto the GO sheets to form GOx-HRP-PAA/GO cascade biohybrid. The GOx-HRP-PAA/GO is viewed as a nanogel of GOx-HRP-PAA assembled onto the GO sheets. This modular concept may be extended to produce environmentally benign, biologically compatible (edible) and efficient biocatalysts for the production of energy/materials as alternatives to fossil fuel-based energy/products.

**GOx = Glucose oxidase**  
**HRP = Horseradish peroxidase**  
**PAA = Polyacrylic acid**  
**GO = Graphene oxide**

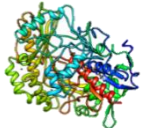



**Scheme 3.1:** Synthesis of GOx-HRP-PAA/GO conjugate using GOx and HRP bienzyme and PAA and GO. HRP and GOx structures are shown above; PAA as green line and GO is represented as a sheet. EDC chemistry is used to crosslink amine groups on the enzymes with the polymer COOH groups.

### 3.3 Experimental

**3.3.1 Materials.** PAA ( $M_v = 450,000$  g/mol where  $M_v$  indicated viscosity average molecular weight), GOx, hydrogen peroxide ( $H_2O_2$ ), o-methoxyphenol, EDC, Sodium Dodecyl Sulfate (SDS),  $H_2SO_4$ , HCl,  $KMnO_4$ , uranyl acetate and graphite were purchased from Sigma-Aldrich (St. Louis, MO). HRP was purchased from Calzyme Laboratories INC, San Luis Obispo, CA, Agarose was purchased from Molecular Biology Hoefer Inc., Allison, MA.

**3.3.2 Synthesis of GO.** Graphene oxide was prepared from graphite using modified Hummers method.<sup>31</sup> Graphite (1.0 g) was dispersed in conc.  $H_2SO_4$  (30 mL) and placed in an ice bath and  $KMnO_4$  (3.0 g) was added in portions with constant stirring. This mixture heated to 50 °C for 3 hr followed by addition of 70 mL distilled water to quench the reaction. After 15 minutes, another 300 mL of distilled water and 30 %  $H_2O_2$  (20 mL) was added and the color changed to bright yellow. The mixture was initially washed with 10% HCl for 3 times followed by washing with distilled water until neutral pH was attained. The resulting graphitic oxide powder was sonicated in buffer solution (10 mM Sodium phosphate at pH 7.0) for 45 minutes and centrifuged (4000 rpm for 1 hr) to remove any unexfoliated graphite. GO was characterized using Raman spectroscopy, XRD and Zeta potential studies as previously reported.<sup>24</sup> The supernatant solution was used for further studies. Key properties of GOx<sup>32</sup> and HRP<sup>33</sup> are shown in chart 3.1.

Enzyme	Molecular weight (kDa)	Total number of residues	Number of Lys residues
GOx			
	160	1166	30
HRP			
	40	306	6

**Chart 3.1:** Key properties of glucose oxidase (GOx) and Horseradish Peroxidase (HRP).



### **3.3.3 Synthesis of Bienzyme-PAA and Bienzyme-PAA/GO conjugates.**

PAA stock solution (2.8 mL, 2 wt % ) was added to 1.7 mL EDC (130 mg/mL) in 10 mM, pH 7.4 PB such that mole ratio of –COOH of PAA and EDC was maintained at 1:1.5. GOx (800  $\mu$ L, 15 mg/mL) and HRP (540  $\mu$ L, 6 mg/mL) were added drop wise and stirred for 6 hr. The conjugation was achieved by covalent attachment of –COOH's of PAA and Lys residues from GOx and HRP (total number of Lys residues are given in Chart 3.1 for GOx and HRP). This conjugate is referred as GOx-HRP-PAA. Similarly, conjugate was synthesized with GOx, without HRP and labeled as GOx-PAA. GOx-HRP-PAA was adsorbed onto GO (0.7 mg/mL) such that weight ratio of total enzyme to GO was 1:1.5 and 1:2. These conjugates then are labeled as GOx-HRP-PAA/GO(1:1.5) and GOx-HRP-PAA/GO(1:2), respectively. All conjugates were dialyzed against PB pH 7.4 for 6 hr for three cycles to remove any unreacted EDC or byproduct formed after coupling using 8 kDa Membrane.

**3.3.4 Zeta Potential Studies.** The charge on each sample was measured using Brookhaven zeta plus zeta potential analyzer (Brookhaven Instruments Corporation, Holtsville, NY) by laser doppler velocimetry. In these measurements, 1.5 mL sample with 0.1 mM equivalent of GOx and HRP were charged into 3 mL polystyrene cuvettes. Smoluchowski fit by the software and matching electrophoretic mobility technique was used to obtain the zeta potential values in mV.

**3.3.5 Agarose Gel Electrophoresis.** Agarose gel electrophoresis was performed using horizontal gel electrophoresis apparatus by Gibco Model 200, Life

Technologies Inc., Grand Island NY. Molecular biology grade agarose (0.5% w/v) was heated in a solution of pH 6, 40 mM Tris acetate buffer and left to gel in the apparatus. After the gel was formed, the samples were mixed with loading buffer containing 50% v/v glycerol and 0.01% m/v bromophenol blue and then loaded into the wells, followed by electrophoresis for 40 mins at 100 V. The gel was subsequently stained using 10% v/v acetic acid and 0.02% m/v coomassie blue overnight, and then destained with 10% v/v acetic acid overnight, photographed and reported.

**3.3.6 Circular Dichroism (CD) studies.** Secondary structure of GOx and HRP native bi-enzyme and conjugates was evaluated using CD study. Structure of enzymes was evaluated in the ultraviolet (UV) range using Jasco 710 spectropolarimeter. UV-CD spectrum for each sample was measured from 195 nm to 250 nm.

**3.3.7 Transmission Electron Microscopy (TEM).** Morphologies of Bienzyme physical mixture, Bienzyme-PAA conjugate and Bienzyme-PAA/GO conjugate hybrid were evaluated using tecnai T 12 TEM operating at an accelerating voltage of 120 kV and at step 3. Aqueous samples were prepared such that concentration of GOx and HRP was 10 nM each. Then this solution was drop casted on copper TEM grid covered with fomvar film. Excess solution was removed by blotting, dried and stained with 0.5 wt % of uranyl acetate, dried for 20 mins and imaged.

**3.3.8 Activity Studies.** Activities were measured using GOx and HRP enzyme colorimetric assays where GOx converts glucose into gluconolactone and  $H_2O_2$ , and HRP uses the  $H_2O_2$  formed and o-methoxyphenol to form oxidation product

with  $\lambda_{\max}$  at 470 nm. The absorbance spectrum at 470 nm was monitored over the period of 1 minute and first 20-40 seconds were used to compute the initial rate. Initial rate of GOx-HRP native bienzyme system in 10 mM, pH 7.4 phosphate buffer (PB) at 25°C was referenced at 100% and used as reference to calculate all the specific activities. Specific activities were calculated for 1  $\mu$ M of GOx and HRP each. While doing activity studies, cuvette contained 1  $\mu$ M each of GOx and HRP in native as well as bienzyme conjugate forms, 1.125 mM o-methoxyphenol, 0.3 mM glucose and remaining solution contained appropriate buffer (10 mM each of pH 2.5 glycine/HCl, pH 4 Citrate, pH 5.5 acetate and pH 7.4 PB). In case of single enzyme conjugates and hybrids, HRP was added at the time of activity studies and are used as controls for comparison purposes.

#### **3.3.9 Activity study with denaturant (SDS) and at high temperature (65°C).**

Activity assay was performed with 4 mM SDS concentration in the cuvette in a mixture of 10 mM each of pH 2.5 glycine/HCl, pH 4 Citrate, pH 5.5 acetate and pH 7.4 PB. For each assay, the cuvette was incubated with appropriate buffer and 4 mM SDS for 10-15 mins before performing the activity studies. All initial rates were compared to native bienzyme system in 10 mM, pH 7.4 PB and specific activity was computed in each case. For high temperature activity studies, cuvette was incubated at 65°C in 10 mM, pH 7.4 PB and initial rates were obtained. Then specific activity was calculated as discussed above.

**3.3.10 Kinetics Studies.** Kinetic constants such as  $K_M$  and  $V_{\max}$  were calculated for bienzyme native system and conjugates by carrying out the activity study with varying concentrations of glucose (0.15 mM to 0.75 mM) using UV

spectrophotometer by Agilent Technologies. Then Lineweaver-Burk plots were prepared using the initial rates of samples. In each of these experiments, GOx and HRP concentrations were maintained at 0.5  $\mu$ M and o-methoxyphenol at 1.125 mM. Lineweaver-Burk plots comprised of inverse or initial rate vs inverse of substrate (glucose) concentration were developed. From these plots, Michaelis constant ( $K_M$ ) and maximum velocity ( $V_{max}$ ) for the bienzyme system was calculated.

### 3.4 Results

In this study, GOx and HRP were conjugated to PAA together covalently and then adsorbed on to GO using non-covalent interactions resulting in bienzyme conjugate hybrids. GOx and HRP were physically mixed together using only non-covalent interactions and labeled as GOx/HRP. For comparison with the bienzyme system, several control samples were also synthesized. Synthesis of the conjugates is discussed briefly here.

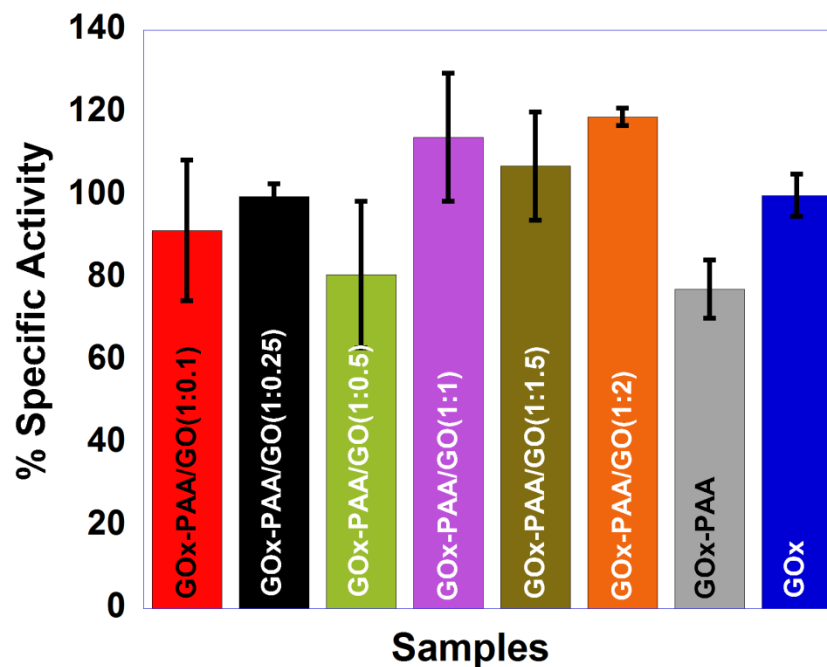
**3.4.1 Synthesis.** To synthesize GOx-HRP-PAA (bienzyme conjugate) and GOx-PAA (single-enzyme conjugate), EDC chemistry was used and all the syntheses were carried out in pH 7.4 phosphate buffer. In case of GOx-PAA and GOx-HRP-PAA, total enzymes to PAA mole ratio were maintained at 1.2:1. The effect of GO in controlling the enzymatic activity of GOx was assayed at increasing concentrations of GO (mass percent) in the composite from 0 % to 31% (7 points), indicated optimum relative specific activity (~ 120 %) at higher GO concentrations (Figure 3.1). Thus in this study, we followed the optimized mass percent of GO (25 and 31%) in all the hybrids. Final mass composition of all individual components

(in about 100 mg scale) is presented in Table 3.1. Agarose gel electrophoresis and zeta potential studies were carried out after removing excess reagents by dialysis (25 kDa cellulose membrane) for 3 times for 6 hr each and used to confirm the conjugation of the PAA and GO to enzyme and enzymes-PAA conjugate, respectively. The data is presented below.

**3.4.2 Agarose Gel Electrophoresis.** Conjugation of PAA to the enzymes and further adsorption to GO was characterized using agarose gel electrophoresis. Covalent conjugation of GOx and/or HRP to PAA was confirmed using agarose gel electrophoresis. The agarose gel is shown in Figure 3.2A. Lane 1 was loaded with GOx-HRP-PAA, lane 2 with GOx-PAA, lane 3 with GOx and lane 4 with HRP. The covalent conjugation of PAA to enzymes should increase the negative charge on conjugates and ultimately increase the electrophoretic mobilities. Conversely, increase in molecular size as a result of polymer conjugation decreases the mobility of the conjugates, and thus streaking rather than discrete entities in case of GOx-HRP-PAA and GOx-PAA was noted. This suggests the formation of enzymes-polymer nanogels<sup>26</sup> with variable molecular weight. HRP was not observed in the gel due to its isoenzyme features with isoelectric points ranging from 3.0 to 9.0.<sup>34</sup> This resulted in HRP spreading to both sides of the agarose gel and was invisible after staining. Control experiments with GOx/PAA and GOx/HRP/PAA, physical mixtures and single and bienzyme conjugate hybrids (1:2) and the agarose gel electrophoresis are displayed in Figure 3.3 (A). The physical mixtures did not show any mobility relative to GOx. GOx-HRP-PAA/GO

conjugates showed similar mobility as of GOx-HRP-PAA, indicating non-covalent conjugation of GOx-HRP-PAA to GO.

**3.4.3 Zeta Potential Studies.** Successful modification of enzymes chemically by PAA and adsorption onto GO was followed in solution phase using zeta potential measurements. The charge and electrophoretic motilities before and after conjugation was established by zeta potential measurements, Figure 3.2B. Conjugation of enzyme(s) to PAA covalently (single and bienzyme conjugates) and GO non-covalently (single and bienzyme conjugate hybrids) should result in increased negative charge on the conjugate due to  $\text{-COOH}$  groups present on PAA and GO. At pH 7.0, zeta potential of bienzyme (-1.1 mV, blue bar) decreased drastically when conjugated to PAA (bienzyme conjugate) and this can be attributed to free  $\text{-COOH}$  ( $\text{pK}_a = 4.2$ )<sup>35</sup> groups present on PAA (-31.7 mV, black bar). Further physical modification with GO was confirmed as the zeta potential dropped down to -39.5 mV (green) and -43.8 mV (red) for bienzyme conjugate hybrids with (1:1.5) and (1:2) ratio of total enzymes to GO (w/w), respectively. Similar results were also noted in the case of single enzyme conjugates where zeta potential of -7.1 mV (GOx-PAA) (grey) was dropped to -37.2 (orange) and -30.8 mV (pink) respectively for single-enzyme conjugate hybrids with ratio of (1:1.5) and (1:2). Zeta potential of PAA and GO was found to be -46.0 and -37.9 mV, respectively, (Figure 3.3 B).

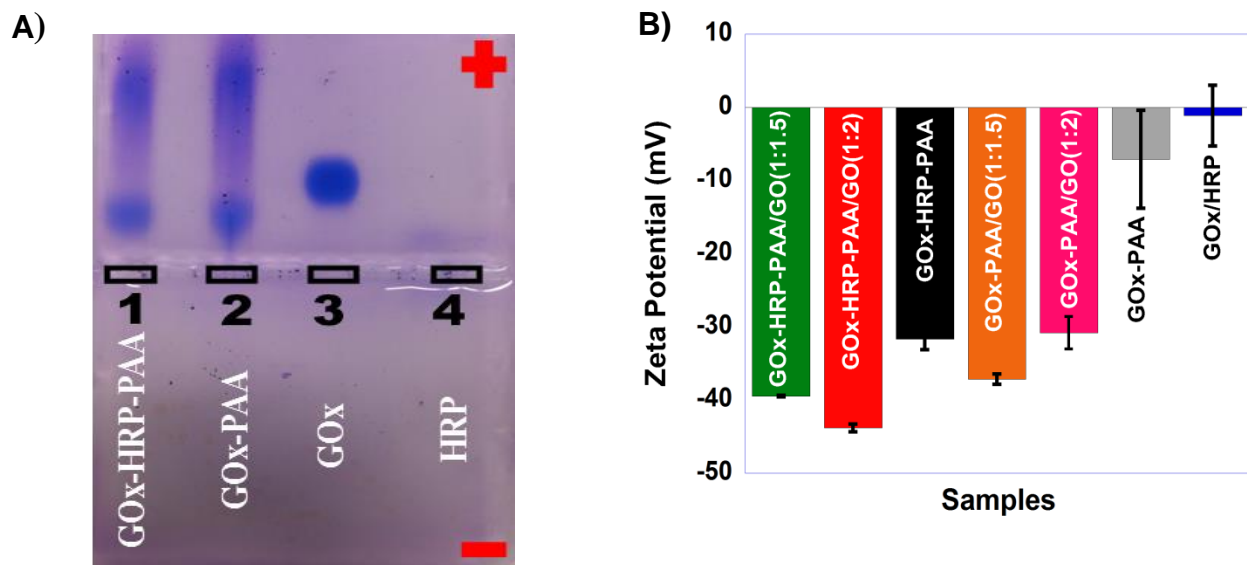


**Figure 3.1.** Activity study at pH 7.4 (phosphate buffer) for GOx-PAA/GO(1:0.1) (green), GOx-PAA/GO(1:0.25) (blue), GOx-PAA/GO(1:0.5) (brown), GOx-PAA/GO(1:1) (orange), GOx-PAA/GO (1:1.5) (yellow) and GOx-PAA/GO(1:2) (light blue), GOx-PAA (black), and GOx (red). Activity study was done at room temperature and product (dimer of o- methoxyphenol) formation was monitored at 470 nm.

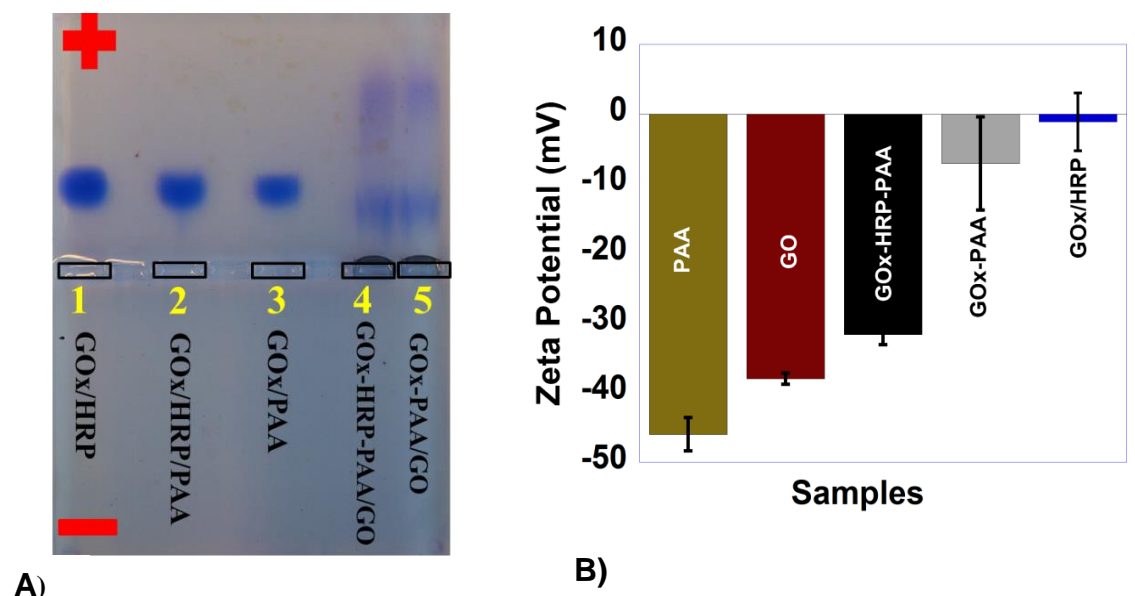
Samples	Mass percent				Description
	GOx	HRP	PAA	GO	
<b>GOx-HRP-PAA/GO(1:1.5)</b>	13	3.3	58	25	Bienzyme conjugate hybrids
<b>GOx-HRP-PAA/GO(1:2)</b>	12	3.0	54	31	
<b>GOx-HRP-PAA</b>	18	4.5	78	0	Bienzyme conjugate
<b>GOx-PAA/GO(1:1.5)</b>	17	0	58	25	Single enzyme conjugate hybrids
<b>GOx-PAA/GO(1:2)</b>	15	0	54	31	
<b>GOx-PAA</b>	22	0	78	0	Single enzyme conjugate
<b>GOx/HRP</b>	80	20	0	0	Unbound Bienzyme

**Table 3.1.** Different conjugates and the mass percent of enzymes, PAA and GO used for synthesis.



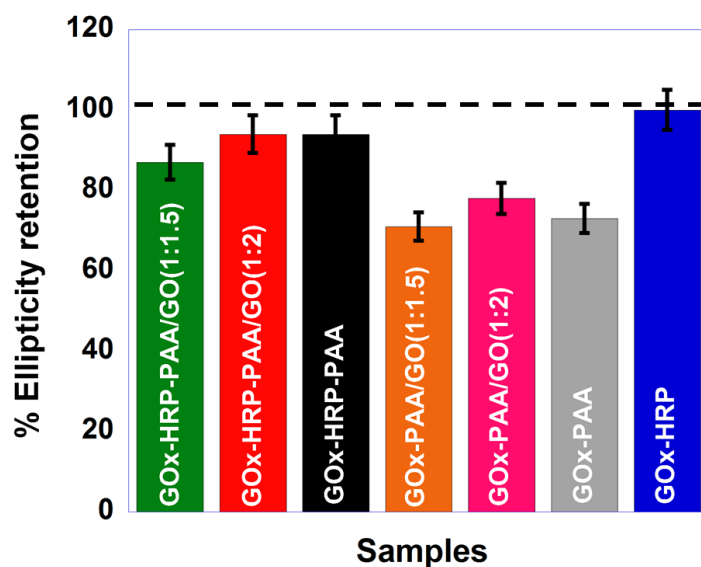


**Figure 3.2.** A) Agarose gel electrophoresis with GOx-HRP-PAA loaded in lane 1, GOx-PAA in lane 2, GOx in lane 3 and HRP in lane 4. Agarose gel electrophoresis was done at pH 6.0, 40 mM Tris acetate buffer. HRP did not get stained well due to a mixture of enzymes which smeared in the lane. B) Zeta potential of GOx-HRP-PAA/GO (1:1.5) (green), GOx-HRP-PAA/GO (1:2) (red), GOx-HRP-PAA (black), GOx-PAA/GO (1:1.5) (brown) GOx-PAA/GO (1:2) (pink), GOx-PAA (grey) and GOx/HRP (blue) were done at 25°C. All measurements were performed in 10 mM sodium phosphate buffer at pH 7.0.

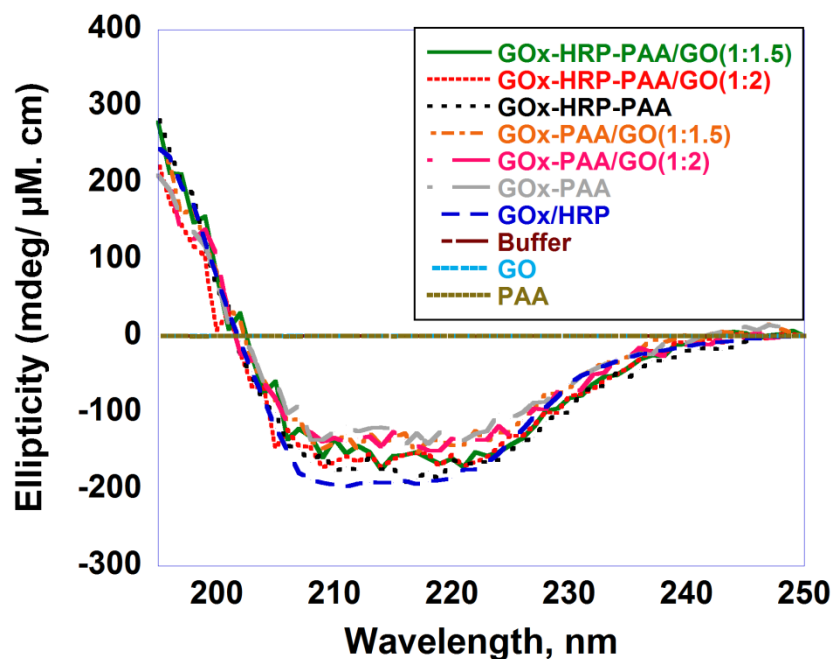


**Figure 3.3** (A) Agarose gel electrophoresis of GOx/HRP (lane 1), GOx/HRP/PAA (lane 2), GOx/PAA (lane 3), GOx-HRP-PAA/GO (1:2) (lane 4) and GOx-PAA/GO (1:2) (lane 5). GOx/HRP/PAA and GOx/PAA are physical mixtures, synthesized without EDC and lane 4 contains single and bienzyme conjugate hybrids. Agarose gel was done at pH 6 in 40 mM Tris acetate buffer. (B) Zeta potential of PAA (brown), GO (maroon), GOx-HRP-PAA (black), GOx-PAA (grey) and GOx/HRP (blue). GO and PAA were used as control samples. Zeta potential was measured at pH 7.4 in 10 mM PB. For agarose gel electrophoresis and Zeta potential studies, protein equivalent of 3-4  $\mu$ M was used for analysis.

**3.4.4 Circular Dichroism (CD) studies.** The change in enzymes' secondary structure after each modification was examined using far-UV CD studies. The secondary structures and relative % ellipticity of the bienzyme, PAA conjugates, GO conjugates and conjugate hybrids were analyzed using far UV circular dichroism (CD) studies. It is expected that after conjugation with PAA and GO, GOx/HRP or GOx were supposed to lose its relative % ellipticity due to the strain imposed on its secondary structure from covalent conjugation with PAA and non-covalent conjugation with GO.<sup>24</sup> Figure 3.4 presents the comparison of the percent retention of the ellipticity of bienzyme and that of their respective PAA and/or GO conjugates. These studies were carried out in PB pH 7.4, 10 mM buffer; in this Figure ellipticity at 222 nm of GOx/HRP is referenced as 100%. The CD spectra of the unmodified bienzyme, single and bienzyme conjugates, and corresponding GO conjugate hybrids, bare GO and PAA are shown in Figure 3.5. Spectra of bare GO and PAA confirms absence of scattering and structure from these samples, (Figure 3.5).

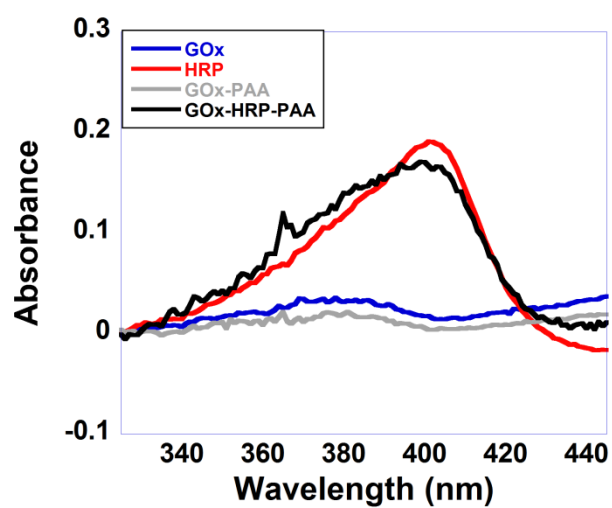


**Figure 3.4.** Comparison of the CD secondary structure retention in PB pH 7.4, 10 mM of GOx-HRP-PAA/GO(1:1.5) (green), GOx-HRP-PAA/GO(1:2) (red), GOx-HRP-PAA (black), GOx-PAA/GO(1:1.5) (orange), GOx-PAA/GO(1:2) (pink), GOx-PAA (grey), and GOx/HRP (blue). Ellipticity at 222 nm in mdeg/  $\mu$ M. cm is used to calculate % ellipticity retention and ellipticity at 222 nm of GOx/HRP is referenced at 100 nm.

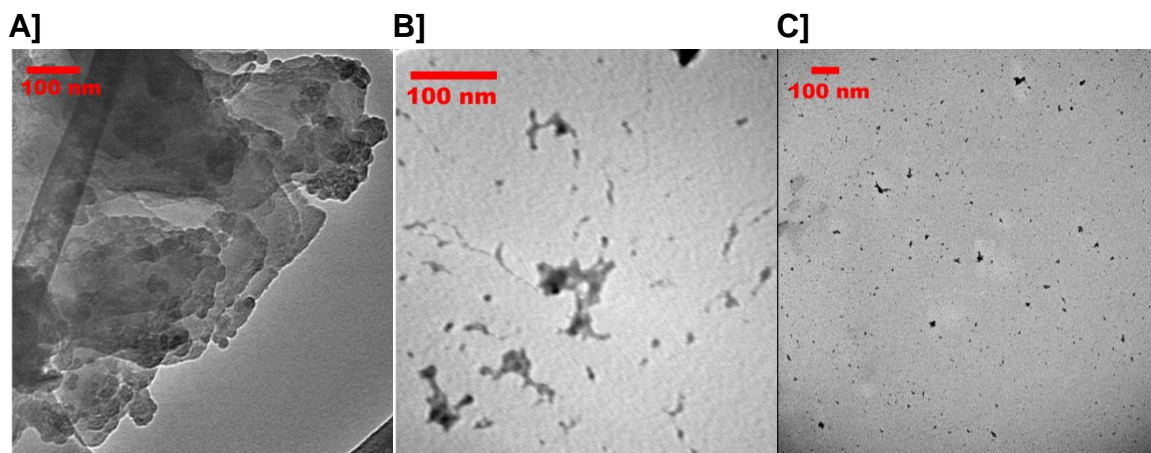


**Figure 3.5.** Circular Dichroism (CD) spectra of GOx-HRP-PAA/GO(1:1.5) (green), GOx-HRP-PAA/GO(1:2) (red), GOx-HRP-PAA (black), GOx-PAA/GO(1:1.5) (orange), GOx-PAA/GO(1:2) (purple), GOx-PAA (grey, GOx-HRP (blue), buffer (maroon), GO (light blue) and PAA (dark brown). CD spectra were monitored from 190-250 nm in PB pH 7.4, 10 mM. For CD experiments protein concentration of 1  $\mu$ M, for each sample, and 0.05 cm cuvette was used.

From Figure 3.4, conjugation of PAA to the enzymes resulted in decreased % ellipticity retention. Blue bar in Figure 3.4 indicates unmodified GOx/HRP which is referenced to 100% CD ellipticity retention. GOx-HRP-PAA/GO (1:1.5) (green bar) and (1:2) (red bar) presented 87% and 94% ellipticity retention and GOx-PAA/GO (1:1.5) (orange bar) and (1:2) (pink bar) showed 71% and 78 % of the same. This % ellipticity of the single and bienzyme conjugate hybrids was lower than single or bienzyme conjugate counterparts. GOx-HRP-PAA (black bar) showed 94% and GOx-PAA (grey bar) showed 73% ellipticity retention. Also, the presence of Fe in HRP soret environment and inside PAA conjugate was confirmed using optical spectroscopy. For example, GOx-HRP-PAA and native HRP showed soret peak ~403 nm confirming the same. The samples were dialyzed to remove any free HRP using a membrane with a cut-off size of 25 kDa. The plot can be found in Figure 3.6 (concentration of HRP was normalized to 2  $\mu$ M). Soret optical spectra for bienzyme conjugate hybrid showed extensive scattering due to GO and are not provided.



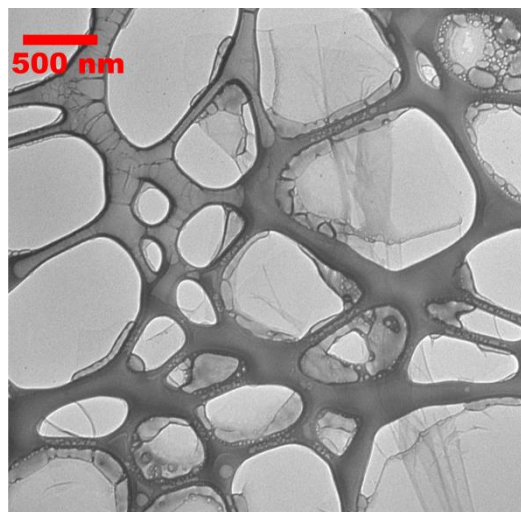
**Figure 3.6.** Optical spectra at 403 nm for GOx (blue), HRP (red), GOx-PAA (grey) and GOx-HRP-PAA (black) to test solet environment.



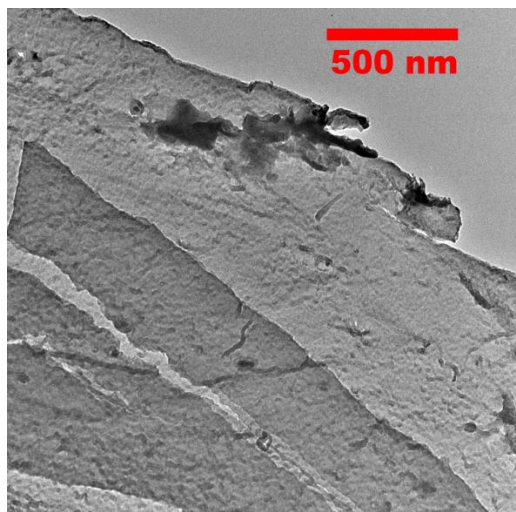
**Figure 3.7.** TEM micrographs of A) GOx-HRP-PAA/GO (1:2), B) GOx-HRP-PAA and C) GOx/HRP. All samples were stained with 0.5% w/w uranyl acetate. GOx-HRP-PAA/GO (1:2) showed nanogels assembled on GO sheets, GOx-HRP-PAA showed nanogels and GOx/HRP showed aggregated particles.



**3.4.5 Transmission Electron Microscopy (TEM).** Morphology of collapsed structure of GOx-HRP-PAA/GO (1:2), GOx-HRP-PAA and GOx/HRP conjugates was examined using TEM. As seen from Figure 3.7A, micrograph of GOx-HRP-PAA/GO (1:2) showed crosslinked enzymes polymer networks assembled on graphene basal plane. Figure 3.7B, showed nanogel morphology for GOx-HRP-PAA, whereas, Figure 3.7C displayed aggregated enzyme particles of GOx/HRP. TEM micrograph of bare GO, Figure 3.8, displayed smoother texture compared to GOx-HRP-PAA/GO (1:2). This suggests successful physical adsorption of GOx-HRP-PAA nanogel onto GO.



A)



B)

**Figure 3.8.** TEM micrographs showing bare GO surface. Bare GO showed more crystalline character and hence smoother in appearance.

**3.4.6 Activity Studies.** GOx has a narrow range of optimal pH (pH 5-6) and HRP has optimal pH of 4.2 at which these enzymes show enzymatic activity.<sup>7,8</sup> The catalytic activity studies of single and bienzyme conjugates, hybrids and unmodified bienzyme were examined at biologically challenging conditions of pH (2.5-7.4), temperature (25 and 65°C) and denaturant concentration (4 mM of surfactants). Oxidase activity of GOx was monitored using glucose as a substrate.<sup>36</sup> Relative specific activity was calculated for each sample by using the initial rate of unmodified GOx activity at 25 °C in pH 7.4 phosphate buffer. These hybrid systems showed exceptional stability at diverse conditions, whereas unmodified enzymes showed negligible activity. In case of single enzyme conjugates and hybrids, HRP was added at the time of activity measurements and were used as controls for comparison only.

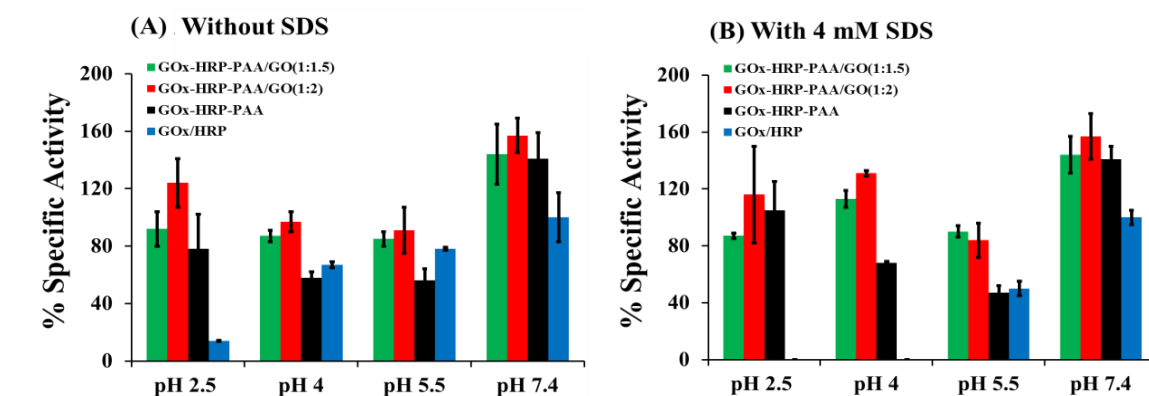
**3.4.6.1 Activity studies at room temperature and pH 7.4.** Benchmark activity measurements were performed using unbound bienzyme, conjugates and hybrids at room temperature and at pH 7.4. Under these conditions, GOx/HRP specific activity was referenced to 100% and this was used to standardize specific activities of all other samples, Figure 3.9A. The kinetic plots of all the conjugates and hybrids as well as GOx/HRP are presented in Figure 3.10. Accordingly, GOx-HRP-PAA/GO(1:1.5), GOx-HRP-PAA/GO(1:2) and GOx-HRP-PAA, showed 144, 157 and 141% activities, respectively. Evidently % specific activity of the PAA and subsequent GO conjugated to GOx/HRP were very high. This observation led us to investigate the robustness of our conjugates at severe conditions for wide range of applications as discussed in the next few sections.

**3.4.6.2 Activity studies at different pH's in presence and absence of a chemical denaturant.** The pH profile of the enzymatic activity of the bio-hybrids was tested in presence of SDS, a denaturant, which reduces the activity of the enzymes. Catalytic activities were established at pH 2.5, 4.0, 5.5 and 7.4 with and without SDS (4 mM).

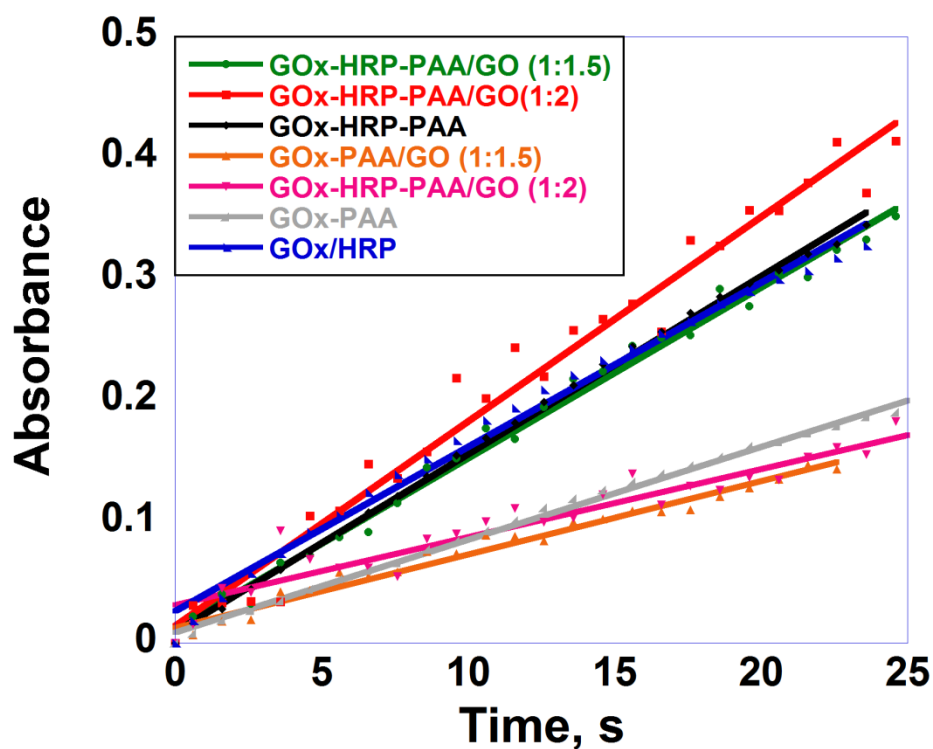
From Figure 3.9A, bienzyme conjugate hybrids activities were 85-95% at pH 2.5, 4.0 and 5.5 except in case of GOx-HRP-PAA/GO(1:2) at pH 2.5 where it showed high activity of 124%. In case of GOx-HRP-PAA, retained activity at pH 2.5 was 78% which was more than activity at pH 4.0 and 5.5 (~60%). Bienzyme showed 14% retention in activity at pH 2.5, which increased with pH and was 100% at pH 7.4. In presence of 4.0 mM SDS, (Figure 3.9B) GOx-HRP-PAA and GOx-HRP-PAA/GO (1:1.5) and (1:2) conjugates and conjugate hybrids, showed 47, 90 and 84% specific activities at pH 5.5, respectively. The highest activity was observed with GOx-HRP-PAA/GO (1:2) with or without SDS. At pH 5.5 single enzyme conjugates and hybrids, GOx-PAA and GOx-PAA/GO showed comparable activities to bienzyme conjugate hybrids (Figure 3.11). In sharp contrast, with 4.0 mM SDS and at lower pH's (2.5 and 4.0), unbound bienzyme showed negligible activity. At pH 7.4, the bienzyme showed 100% activity, which was double than that of its activity at pH 5.5 (50%).

We tested the recyclability of GOx-HRP-PAA/GO (1:2) and GOx-PAA/GO (1:2). Single enzyme conjugate hybrid failed to show any recyclability whereas bienzyme conjugate hybrid (GOx-HRP-PAA/GO (1:2)) showed recyclability up to two cycles in pH 2.5 and up to three cycles in pH 7.4 in absence of SDS. When

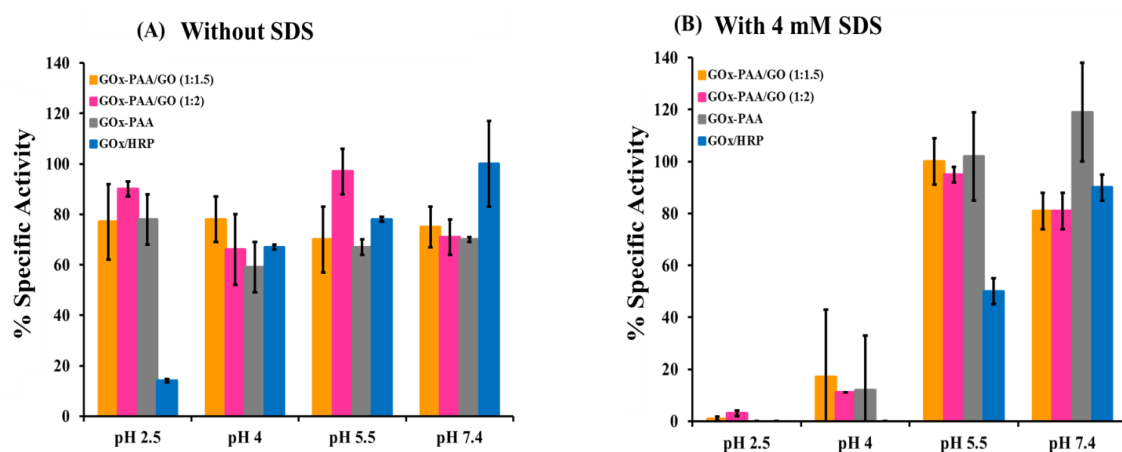
recyclability studies were performed in presence of 4 mM SDS, the bienzyme conjugate hybrid showed recyclability up to only one cycle at pH 2.5 and 7.4. Corresponding activity at each cycle can be found in Figure 3.12.



**Figure 3.9.** (A) Activity study as a function of increasing pH without SDS (B) Activity study at increasing pH's with 4.0 mM SDS (denaturant) – GOx-HRP-PAA/GO (1:1.5) (green), GOx-HRP-PAA/GO (1:2) (red), GOx-HRP-PAA (black) and GOx/HRP (blue). Activity of single enzyme GOx-PAA and GOx-PAA/GO (1:1.5) and (1:2) is presented in SI Figure S7. Initial activity of each sample (20-40 sec) was measured for each sample and compared to GOx/HRP which was referenced to 100%.

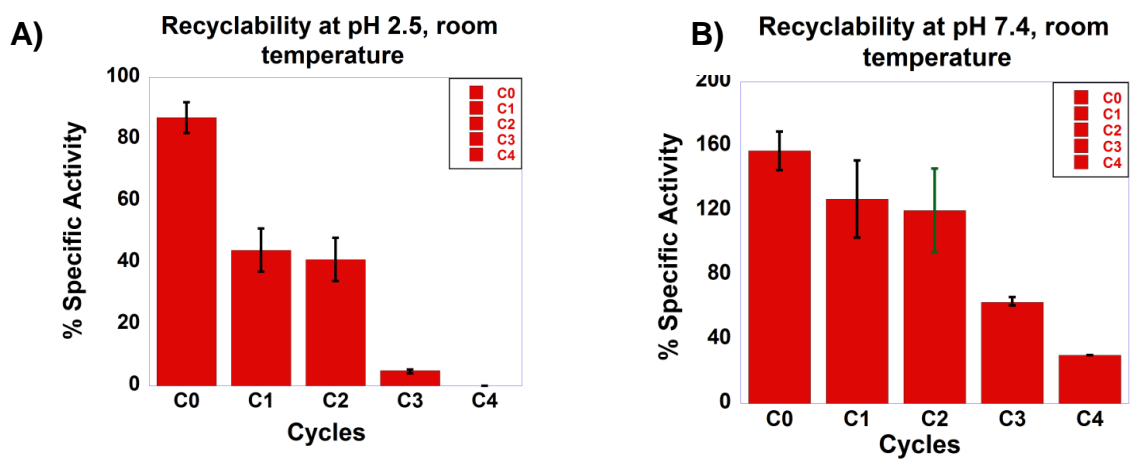


**Figure 3.10.** Kinetic traces of GOx-HRP-PAA/GO(1:1.5) (green), GOx-HRP-PAA/GO(1:2) (red), GOx-HRP-PAA (black), GOx-PAA/GO (1:1.5) (orange), GOx-PAA/GO (1:2) (pink), GOx-PAA (grey) and GOx/HRP (blue) in 10 mM , pH 7.4 PB. Activity was established using 1.125 mM o-methoxyphenol, 0.3 mM glucose and 1  $\mu$ M equivalent of each of GOx and HRP equivalents.



**Figure 3.11.** (A) Enzyme activities as a function of pH. (B) Enzyme activities as a function of pH, in the presence of added 4 mM SDS. GOx-PAA/GO(1:1.5) (orange), GOx-PAA/GO(1:2) (pink), GOx-PAA (grey) and GOx-HRP (blue). Activity studies were done in glycine hydrochloride buffer (pH 2.5), citrate buffer (pH 4), acetate buffer (pH 5.5) and phosphate buffer (pH 7.4).

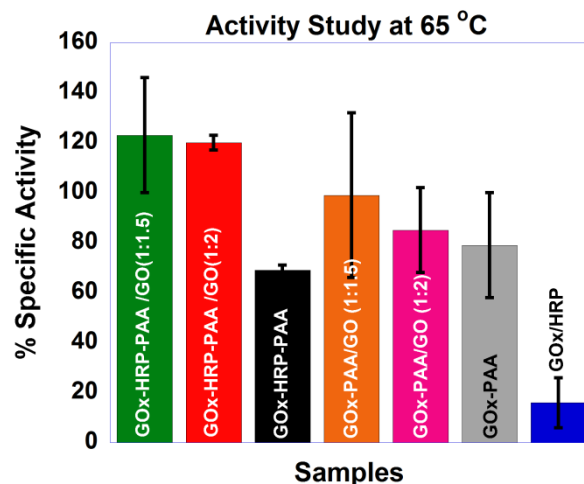




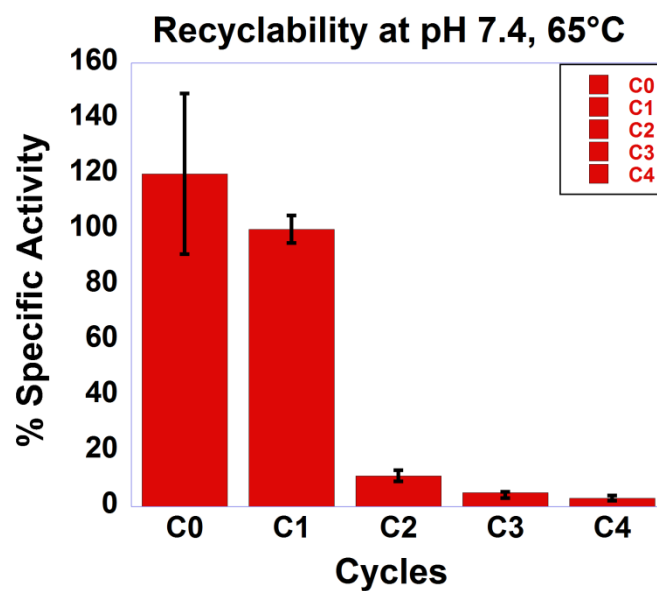
**Figure 3.12.** Recyclability study of GOx-HRP-PAA/ GO (1:2) A) at pH 2.5 and B) at pH 7.4 in absence of SDS and at room temperature. All the % specific activities are compared to GOx/HRP at room temperature at pH 7.4 reference point (100%).

**3.4.6.3 Activity studies at 65°C.** The optimal temperature for catalytic activity of GOx is ~60°C.<sup>2</sup> Therefore, activity studies were performed at 65°C to test the robustness and effectiveness of the bienzyme conjugates and hybrids and to evaluate the impact of GO on thermal stability of the conjugates. Figure 3.13 summarized the activity study plot of the GOx/HRP bienzyme and other conjugates and hybrids. The activity retention was calculated by using initial rate of free bienzyme at 25° C as the reference (100%). GOx-HRP-PAA/GO showed ~120% activity which was 40% higher than single enzyme conjugate as well as hybrids. GOx-PAA/GO conjugate hybrids showed 70-80% activity. GOx/HRP showed ~12% activity while bienzyme and single enzyme conjugates retained 60-80% activity.

To test the robustness of the bienzyme conjugate hybrid, recyclability studies were performed at 65°C in pH 7.4 using GOx-HRP-PAA/GO (1:2). It showed recyclability up to one cycle. Recyclability study graph can be found in Figure 3.14.



**Figure 3.13.** Activity study at 65°C for the samples of dual and single enzyme systems. % Specific activity of GOx-HRP-PAA/GO(1:1.5) (green), GOx-HRP-PAA/GO (1:2) (red), GOx-HRP-PAA (black), GOx-PAA/GO(1:1.5) (orange), GOx-PAA/GO (1:2) (pink) GOx-PAA (grey) and GOx/HRP (blue), were compared to 100% specific activity of GOx/HRP at room temperature and at pH 7.4.



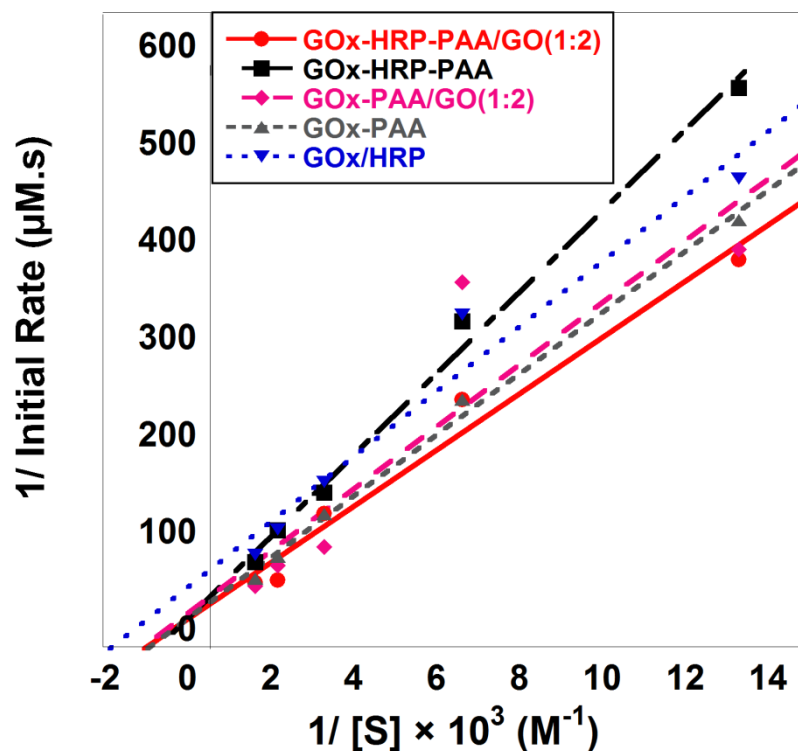
**Figure 3.14.** Recyclability study of GOx-HRP-PAA/GO (1:2) at 65° C in pH 7.4.

Bienzyme conjugate hybrid showed recyclability up to one cycle.

**3.4.7 Kinetics studies.** The enzymatic catalytic rates were computed using Lineweaver-Burk plots, which were assembled by plotting  $1/\text{initial rate}$  vs  $1/\text{substrate concentration}$  and Michaelis-Menton constant ( $K_M$ ) and maximum catalytic rate ( $V_{\max}$ ) were calculated. The inverse of Y-intercept and negative inverse of X-intercept of the Lineweaver-Burk plot were used to determine the  $V_{\max}$  and  $K_M$ , respectively. Higher  $K_M$  indicates lower affinity of the substrate towards the enzyme and vice versa. These studies helped investigate the catalytic efficiency and  $K_{\text{cat}}$  (catalytic rate constant) of each system. In case of biological catalysts such as enzymes and modified enzymes catalytic turnover numbers are presented in terms of  $K_{\text{cat}}$  values.<sup>37</sup> In these studies, increasing amounts of glucose was used and initial rates were calculated. Lineweaver-Burk plots (GOx-HRP-PAA/GO(1:2), GOx-PAA/GO(1:2), GOx-HRP-PAA, GOx-PAA and GOx/HRP) are shown in Figure 3.15). The corresponding  $K_M$ ,  $V_{\max}$ ,  $K_{\text{cat}}$  (Turnover numbers) and  $K_{\text{cat}}/K_M$  (catalytic efficiency) are presented in Table 3.2.

3D plot of catalytic efficiency and  $K_{\text{cat}}$  of all the conjugates are presented in Figure 3.16. Kinetic plots of GOx-HRP-PAA/GO(1:1.5) and GOx-PAA/GO(1:1.5) were not computed since conjugate hybrid, GOx-HRP-PAA/GO(1:2) and GOx-PAA/GO(1:2) showed better catalytic activity at higher temperature and at lower pH's. GOx-HRP-PAA showed highest  $K_{\text{cat}}$  of  $69 \times 10^{-2} \text{ s}^{-1}$  followed by GOx-HRP-PAA/GO(1:2), GOx-PAA, GOx-PAA/GO(1:2) and GOx-HRP with values of  $68 \times 10^{-2}$ ,  $68 \times 10^{-2}$ ,  $57 \times 10^{-2}$  and  $32 \times 10^{-2} \text{ s}^{-1}$  respectively. In case of catalytic efficiency, GOx-HRP-PAA/GO(1:2) showed highest of  $69 \text{ mM}^{-1}\text{s}^{-1}$  and GOx-HRP-PAA showed the lowest of  $47 \text{ mM}^{-1}\text{s}^{-1}$ . GOx/HRP, GOx-PAA and GOx-PAA/GO (1:2)

had catalytic efficiency of 59, 63 and 63  $\text{mM}^{-1}\text{s}^{-1}$  respectively. In Table 3.2,  $K_M$  and  $V_{\text{max}}$  are presented.  $K_M$  values indicate the affinity of the conjugate or the enzyme towards the substrate. Lower the  $K_M$  value higher the affinity and vice versa. GOx/HRP showed the lowest  $K_M$  and  $V_{\text{max}}$  of 0.55 mM and 0.016  $\mu\text{M}^{-1}\text{s}^{-1}$  respectively, whereas, GOx-HRP-PAA showed the highest  $K_M$  and  $V_{\text{max}}$  values of 1.46 mM and 0.035  $\mu\text{M}^{-1}\text{s}^{-1}$  respectively. However,  $K_M$  and  $K_{\text{cat}}$  values of native GOx reported elsewhere were 1.34 mM<sup>38</sup> and  $16 \times 10^{-2} \text{ s}^{-1}$ <sup>39</sup>, respectively, which was very different from our values (0.55 mM and  $32 \times 10^{-2} \text{ s}^{-1}$ ) and this is to be expected for cascade catalysis. The diffusional characteristics of substrates for free enzymes vs bound enzymes are responsible for these differences.

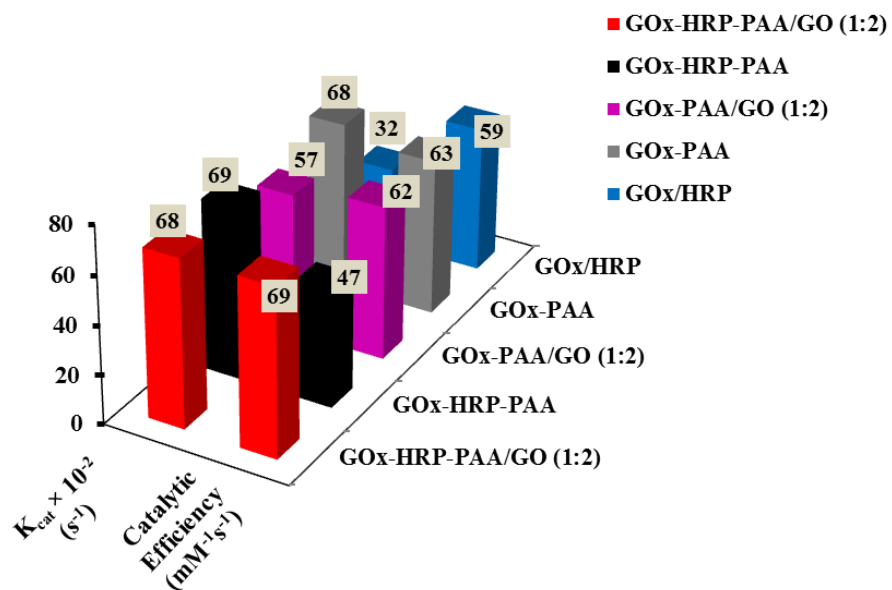


**Figure 3.15.** Lineweaver-Burk plot of GOx-HRP (blue), GOx-HRP-PAA (black), GOx-HRP-PAA/GO(1:2) (red), GOx-PAA (grey) and GOx-PAA/GO(1:2) (purple) with increasing glucose concentrations (0.075 mM- 0.6 mM), GOx and HRP concentrations were maintained at 0.5 μM and 1.125 mM o-methoxyphenol in PB pH 7.4, 10 mM. Product (dimer of o-methoxyphenol) formation was measured at 470 nm.

<b>Samples</b>	<b><math>K_M</math> (mM)</b>	<b><math>V_{max}</math> (<math>\mu M^{-1}.s^{-1}</math>)</b>	<b><math>K_{cat} \times 10^{-2}</math> (<math>s^{-1}</math>) Turnover Number (TON)</b>	<b>Catalytic Efficiency (<math>mM^{-1}s^{-1}</math>)</b>
<b>GOx-HRP- PAA/GO(1:2)</b>	1.00	0.034	68.9	69.0
<b>GOx-HRP-PAA</b>	1.46	0.035	69.8	47.7
<b>GOx- PAA/GO(1:2)</b>	0.91	0.029	57.3	63.4
<b>GOx-PAA</b>	1.08	0.034	68.8	63.4
<b>GOx/HRP</b>	0.55	0.016	32.6	59.6

**Table 3.2** Catalytic constants  $K_M$ ,  $V_{max}$ ,  $K_{cat}$  [Turnover Number (TON)] and catalytic efficiency of conjugates and corresponding unmodified protein.





**Figure 3.16** Catalytic efficiency and  $K_{cat}$  of GOx-HRP-PAA/GO(1:2) (red), GOx-HRP-PAA(black), GOx-PAA/GO(1:2) (pink), GOx-PAA (grey) and GOx/HRP (blue) in PB pH 7.4 and 10 mM with enzyme concentration of 0.5  $\mu M$ , varying glucose (0.075 mM- 0.6 mM) and o-methoxyphenol (1.125 mM).

### 3.5 Discussion

Here, GOx and HRP are modified by covalent attachment with PAA using EDC chemistry and subsequently adsorbed on GO to prepare highly stable quaternary hybrid biocatalysts of GOx-HRP-PAA/GO. Synergetic effect from the host materials, which are capable of enhancing enzymes' thermodynamic stability, has bestowed substrate channeling between the enzymes and thermal and chemical stability at various denaturing conditions. GO nanolayers with oxygen functional groups showed affinity with PAA by H-bonding interactions.<sup>22</sup> We have demonstrated that PAA conjugation is highly effective in protecting enzymes from various stresses like temperature, aggregation and proteases.<sup>14</sup> For example, catalase-PAA conjugates were thermally stable at ~90 °C and the same conjugates improved the shelf life of catalase by 8 weeks at 8 °C.<sup>14</sup> Going forward, we wish to investigate the stability enhancement of multi-enzyme polymer conjugate by employing another host material. We also wish to explore if rendering these multi-enzymes polymer conjugates more functional by the presence of another host matrix. We demonstrate a general approach combining conjugation and assembly for design of the enzymes-polymer hybrids on solid supports for catalytic applications. It is important to note that the catalytic properties presented by these hybrid materials cannot be realized from just simple enzymes-polymer conjugates or physical mixtures.

Successful syntheses of single and bienzyme conjugates and hybrids were verified using agarose gel electrophoresis, TEM and zeta potential studies. Covalent conjugation of enzymes with PAA was confirmed using agarose gel at

pH 6.0, The presence of –COOH groups in PAA imparted more negative charges to the conjugates compared to unmodified enzymes and thus the PAA conjugates showed ~120% more mobility as compared to GOx. The streaking bands from enzymes-polymer conjugates resulted from polydisperse PAA-enzyme nanogel formation. These observations in agarose gels were corroborated by observations from zeta potential studies as well. TEM images of collapsed GOx-HRP-PAA/GO (1:2) showed assembly of nanogels of GOx-HRP-PAA onto GO sheets whereas GOx/HRP showed aggregated particles. Nanogel formation of GOx/HRP when conjugated to PAA was expected as we have previously observed nanogels from single enzyme conjugation to PAA.<sup>23</sup>

Zeta potential is a handy tool to monitor electrostatic changes around negatively charged GO basal plane at successive steps.<sup>24</sup> The zeta potential of single and bienzyme conjugate and hybrids are dictated by PAA and/or GO because of their large size compared to single enzymes molecule. The interaction of enzymes conjugates with GO did not result in a big shift of surface potential, which indicated that electrostatic interactions are less dominant at this interface leading us to believe that most of the amino groups in the surface of the enzymes are modified by PAA. In this scenario a possible driving force is the hydrogen bonding between carboxyl / amide groups of enzymes-PAA conjugates and oxygen based functional groups at the GO interface.<sup>22</sup>

CD study was carried out to investigate the effect of polymer conjugation and subsequent immobilization onto GO on the secondary structure of the enzyme, which is vital for biological function and its biocatalytic activity. Conjugation with

PAA and further adsorption to GO resulted in some secondary structural changes to the enzymes as maximum of 30% ellipticity loss was noted. The reduction in the ellipticity could be attributed to the unfavorable hydrophobic interaction of the enzymes interior with GO. Despite these adverse interactions, enzymes within PAA and GO matrix may still be protected and retain some of its secondary structure.<sup>24</sup> More importantly, catalytic activity determination suggests that enzymatic activity of the biocatalysts is not compromised due to perceived structural denaturation. This was verified by extensive catalytic activity measurements at different pH with and without denaturant (4.0 mM SDS) and at high temperature (65 °C) were carried out with a variety of these samples and controls.

Although thermal stability and shelf life of different enzyme-polymer conjugates are well documented, stability of enzymes against denaturants and at low pHs are poorly understood. We discovered that some enzymes may be protected from acid denaturation by conjugating with PAA. For example, GOx-HRP-PAA conjugate showed nearly 80% activity at pH 2.5 whereas GOx/HRP had negligible activity (~14%) under similar conditions. This indicates that both GOx and HRP are stabilized within PAA due to the marginal reduction of the conformational entropy of the denatured state of the enzyme(s) compared to the unmodified enzyme(s).<sup>27</sup> This is first example of enzymes(s)-polymer conjugates wherein two enzymes were stabilized simultaneously within a single polymer network.

In GOx-HRP-PAA/GO, improvement in stabilization may be due to the presence of GO layers<sup>40</sup> despite diffusional limitation of the substrate and the

products. Interestingly, we found that immobilization of GOx-HRP-PAA onto GO resulted in remarkable quantitative retention (100%) in catalytic activities over a broad pH range. Thus, despite loss of % ellipticity from CD studies, minor structure deformation can improve the enzymatic activity by improved access to the active sites.<sup>24</sup> TEM of GOx and HRP conjugated to PAA and assembled onto GO clearly showed the successful decoration of enzymes polymer conjugates in the GO layers. This supports the above hypothesis that GO is acting as another shield against various stresses like pH and SDS.

GOx is a very robust enzyme and its SDS denaturation is possible only at lower pH values (~3.0).<sup>41</sup> Also, under similar low pH conditions, HRP is enzymatically deactivated.<sup>42,43</sup> Here, a modular approach is shown to stabilize the pH profile of GOx as well as HRP with SDS. Polymer sheath of PAA around enzymes stabilizes them from thermal denaturation as shown previously.<sup>46</sup> But, stability to chemical denaturants like SDS has never been addressed before. At pH 2.5-7.4 with SDS, these bienzyme conjugates and hybrids indicated high activities compared to single enzyme counterparts or unmodified bienzyme system. Only at pH 5.5 single enzyme conjugate hybrids showed comparable activities to bienzyme conjugate hybrids. These results indicate that PAA is a good candidate to induce denaturant resistivity to the enzymes as SDS showed hydrophobic binding with PAA with favorable enthalpy and entropic contributions.<sup>44</sup> PAA conjugation could also alter the pKa of active site by shielding from the bulk and thereby responsible for retention of activity but experimental access to such information may not be easy. Furthermore, PAA conjugation has not only improved the stability of the enzymes

against SDS but also stability of enzymes at low pH conditions. Negatively charged COOH groups of PAA acts as an electrostatic repulsion barrier for SDS-like anionic surfactant to get access to the enzyme surface in order to unfold the molecule. In addition, GO sheets further enhanced this stability despite diffusional problem of the substrates in presence of multiple GO layers around the enzyme(s). GO can also interact with SDS, which in turn results in reduced interaction of SDS towards enzymes.<sup>45</sup> These factors may help in stabilizing the enzymes against high concentration of the denaturant.

We mentioned previously that some of our conjugated displayed activities of higher than 100%, which has been attributed to substrate channeling across the matrix. Despite diffusional limitation of the substrate and the products across GO and PAA matrix, H<sub>2</sub>O<sub>2</sub> (a product of GOx reaction and substrate for HRP reaction) are able to internally diffuse within the matrix. This effect might help overcome problems of bulk diffusion to the matrix affording high initial catalytic rates of reactions. Furthermore, this robust bienzyme conjugate and hybrid platform maybe exploited for high temperature enzyme catalysis with substrate channeling.

To determine thermal stability of enzymes conjugates, catalytic activities were established at 65°C and compared to appropriate control samples. For example, GOx is inactive above 50°C and HRP presents reduced activity (65%) at 42°C.<sup>2,6</sup> However, when GOx (and HRP) was conjugated with PAA it seemed to have regained some of the activity (60-80%) since the conformational entropy of the denatured state is reduced as result of PAA confinement. Therefore, heat of denaturation of enzyme increases<sup>46</sup> and enzyme is stabilized more than its

unmodified counterparts. This stabilization is enhanced when the PAA conjugated GOx (and HRP) are adsorbed onto GO as a consequence of further reduction in entropy and possibly due to elevated substrate channeling. This is proved by the activity data shown in Figure 6 wherein GOx-HRP-PAA/GO and GOx-PAA/GO showed higher % specific activity retention compared to single and bienzyme conjugated samples (GOx-HRP-PAA/ GOx-PAA). Additionally, at high temperatures, the rate of the reaction can increase by several folds in accordance with the Arrhenius equation. Conversely, H<sub>2</sub>O<sub>2</sub> decomposition at elevated temperatures may be an opposing effect to above two. But in our conjugates, both donor and acceptor enzymes are in a close proximity that H<sub>2</sub>O<sub>2</sub> transfer become internally very efficient prior to the decomposition step. This is, again, a very rare example of enzymes cascading with high retention of activity at thermally denaturing conditions.

To better understand and compare the effectiveness of the substrate channeling of current system we computed the degree of substrate channeling (DSC). DSC is calculated by using the ratio of initial rate of the bienzyme conjugate hybrids (1:2) system to that of the bienzyme alone under comparable conditions. These DSC values are then compared to few relevant examples of multienzyme systems published in literature.<sup>47, 48, 49, 50, 51</sup> and presented in Table 3.3.<sup>17</sup> To our best knowledge, only the current system demonstrated active substrate channeling at diverse conditions including high temperature and with denaturant of 4.0 mM. Thus, effective substrate channeling can be achieved using PAA in conjunction with GO.

Kinetic data showed that adsorption of GOx-HRP-PAA to GO increases the catalytic efficiency of the GOx/HRP (unmodified bienzyme) system. Also, highest  $K_{cat}$  of the GOx-HRP-PAA showed the importance of bienzyme conjugation instead of single enzyme conjugation. Furthermore, high catalytic efficiency of GOx-HRP-PAA/GO (1:2) may be due to the presence of PAA matrix, which is a hydrophilic polymer that aids in transport of the glucose to the catalytic site within GOx and subsequent removal of the products. This constant replenishment of substrate and further depletion of products from the enzyme active site may be responsible for the enhancement of the  $K_{cat}$  and catalytic efficiency of the bi-enzyme conjugates. Also, high  $K_M$  indicated the decrease in selectivity of glucose towards GOx of the GOx-HRP-PAA. This could be due to the change in conformation of the active site of the enzyme, which is supported by our CD data. This resulted in increase in  $V_{max}$ , which may be related to the hydrophilic PAA matrix. The conclusions drawn from the kinetics studies are rudimentary and require extensive investigation.



No.	Enzymes used in Multi-enzyme systems	Degree of Substrate Channeling	Temperature of the Study	pH of the Study	Conc. of Surfactant (SDS)(mM)
1	Krebs Cycle Enzymes <sup>47</sup>	1-2	25	7-8	Not Applicable (NA)
2	Ferredoxin and Hydrogenase <sup>48</sup>	1	25	7-8	NA
3	GOx and HRP <sup>49</sup>	20-30	25	7-8	NA
4	Cellulosomes <sup>50</sup>	2-4	37	6-7	NA
5	Tryptophan Synthase <sup>51</sup>	Infinite	25	6-7	NA
6	<b>This Work (GOx and HRP)</b>	<b>1.3</b>	<b>25</b>	<b>7.4</b>	<b>4.0</b>
7	<b>This Work (GOx and HRP)</b>	<b>Infinite</b>	<b>25</b>	<b>2.5</b>	<b>4.0</b>
8	<b>This work (GOx and HRP)</b>	<b>7.5</b>	<b>65</b>	<b>7.4</b>	<b>NA</b>

**Table 3.3.** Comparison of substrate channeling efficiency of current catalytic system with other relevant reports.

### 3.6 Conclusion

This is the first example of bienzyme (HRP and GOx) stabilization using PAA and GO sheets and proof-of-concept of bienzyme cascade catalytic effects. GOx/HRP (bienzyme) and GOx were covalently modified with PAA using EDC chemistry and then assembled on GO using non-covalent interactions. These versatile bienzyme conjugates have been used to enhance: (1) stability of these enzymes under harsh conditions of pH (2.5-7.4) and denaturants (SDS); and (2) enhanced biocatalytic activities of the catalytic cascade in the dual-host system, when compared to a mixture of the two enzymes in the solution. Furthermore, the bienzyme activity improved at higher temperatures compared to their single enzyme counterparts. This new platform bestowed stabilization of two different enzymes simultaneously to implement substrate channeling at high temperature, broad pH and chemically denaturing conditions with ~100% retained enzymatic activity. Polymer wrapping followed by contact with GO resulted in reducing the substrate specificity of the enzymes because of loss in ellipticity retention but highest catalytic efficiency ( $K_{cat}$ ) of GOx-HRP-PAA/GO (1:2) is obtained as a bonus. Therefore, this bienzyme composite cascade mechanism proved to be highly efficient and showed stability at high temperature, which has not achieved by unbound enzymes or polymer conjugates. This combination of a 2D host material for a enzymes-polymer guest opens up a new platform for multienzyme cascading for broad spectrum of applications, at diverse and biologically inaccessible conditions. This is one of the first enzyme hybrids with substrate channeling demonstrated at diverse and challenging conditions. The versatility of

this system to protect more than two enzymes needs to be tested, which could lead to the design of micro biofuel cells and biobatteries. Also, in the long term, this modular methodology may be used to produce environmentally benign, biocompatible, edible and efficient biocatalysts for energy production as alternatives to fossil fuel-based energy.

### 3.7 References

1. Cooper, V. A.; Nicell, J. A. *Water Res.* **1996**, *30*, 954-964.
2. Wong, C.; Wong, K.; Chen, X. *Appl. Microbiol. Biotechnol.* **2008**, *78*, 927-938.
3. Guo, X.; Liang, B.; Jian, J.; Zhang, Y.; Ye, X. *Microchim. Acta* **2014**, *181*, 519-525.
4. Delvaux, M.; Walcarius, A.; Demoustier-Champagne, S. *Biosens. Bioelectron.* **2005**, *20*, 1587-1594
5. Ramachandran, S.; Fu, E.; Lutz, B.; Yager, P. *Analyst* **2014**, *139*, 1456-1462.
6. Lavery, C. B.; MacInnis, M. C.; MacDonald, M. J.; Williams, J. B.; Spencer, C. A.; Burke, A. A.; Irwin, D. J. G.; D'Cunha, G. B. *J. Agric. Food Chem.* **2010**, *58*, 8471-8476.
7. Munoz-Munoz, J. L.; Garcia-Molina, F.; Varon, R.; Rodriguez-Lopez, J. N.; Garcia-Canovas, F.; Tudela, J. *Biosci. biotechnol. and biochem.* **2007**, *71*, 390-396.
8. Jo, S. M.; Lee, H. Y.; Kim, J. C. *Int. J. Biol. Macromol.* **2009**, *45*, 421-426
9. He, C.; Liu, J.; Xie, L.; Zhang, Q.; Li, C.; Gui, D.; Zhang, G.; Wu, C. *Langmuir* **2009**, *25*, 13456-13460.
10. Gouda, M. D.; Singh, S. A.; Rao, A. G. A.; Thakur, M. S.; Karanth, N. G. *J. Biol. Chem.* **2003**, *278*, 24324-24333
11. Paz-Alfaro, K. J.; Ruiz-Granados, Y. G.; Uribe-Carvajal, S.; Sampedro, J. G. *J. Biotechnol.* **2009**, *141*, 130-136.
12. Sarath Babu, V. R.; Kumar, M. A.; Karanth, N. G.; Thakur, M. S. *Biosens. Bioelectron.* **2004**, *19*, 1337-1341.
13. Eremin, A. N.; Budnikova, L. P.; Sviridov, O. V.; Metelitsa, D. I. *Appl. Biochem. Microbiol.* **2002**, *38*, 151-158.

- 
14. Riccardi, C. M.; Cole, K. S.; Benson, K. R.; Ward, J. R.; Bassett, K. M.; Zhang, Y.; Zore, O. V.; Stromer, B.; Kasi, R. M.; Kumar, C. V. *Bioconjugate Chem.* **2014**, *25*, 1501-1510.
15. Kumar, C. V.; Chaudhari, A. *J. Am. Chem. Soc.* **2000**, *122*, 830-837.
16. Panchagnula, V.; Kumar, C. V.; Rusling, J. F. Ultrathin Layered Myoglobin-Polyion Films Functional and Stable at Acidic pH Values. *J. Am. Chem. Soc.* **2002**, *124*, 12515-12521.
17. Zhang, Y. H. P. *Biotechnol. Adv.* **2011**, *29*, 715-725.
18. Santacoloma, P. A.; Sin, G. r.; Gernaey, K. V.; Woodley, J. M. *Org. Process Res. Dev.* **2010**, *15*, 203-212.
19. Wang, Y.; Li, Z.; Wang, J.; Li, J.; Lin, Y. *Trends Biotechnol.* **2011**, *29*, 205-212.
20. Zhang, Y.; Wu, C.; Guo, S.; Zhang, J. *Nanotechnol. Rev.* **2013**, *2*, 27-45.
21. Shen, H.; Liu, M.; He, H.; Zhang, L.; Huang, J.; Chong, Y.; Dai, J.; Zhang, Z. *ACS Appl. Mater. Interfaces* **2012**, *4*, 6317-6323.
22. Kavitha, T.; Kang, I. K.; Park, S., Y. *Langmuir* **2013**, *30*, 402-409.
23. Zhang, Y.; Zhang, J.; Huang, X.; Zhou, X.; Wu, H.; Guo, S. *Small* **2012**, *8*, 154-159.
24. Pattammattel, A.; Puglia, M.; Chakraborty, S.; Deshapriya, I. K.; Dutta, P. K.; Kumar, C. V. *Langmuir* **2013**, *29*, 15643-15654.
25. Kumar, C. V.; Chaudhari, A. *Chem. Commun.* **2002**, *20*, 2382-2383.
26. Zore, O. V.; Lenehan, P. J.; Kumar, C. V.; Kasi, R. M. *Langmuir* **2014**, *30*, 5176-5184.
27. Kumar, C. V.; Chaudhari, A. *Chem. Commun.* **2002**, *21*, 2382-2383.
28. Jeykumari, D. R. S.; Narayanan, S. S. *Biosens. Bioelectron.* **2008**, *23*, 1686-1693.
29. Rocha-Martín, J.; Rivas, B.; Muñoz, R.; Guisán, J. M.; López-Gallego, F. *ChemCatChem* **2012**, *4*, 1278-1288.
30. Cao, X.; Li, Y.; Zhang, Z.; Yu, J.; Qian, J.; Liu, S. *Analyst* **2012**, *137*, 5785-5791.
31. Hummers, W. S.; Offeman, R. E. *J. Am. Chem. Soc.* **1958**, *80*, 1339-1339.
32. Carlsson, G. H.; Nicholls, P.; Svistunenko, D.; Berglund, G. I.; Hajdu, J. *Biochem.* **2005**, *44*, 635- 642.

- 
33. Kimmoju, P. R.; Chen, Z. W.; Bruckner, R. C.; Mathews, F. S.; Jorns, M. S. *Biochem.* **2011**, *50*, 5521-5534
34. Fieldes M. A. *Electrophoresis* **1992**, *13*, 82-86.
35. Liu, Y.; Wang, W.; Jin, Y.; Wang, A. *Sep. Sci. Technol.* **2011**, *46*, 858-868.
36. Gibson, Q. H.; Swoboda, B. E. P.; Massey, V. *J. Biol. Chem.* **1964**, *239*, 3927-3934.
37. Axley, M. J.; Bock, A.; Stadtman, T. C.; *Proc. Natl. Acad. Sci. USA.* **1991**, *88*, 8450-8454.
- 38 Shin, K. S.; Youn, H. D.; Han, Y. H.; Kang, S. O; Hah, Y. C. *Eur. J. Biochem.***1993**, *215*, 747-752.
- 39 Witt, S.; Wohlfahrt, G.; Schomburg, G.; Hecht, H. J.; Kalisz, H. M. *Boichem. J.* **2000**, *347*, 553-559.
40. Jin, L.; Yang, K.; Yao, K.; Zhang, S.; Tao, H.; Lee, S.-T.; Liu, Z.; Peng, R. *ACS Nano* **2012**, *6*, 4864-4875.
41. Jones, M. N.; Manley, P.; Wilkinson, A. *Biochem. J.* **1982**, *203*, 285-291.
42. Bovaird, J. H.; Ngo, T. T.; Lenhoff, H. M. *Clin. Chem.* **1982**, *28*, 2423-2426
43. Laurenti, E.; Suriano, G.; Ghibaudi, E. M.; Ferrari, R. P. *J. Inorg. Biochem.* **2000**, *81*, 259-266.
44. Wang, C.; Tam, K. C. *J. Phys. Chem. B* **2005**, *109*, 5156-5161.
45. Liang, Y.; Wu, D.; Feng, X.; Müllen, K. *Adv. Mater.* **2009**, *21*, 1679-1683.
46. Mudhivarthi, V. K.; Cole, K. S.; Novak, M. J.; Kippit, W.; Deshapriya, I. K.; Zhou, Y.; Kasi, R. M.; Kumar, C. V. *J. Mater. Chem.* **2012**, *22*, 20423-20433.
47. Moehlenbrock, M., J.; Toby, T., K.; Waheed, A.; Minter, S., D. *J. Am. Chem. Soc.* **2010**, *132*, 6288-6289
48. Agapakis, C., M.; Ducat, D., C.; Boyle, P., M.; Wintermute, E., H.; Way, J., C.; Silver, P., A.; *J. Biol. Eng.* **2010**, *4*, 3-18
49. Wilner, O., I.; Weizmann, Y.; Gill, R.; Lioubashevski, O.; Freeman, R.; Willner, I. *Nat. Nanotechnol.* **2009**, *4*, 249-254
50. Fierobe, H., P.; Mingardon, F.; Mechaly, A.; Belaich, A.; Rincon, M., T.; Pages, S.; Lamed, R.; Tardiff, C.; Belaich, J., P.; Bayer, E., A.; *J. Biol. Chem.* **2005**, *280*, 16325-16334
51. Hyde, C., C.; Ahmed, S.,A.; Padlan, E.,A.; Miles, E.,W.; Davies, D., R. *J. Bio./ Chem.* **1988**, *263*, 17857–17871.

---

## Chapter 4

### 4. Biocompatible Multienzyme-Polyacrylic Acid Conjugates for High Temperature Catalysis

#### 4.1 Abstract

Modular approach of conjugation of multiple of enzymes with different pI values to hydrophilic polyacrylic acid (PAA) is presented here. Glucose oxidase (GOx), acid phosphatase (AP), lactate dehydrogenase (LDH), horseradish peroxidase (HRP) and lipase (Lip) were used as model enzymes. The multienzyme complexes (MEC) thus formed showed activity enhancement at room temperature (25 °C) and at high temperature (65 °C). The synthesis of MEC's were carried out using two distinct protocols – (1) parallel and (2) sequential synthesis to form 5-P and 5-S, respectively. The synthesis of MEC's were confirmed using agarose gel electrophoresis, zeta potential, dynamic light scattering (DLS) and the structural modifications of enzymes after conjugation to PAA was studied using circular dichroism spectroscopy. Transmission electron microscopy was used for morphological examination of MEC's. The formation of 5-P and 5-S resulted in unprecedented increase in activity of AP to 19.5 and 6.5 times in case of 5-P and 5-S, respectively at room temperature. This can be related to increase in catalytic efficiency of AP ( $9.11 \times 10^{-5}$ ) to  $1.55 \times 10^{-3}$  and  $1.68 \times 10^{-3}$ , for 5-P and 5-S respectively. In other example, at high temperature GOx lost its activity completely whereas, 5-P and 5-S retained 132 and 152 % of its activity. Similar observations were made, in case of AP activity assay at high temperature, where AP completely lost its activity whereas, 5-P and 5-S retained 100 and 300 % of activity.

Conversely, at room temperature, reduction in activity was observed for 5-P and 5-S for HRP and LDH activity assays. This is related to the decrease in substrate affinity of 5-P and 5-S towards o-methoxyphenol and NADH which acts as substrates for HRP and LDH activity assay. These robust MEC's can be used in future for biofuel cell applications in biocompatible and environmentally friendly manner.

## 4.2 Introduction

We describe an easy, modular and general method to synthesize highly active and stable multi-enzyme polyacrylic conjugates (MECs). Enzyme catalysis is a billion dollar industry,<sup>1,2,3</sup> and the development of stable, active and multi-purpose biocatalysts, which can be used to enhance the rate of one or more chemical transformations, is important to reduce processing costs as well as the impact on the environment. In this present study, glucose oxidase (GOx), horseradish peroxidase (HRP), lipase (Lip), acid phosphatase (AP) and lactate dehydrogenase (LDH) are used as model enzymes and poly (acrylic acid) as a polymer to tether these enzymes together in covalent networks of nanogels to form multienzyme complex (MEC). While we have previously reported polymer conjugated cascading bi (2) enzymes, this is the first example of polymer based covalent conjugation of non-cascading multi (5) enzymes and evaluation of their catalytic features. The two different methods used to synthesize MECs are presented in Scheme 4.1.

In this case, enzymes that catalyze redox transformations (oxidoreductases) such as GOx and HRP are useful for sensing, catalysis and waste water

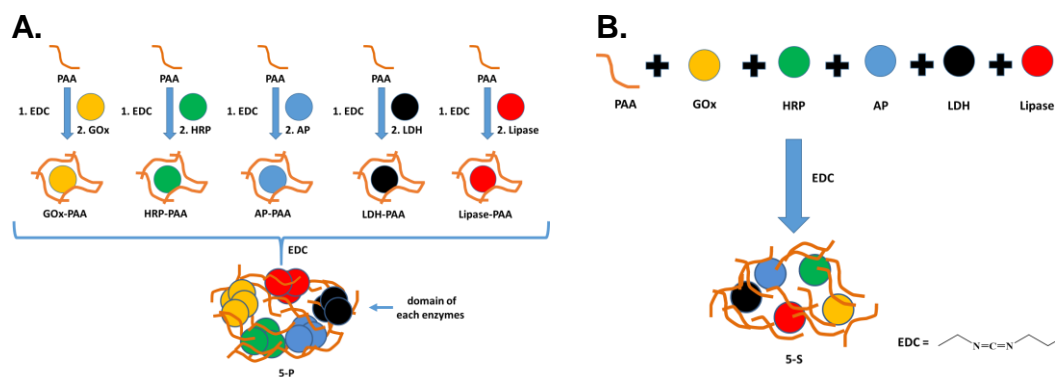


remediation, and serve as a cascade dyad, <sup>4, 5, 6, 7, 8</sup> while, LDH is valuable for production of enantiopure (-) lactate which is precursor to many pharmaceutical drugs such as anti-hypertensives and semi-synthetic penicillins. <sup>9</sup> Enzymes that catalyze hydrolysis (hydrolases) such as AP is used widely for waste remediation, metal recovery <sup>10</sup> and determination of surfactants, <sup>11</sup> while, Lipases are employed for production of pharmaceutical drugs, cosmetics, leather, detergents, foods, perfumery, medical diagnostics and other synthetic materials. <sup>12, 13, 14</sup> However, LDH, GOX and HRP displayed significantly reduced activities at 50 °C, while Lip and AP presented rapid decrease in activity above 40 °C. <sup>4, 15, 16, 17</sup> To effectively harness the activity of these enzymes, they need to be individually stabilized over wide range of temperatures. More importantly, by developing strategies to covalently stabilize five enzymes within a single scaffold, their individual catalytic properties can be combined within one system for potential applications in biofuel cells and other catalytic applications.

In a previous example, 3 enzymes glucose oxidase, lactate oxidase and galactose oxidase were non-covalently immobilized on electrode using polyethylene glycol as a spacer and used for quantification of glucose, lactate and galactose at millimolar concentrations.<sup>18</sup> In another example, 13 different enzymes were physically adsorbed onto carbon nanotubes/carbon paper (also called non-immobilized), and used an enzymatic biofuel cascade reactor for sugar battery applications. Although, this system failed to target the enzyme stability at high temperature. <sup>19</sup> We recently reported the only example of covalent conjugation of 2 enzymes (GOx and HRP) using polyacrylic acid for efficient catalysis at low pH,

with denaturant and at high temperatures (65 °C).<sup>4</sup> Covalent conjugation of several enzymes (more than 2) using polymers and stabilization of these multi-enzyme conjugates will become very useful high temperature, renewable, multi-purpose catalysis, biofuel cells and other enzyme cascade reactions. Furthermore, design of biocompatible MEC will be important for development of implantable therapeutic devices. In all above cases, MEC's studied were cascade systems and non-cascading multienzyme systems were not studied yet. Therefore, here non-cascading enzyme systems were studied (except GOx and HRP, which were cascading in current MEC).

In this paper, MECs were synthesized using 2 different routes (Scheme 4.1). In Route 1, parallel synthesis strategy was used to produce MEC. In step 1, Individual enzyme-PAA conjugates were synthesized using GOx (yellow), HRP (green), AP (blue), LDH (black) and lipase (red) and PAA (brown string) to form GOx-PAA, HRP-PAA, AP-PAA, LDH-PAA and Lip-PAA. In step 2, these enzyme-PAA conjugates were mixed together and crosslinked further using 1-Ethyl-3-(3-dimethylaminopropyl) carbodiimide (EDC) to form MEC (5-P, Scheme 4.1A). In Route 2, sequential synthesis of MEC was used. PAA and 5 enzymes were stirred together for 10-20 minutes and then crosslinked using EDC to form MEC (5-S, Scheme 4.1B).



**Scheme 4.1.** Two different routes to synthesize MEC's. In Route 1 (A) individual enzyme-PAA conjugates were synthesized using EDC chemistry and then they were further crosslinked to make 5-P. In Route 2 (B), PAA and all 5 enzymes were mixed and stirred for 20 minutes and finally they are crosslinked using EDC to make 5-S. In above figures enzymes- GOx, HRP, AP, LDH and Lip were represented by yellow, green, blue, black and red circles, respectively and PAA was shown by brown string. 5-P and 5-S were illustrated as shown in A and B respectively.

## 4.3 Experimental

**4.3.1 Materials.** PAA ( $M_v = 450,000$  g/mol where  $M_v$  indicated viscosity average molecular weight), GOx, Lipase, hydrogen peroxide ( $H_2O_2$ ), glucose, o-methoxyphenol, EDC, NADH, sodium pyruvate, 4-nitrophenyl acetate, 4-nitrophenyl phosphate and uranyl acetate were purchased from Sigma-Aldrich (St. Louis, MO). HRP and LDH was purchased from Calzyme Laboratories INC, San Luis Obispo, CA. AP was purchased from MP Biomedicals, Solon, OH. Agarose was purchased from Molecular Biology Hoefer Inc., Allison, MA.

**4.3.2 Synthesis of MEC's.** MEC's were synthesized using two different synthesis routes. It comprised of parallel (2-steps) and sequential synthesis (1-step) of MEC using 5 enzymes, details below. Important features of the 5 enzymes are presented in chart 4.1.

**4.3.3 Parallel synthesis of 5-P** Synthesis of MEC was performed using 2 step parallel process. In step 1, individual enzyme-PAA conjugates were synthesized using EDC chemistry. First 2% w/v stock solution of PAA was prepared by dissolving PAA in DI and pH is adjusted to 7. This PAA (2.8 mL) was added to phosphate buffer, 10 mM, pH 7.4 (PB) and further activated by EDC. Molar ratio of EDC to  $-COOH$  was maintained at 1.5:1. The mixture was stirred for 10-20 min and then GOx dissolved in PB was added dropwise such that molar ratio of enzyme: PAA was maintained at 1:1 and total solution volume is 10 mL. This solution was stirred for 6 hr. Covalent conjugation was achieved through carboxyl groups on PAA and lysine amino groups on enzymes. In similar manner other enzyme-PAA conjugates were synthesized. In step 2, each enzyme-PAA

conjugates were mixed and crosslinked using EDC and EDC: -COOH ratio was maintained at 1.5:1.

**4.3.4 Sequential synthesis of 5-S.** Synthesis of MEC was carried out by 1-step process. For synthesis 5.6 mL of PAA from stock and 5 enzymes (such that molar ratio of total enzymes: PAA was maintained at 1:1) were mixed and stirred for 10-20 min. After that EDC is added such that molar ratio of EDC: -COOH from PAA is maintained at 1.5:1. The sample was dialyzed using 25 kDa dialysis membrane in pH 7.4 PB to remove unreacted EDC and EDC-urea byproducts.

**4.3.5 Zeta Potential Studies.** Zeta potential of unmodified enzyme, enzyme-PAA and MEC's were measured using Brookhaven zeta plus zeta potential analyzer (Brookhaven Instruments Corporation, Holtsville, NY) by laser doppler velocimetry. In each experiment, 1.5 mL of sample is used and the enzyme concentration is maintained at 0.01 mM. Smoluchowski fit by the software and matching electrophoretic mobility technique was employed to acquire the zeta potential values in mV.

**4.3.6 Agarose Gel Electrophoresis.** Agarose gel electrophoresis was done using horizontal gel apparatus by Gibco Model 200, Life Technologies Inc., Grand Island NY. Molecular biology grade agarose (0.5% w/v) was heated in microwave in pH 7, 40 mM Tris acetate buffer and left to gel in apparatus. After the gel was formed samples were loaded after mixing them with loading buffer containing 50% v/v glycerol and 0.01% m/v bromophenol blue and electrophoresis was carried out for 40 min at 100 V. Then gel was stained using 10% v/v acetic acid and 0.02% m/v

coomassie blue overnight, and then destained with 10% v/v acetic acid overnight, photographed and described.

**4.3.7 Circular Dichroism (CD).** Secondary structure of unmodified enzymes, enzyme-PAA and MEC's were evaluated using CD spectroscopy. Structure of enzymes was evaluated in the ultraviolet (UV) range (195 nm to 250 nm) using Jasco 710 spectropolarimeter. CD spectra of each sample was normalized for 1  $\mu$ M of total enzyme concentration.

**4.3.8 Transmission Electron Microscopy (TEM).** Morphology of all the samples were analyzed using tecnai T 12 TEM functioning at an accelerating voltage of 120 kV and at step 3. Aqueous samples of Glucose oxidase (GOx), GOx-PAA (GOx-polyacrylic acid) and 5-P were prepared at enzyme concentration of 5-10 nM. These samples were drop casted on TEM grids covered with fomvar film. Excess solution was removed by blotting. TEM grids bearing samples were then stained with 0.5 wt % of uranyl acetate, dried for 20 mins and imaged.

**4.3.9 Dynamic Light Scattering (DLS).** Size of the enzymes, enzyme-PAA and MEC's were evaluated using CoolBatch+ dynamic light scattering apparatus with Precision Detectors (PD2074 N) (Varian Inc.,) used in combination with a 0.5 x 0.5 cm<sup>2</sup> square cuvette and 658 nm excitation laser source at 90° geometry. Samples corresponding to 0.5 nM of total enzymes in PB were filtered through 0.2 -micron filter (PVDF, 13 mm, Fisher Scientific) and equilibrated for 300 s at 25 °C; 5 repetitions with 60 accumulations were recorded. Precision Elucidate Version 1.1.0.9 software was used to run the experiment and Deconvolve Version 5.5 was used to process the data.

**4.3.10 Catalytic activity measurements.** Activity studies of unmodified enzymes, enzyme-PAA and MEC's (5-P, 5-S) were carried out using appropriate enzymatic assay methods. Activities for GOx was performed using appropriate assay methods for samples containing GOx, such as GOx, GOx-PAA, 5-P and 5-S. Equivalent concentration of enzyme for each activity assay was maintained as 1  $\mu$ M and appropriate substrates were added using buffered solvents (Tris acetate or PB). Detailed activity assay protocols are presented in following sections.

**4.3.10.1 Glucose oxidase (GOx) activity.** Activity of unmodified GOx, GOx-PAA, 5-P and 5-S were measured using cascade system by employing GOx and HRP as enzymes.<sup>20</sup> GOx catalyzed glucose to gluconolactone and H<sub>2</sub>O<sub>2</sub> and HRP then oxidized o-methoxyphenol using H<sub>2</sub>O<sub>2</sub> to oxidant product, which was traced at ( $\lambda_{\text{max}}$ ) 470 nm using UV spectroscopy. Specific activities were measured by keeping 1  $\mu$ M of GOx and HRP in unmodified as well as in conjugate forms, 0.125 mM o-methoxyphenol, 0.3 mM glucose in 10 mM, pH 7.4, phosphate buffer (PB). Activity studies were carried out for 1 min and first 20-40 sec were used for calculating initial rate. Initial rate of GOx in PB at 25°C was referenced at 100% and used to calculate all the specific activities relating to GOx based enzyme systems.

**4.3.10.2 Horseradish peroxidase (HRP) activity.** Catalytic activities of unmodified HRP, HRP-PAA, 5-P and 5-S were computed using H<sub>2</sub>O<sub>2</sub> and o-methoxyphenol.<sup>21</sup> Therefore, while performing activity studies equivalent of 1  $\mu$ M HRP in all samples were added to cuvette containing 0.375 mM o-methoxyphenol and 0.125 mM H<sub>2</sub>O<sub>2</sub> in PB. Oxidant product of o-methoxyphenol with  $\lambda_{\text{max}}$  at 470

nm was quantified using colorimetric methods. Activity studies were carried out for 1 min and initial 10-20 sec were used to compute the initial rate. This rate of HRP in PB at 25°C was referenced as 100% and used to calculate the specific activities of samples containing HRP.

**4.3.10.3 Lipase (Lip) activity.** The catalytic activity of lip was carried out using 4-nitrophenyl acetate (4-NPA) as a substrate based on reported protocols.<sup>22</sup> A stock solution was prepared using 63 mg of 4-NPA dissolved in 10 mL methanol. A 1 mL aliquot of 4-NPA of stock solution was dissolved in 100 mL DI. Final concentration of 4-NPA was maintained at 0.0175 mM in the cuvette while carrying out activity studies in 10 mM, pH 7 Tris acetate buffer. Activity studies were carried out for 3 min and initial rate for 60-80 sec was used for calculation of specific activity for 1  $\mu$ M of HRP. Esterification of 4-NPA to 4-nitrophenol was monitored using colorimetric methods at 405 nm using UV spectrometer. This initial rate for Lip was used as reference (100%) to calculate the specific activities of all other samples containing Lip.

**4.3.10.4 Acid phosphatase (AP) activity.** The catalytic activity of AP was established using 4-nitrophenyl phosphate (4-NPP) as a substrate by methods previously reported.<sup>23</sup> While performing the activity studies concentration of AP and 4-NPP was maintained at 1  $\mu$ M and 5 mM in the cuvette, respectively. The sample was first stirred in PB in the cuvette and then substrate was added. Enzymatic catalysis of 4-NPP to 4-nitrophenol was quantified at 405 nm using UV spectrometer. Activity studies were carried out for 3 minutes and initial rate for 60-80 sec was used for calculation of specific activity. Initial catalytic rate for AP at 25



°C was referenced at 100%. Therefore, catalytic activity of other samples such as AP-PAA, 5-P and 5-S were computed keeping AP as a reference.

**4.3.10.5 Lactate dehydrogenase (LDH) activity.** The catalytic activity of LDH was monitored using NADH as a substrate in presence of sodium pyruvate using 10 mM, pH 8 Tris buffer.<sup>24</sup> The concentration of LDH, NADH and sodium pyruvate was maintained at 0.1  $\mu$ M, 0.067 mM and 0.45 mM, respectively, in the cuvette. The oxidation of NADH to NAD was monitored at 340 nm using UV spectrometer.



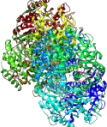

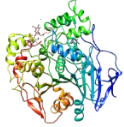
**4.3.11 Activity studies at high temperature (65 °C).** The temperature-controlled catalytic activities were determined at 65 °C using 5 unmodified enzymes (GOx, HRP, LDH, AP, Lip), enzyme-PAA, 5-P or 5-S conjugates with appropriate substrates, solvents and buffers using protocols similar to the ones described in Section 4.3.10.

**4.3.12 Kinetic studies.** To gather kinetic parameters such as  $K_M$  and  $V_{max}$ , Lineweaver Burk plots were used. Identical activity assays were used that assisted in gathering activity studies information. In case of each enzyme and the corresponding enzyme-PAA and MEC conjugates varying substrate concentrations were used to construct Lineweaver Burk plots. The information on the substrate concentration for each enzyme assays is given as follows-

In case of GOx activity assay, glucose was used as a substrate and its concentration was varied in the range of 0.075 – 0.45 mM. o-methoxyphenol was used as a substrate for HRP activity assay and the concentration range used was in the range of 0.0163 – 0.097 mM. In case of Lip activity assay, 4-

nitrophenylacetate was used as a substrate in the range of 0.007 – 0.012 mM. For LDH activity assay, NADH was used as a substrate in the range of 0.0075 – 0.15 mM. Lastly, in case of AP activity assay, 4-nitrophenylphosphate was used as a substrate in the range of 2.7 – 16.2 mM. Thus, all the kinetic parameters were extracted using Lineweaver Burk plots.

**Chart 4.1.** Key properties of glucose oxidase (GOx), horseradish peroxidase (HRP), lactate dehydrogenase (LDH), acid phosphatase (AP) and Lipase (Lip).

<b>Enzyme s</b>	<b>GOx</b> 	<b>HRP</b> 	<b>LDH</b> 	<b>AP</b> 	<b>Lip</b> 
Molecular Weight	160000	40000	146400	45080	57100
pI	4.6	5.1	5.5	5.8	3.8
Number of Lys residues	30	6	104	16	20

## 4.4 Results

In this study, GOx, HRP, AP, LDH and Lip were conjugated to PAA by parallel and sequential strategies to form MECs. In the parallel synthetic method, individual enzyme-PAA conjugates were synthesized first (GOx-PAA, HRP-PAA, etc.) and then these enzyme-PAA conjugates were further treated with EDC to produce MEC, 5-P. In sequential synthesis route, all 5 enzymes and PAA were mixed together in specific ratios and then crosslinked covalently to form MEC, 5-S.

### 4.4.1 Synthesis of MEC's.

*4.4.1.1 Synthesis of 5-P:* The MEC, 5-P, was synthesized in two steps. In step 1, individual enzyme-PAA conjugates were synthesized. For example, PAA was first activated using EDC and GOx was then added dropwise to form covalently conjugated GOx-PAA. Molar ratio of EDC:-COOH and total protein: PAA was maintained at 1.5:1 and 1:1, respectively. Crosslinking between PAA and enzyme was achieved by -COOH groups on PAA and lysine NH<sub>2</sub> groups on GOx. The conjugation reaction was carried out for 6 hr. followed by using 25 kDa dialysis membrane in pH 7.4 PB for 3 cycles of 5 hr. each. Final concentration of enzyme in the GOx-PAA conjugate was 12.5 µM. Similarly, other enzyme-PAA conjugates were synthesized. In step 2, purified enzyme-PAA conjugates were crosslinked further using EDC chemistry. In this case, all 5 enzyme-PAA conjugates (GOx-PAA, HRP-PAA, etc.) were mixed in equal molar proportions and stirred for 10-20 minutes. Then, EDC was added such that molar ratio of EDC:-COOH was kept at 1.5:1. Crosslinking was attained by unreacted enzyme lysine amino groups, aspartate and glutamate carboxyl groups and carboxyl groups on PAA via amide

and ester formation. Error! Bookmark not defined. After 6 hr., the samples were purified by dialysis to remove unreacted EDC and EDC-urea. Final concentration of each enzyme in 5-P was 6.5  $\mu$ M.

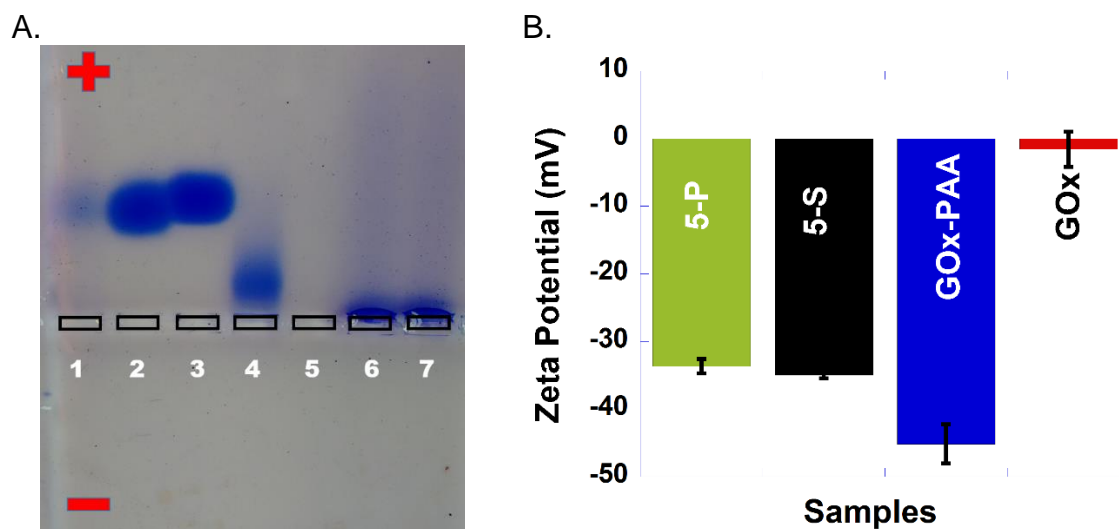
**4.4.1.2 Synthesis of 5-S:** Sequential synthesis of MEC was carried out in one step. All 5 enzymes and PAA were mixed together in specific molar ratio such that total enzyme: PAA concentration was 1:1. Also, all proteins were added in equal molar ratios. This solution was stirred in PB for 20 min. Then, EDC was added to carry out the crosslinking to form the covalently conjugated MEC, 5-S. Final concentration of each enzyme in the 5-S was 6.5  $\mu$ M, similar to 5-P.

Successful synthesis of enzyme-PAA, 5-P and 5-S was confirmed using agarose gel electrophoresis, zeta potential and TEM and the data is presented below.

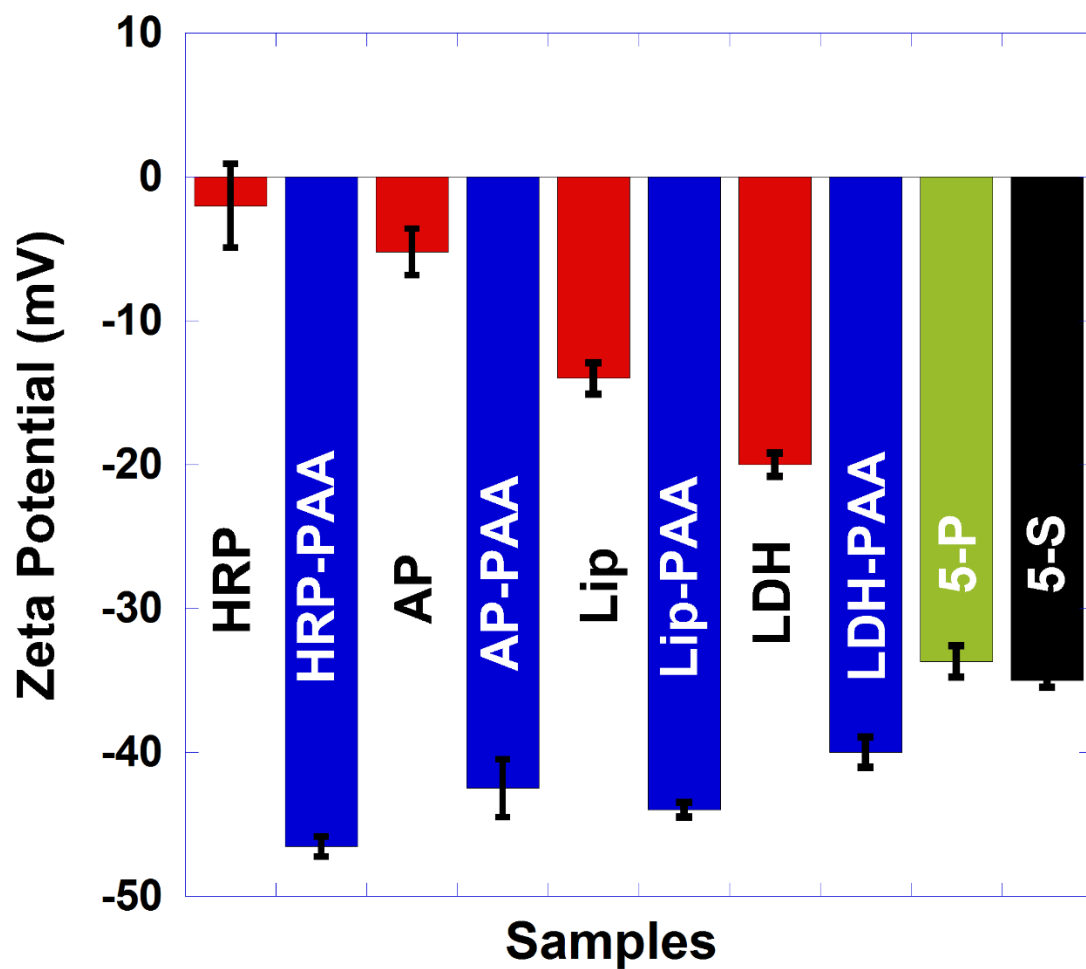
**4.4.2 Agarose gel electrophoresis.** Agarose gel electrophoresis studies were performed at pH 7.4, 40 mM Tris acetate buffer to confirm the successful conjugation of enzymes and PAA to form MEC's. Figure 4.1A presents the gel electrophoresis data of the same. Lane 1 -7 were loaded with- lipase, GOx, LDH, AP, HRP, 5-P and 5-S respectively. Agarose gel electrophoresis technique is based on the electrophoretic mobilities and molecular weight of the samples. Due to PAA crosslinking to the enzymes enzyme-PAA and MEC's should exhibit more negative charge due to free carboxyl groups on PAA and therefore should move more towards positive side in the gel. Contrariwise, if the sample has very high molecular weight due to extensive crosslinking it should resist the movement through the gel and will be stuck. Based on the gel (Figure 4.1A), all the enzymes

traveled towards positive side of the gel due to net negative charge on them. HRP, due to its isoenzyme features (pI - 3 to 9), was not stained and was not visible in lane 5.<sup>4</sup> Whereas, 5-P and 5-S was stuck in the wells due to very high molecular weight by extensive crosslinking to PAA. There was no sign of free enzyme present in MEC's as there was no visible band at the same height compared to that of enzymes in lane 1-5. This proves the successful synthesis of 5-P and 5-S without the presence of free enzyme. Similarly, zeta potential studies were carried out to substantiate the confirmation of the synthesis and the data is presented below.

**4.4.3 Zeta potential study.** Zeta potential measurements were carried out in pH 7.4 PB to establish the charge and the electrophoretic mobility on the conjugates and enzymes. Successful conjugation of PAA to enzyme and formation of MEC can be tracked by charge on the samples. As enzymes get conjugated to PAA covalently, due to the presence of  $-\text{COOH}$  groups on the PAA, cumulative charge on the enzyme-PAA and MEC should decrease compared to unmodified enzymes. This was established by zeta potential studies. Figure 4.1B shows the zeta potential of GOx and GOx-PAA, 5-P and 5-S and was determined to be -1.50 mV, -45.0, -33.5 and -35.0 mV, respectively. Similar observations were found in case of other enzymes such as, HRP, AP, Lip and LDH. For example, HRP, AP, Lip and LDH showed zeta potential of -2.00, -5.22, -14.0 and -20.0 mV. This decreased considerably when conjugated to PAA. Therefore, HRP-PAA, AP-PAA, Lip-PAA and LDH-PAA showed zeta potential of -46.5, -42.5, -44.0 and -40.0 mV. This confirms effective synthesis of enzyme-PAA, 5-P and 5-S. The data for HRP, AP, Lip and LDH is presented in Figure 4.2.



**Figure 4.1.** (A) Agarose gel electrophoresis of enzymes (Lipase, GOx, LDH, AP and HRP), 5-P and 5-S loaded in lanes 1-7 respectively. Agarose gel electrophoresis was performed in pH 7.4, 40 mM Tris acetate. (B) Zeta potential studies of 5-P (green), 5-S (black), GOx-PAA (blue) and GOx (red) done at 25 °C in pH 7.4, 10 mM PB.

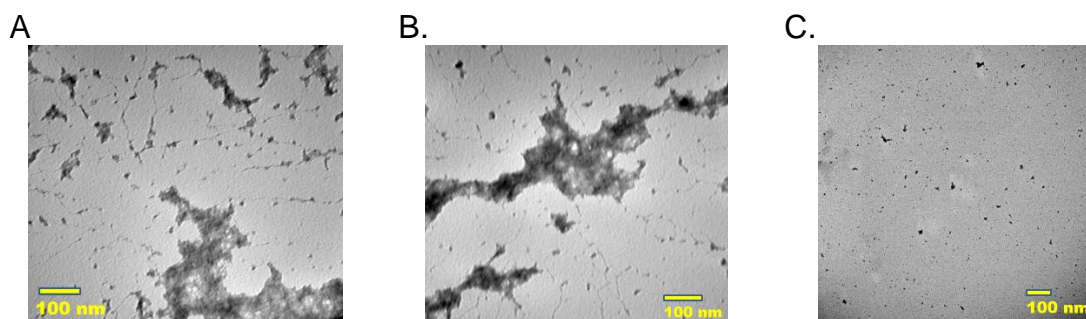


**Figure 4.2.** Zeta potential of unmodified enzymes, enzyme-PAA and multienzyme complexes (MEC's), experiment was performed in pH 7.4 PB at 25 °C. Zeta potential of HRP, HRP-PAA, AP, AP-PAA, Lip, Lip-PAA, LDH, LDH-PAA, 5-P and 5-S are given in the figure.

**4.4.4 Transmission Electron Microscopy (TEM).** Morphologies of MEC's, enzyme-PAA and unmodified enzymes were analyzed using TEM. Samples 5-P, 5-S and GOx were imaged using tecnai t20 TEM, Sample 5-P and 5-S showed extensive crosslinked nanogels structure whereas GOx (C) showed aggregated particles, Figure 4.3 (A-C). Morphology of GOx-PAA which also presented nanogels have been previously reported. <sup>4</sup>

**4.4.5 Dynamic Light Scattering (DLS).** The hydrodynamic radius of MEC's, enzyme-PAA and native enzymes were determined by DLS. All the samples were diluted using pH 7.4 PB such that the equivalent enzyme concentration while doing the DLS is 0.5 nM. The enzymes GOx, HRP, AP, Lip and LDH showed hydrodynamic radius of 6.02, 1.84, 9.10, 1.49 and 3.44 nm, respectively. Some of the enzymes showed aggregation and consequently higher radius compared to single unmodified enzyme. Conjugating the enzymes PAA should result in further increase in hydrodynamic radius of the conjugates. This hypothesis was proven by recording the size of GOx-PAA, HRP-PAA, AP-PAA, Lip-PAA and LDH-PAA, which was 22.3, 26.8, 32.6, 16.7 and 16.6 nm, respectively. Size of MEC's showed variable sizes of conjugates. This is due to random nature of conjugation and incorporation of different sized proteins. Therefore 5-P and 5-S showed sizes in range of 80 to 100 nm. The data for sizes of samples is gathered and presented in Table 4.1.





**Figure 4.3.** Transmission electron microscopy was performed for imaging (A) 5-P, (B) 5-S and (C) GOx. Samples were diluted using pH 7.4 PB such that equivalent protein concentration was 5-10 nM and stained using 0.5 wt % uranyl acetate.

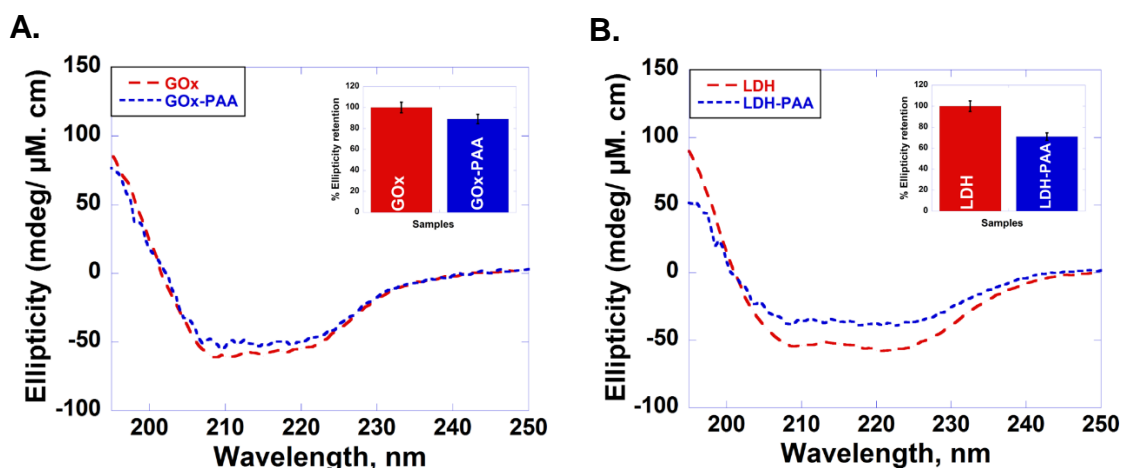
**Table 4.1.** DLS data of MEC's, enzyme-PAA and enzymes illustrating the size of the samples. Data is gathered at pH 7.4 PB at 25 °C.

Sample	Size (radius, nm)	Sample	Size (radius, nm)
GOx	6.02	GOx-PAA	22.3
HRP	1.85	HRP-PAA	26.8
AP	9.10	AP-PAA	32.6
Lip	1.49	Lip-PAA	16.7
LDH	3.44	LDH-PAA	16.6
5-P	97.8	5-S	86.9

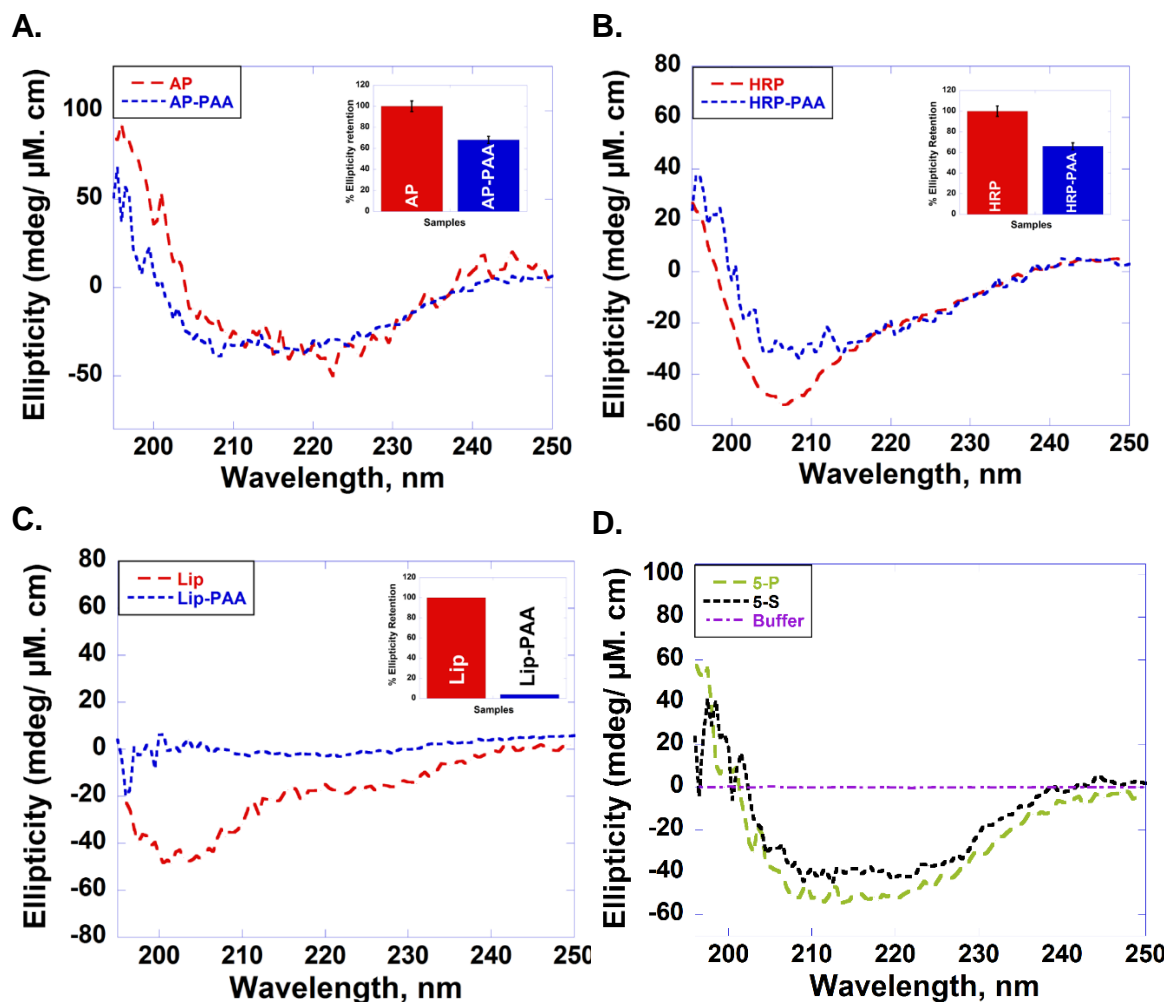
**4.4.6 Circular Dichroism (CD) studies.** Circular dichroism (CD) studies were done for evaluating the secondary structure of the protein before and after the conjugation with PAA. It is expected that conjugation of PAA to enzymes will result in reduction in relative ellipticity compared to unmodified enzymes. This is due to the physical strain put on enzymes due to covalent nature of conjugation to PAA. This was examined using far-UV CD experiments. These studies were carried out in pH 7.4 PB at room temperature.

Figure 4.4 gives the CD spectra of GOx, GOx-PAA (A) and LDH, LDH-PAA (B). Also, inset figure gives the relative % ellipticity retention of enzyme –PAA and unmodified enzyme. To calculate relative % ellipticity retention, signal intensity of samples at 222 nm was used. The signal intensity at that wavelength for unmodified enzyme was referenced at 100% and based on that relative intensity of enzyme-PAA was calculated on per cent basis. The CD spectra and relative % ellipticity retention of AP, AP-PAA (A), HRP, HRP-PAA (B), Lip, Lip-PAA (C), 5-P and 5-S (D) is given in Figure 4.5. To calculate the relative % ellipticity retention signal intensity at lowest position in CD spectra was used which was at 222 nm for GOx, LDH and AP and at 208 nm for Lip and HRP. CD spectra for MEC's were given to show that the enzyme secondary structure was preserved after extensive crosslinking and PAA conjugation. Relative % ellipticity retention showed reduction in retention of secondary structure compared to unmodified enzyme due to PAA conjugation, as expected. GOx-PAA, LDH-PAA, AP-PAA, HRP-PAA and Lip-PAA showed reduction in % relative ellipticity retention to 89, 71, 68, 66 and 4 %. The effect of reduction in relative secondary structure of enzymes in enzyme-PAA and

preservation of secondary structure of enzymes in 5-P and 5-S on activity of MEC, enzyme-PAA and enzymes at room temperature (25 °C) and at high temperature (65 °C) is monitored and presented below.



**Figure 4.4.** Circular dichroism (CD) spectra of (A) GOx (red), GOx-PAA (blue) and (B) LDH (red) and LDH-PAA (blue). CD spectra was monitored from 190-250 nm in pH 7.4 PB at room temperature (25 °C). The inset figure gives the relative ellipticity retention, when peak at 222 nm for unmodified enzyme is referenced at 100 % and relative signal intensity of enzyme-PAA is compared to that.

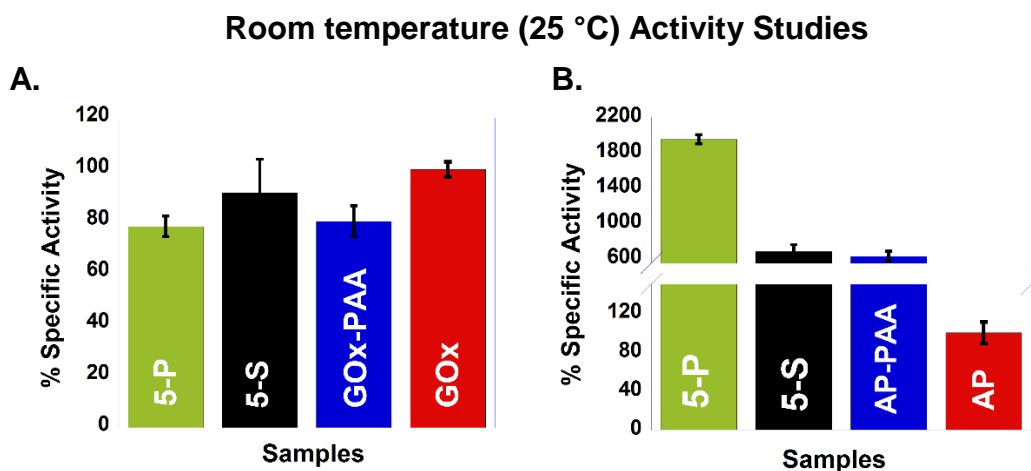


**Figure 4.5.** Circular dichroism (CD) spectra of (A) AP (red), AP-PAA (blue) and (B) HRP (red) HRP-PAA (blue) (C) Lip (red), Lip-PAA (blue) (D) 5-P (green) and 5-S (black). CD spectra was monitored from 190-250 nm in pH 7.4 PB at room temperature (25 °C). The inset figure gives the relative ellipticity retention, when peak at 222 or 202 nm for unmodified enzyme is referenced at 100 % and relative signal intensity of enzyme-PAA is compared to that.

**4.4.7 Activity studies.** Activity studies of enzymes, enzyme-PAA and MEC's were carried out at room temperature at pH 7.4 using 10 mM PB. Appropriate substrates and assay procedures were used to test the activity of the samples. For GOx, HRP, AP, LDH and Lip substrates such as glucose, o-methoxyphenol, 4-nitrophenyl phosphate, NADH and 4-nitrophenyl acetate were used, respectively. Relative % specific activity of each sample was calculated by referencing initial rate of corresponding unmodified enzyme as 100%.

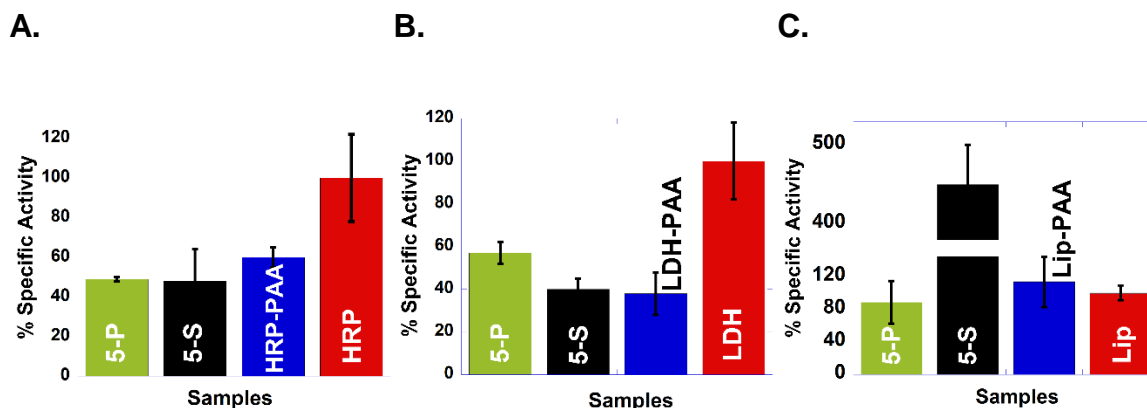
**4.4.7.1 Activity studies at room temperature.** The structural dependence of enzymes and enzyme-PAA and MEC's on activities were evaluated using activity measurements at room temperature. Figure 4.6 gives the relative % specific activities for GOx (A) and AP (B) and the same for HRP, LDH and Lip is given in Figure 4.7. Activities studies carried out with GOx and samples carrying GOx such as GOx-PAA, 5-P and 5-S and showed % specific activities of more than ~75%. All % specific activities were referenced using initial rate of GOx at room temperature at pH 7.4 PB as 100%. Precisely GOx-PAA, 5-P and 5-S showed activities of 80, 78 and 91% respectively. In other case, AP showed large increase in % specific activity, where, AP-PAA, 5-P and 5-S showed activity of 626, 1940 and 970%, respectively. Similar results were obtained in case of Lip, where Lip-PAA, 5-P and 5-S showed activity of 114, 89 and 450%, respectively. This unprecedented increase in activity of AP and Lip could be attributed to increased access of active site to the substrate. In case of HRP and LDH the enzyme-PAA and MEC's showed decrease in activities. For HRP, HRP-PAA, 5-P and 5-S

showed activities of 60, 49 and 54%, respectively. Whereas, LDH conjugates such as, LDH-PAA, 5-P and 5-S showed activities of 38, 57 and 40%, respectively.



**Figure 4.6.** Activity studies were carried out at room temperature (25 °C) in pH 7.4, 10 mM, PB for GOx and AP containing samples and data is presented. % specific activity is plotted on Y axis. To calculate % specific activity, initial rate of unmodified enzyme at 25 °C was referenced at 100% and all other samples were compared to that. In above figure % specific activity of GOx containing samples (A) and AP containing samples (B) were presented 5-P, 5-S are represented as green and black. GOx, GOx-PAA, AP and AP-PAA are represented as red, blue, red and blue respectively.

### Room Temperature (25 °C) Activity Studies



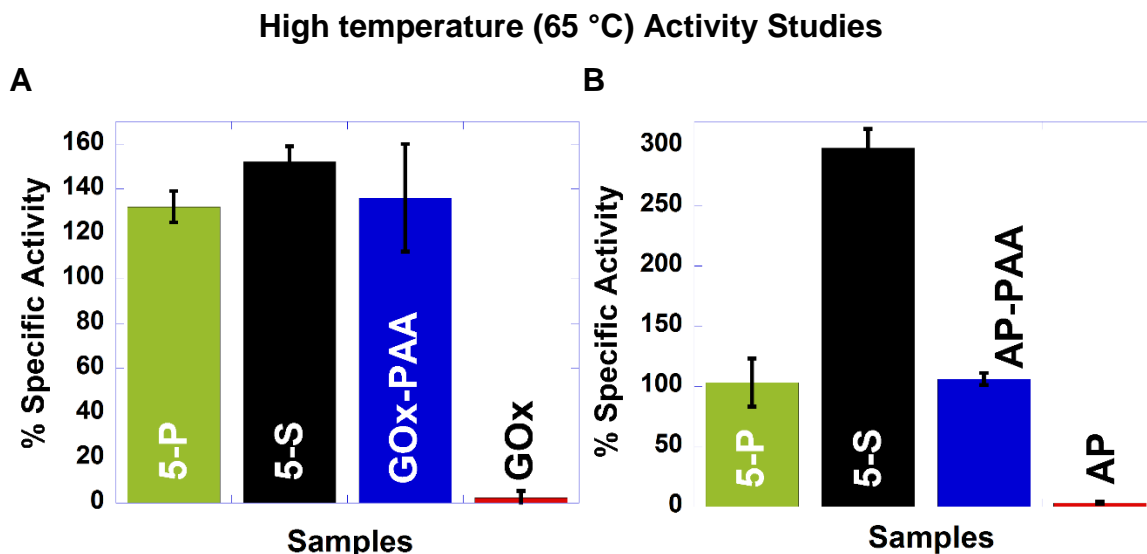
**Figure 4.7.** Activity studies were carried out at room temperature (25 °C) in pH 7.4, 10 mM, PB for HRP, LDH and Lip containing samples and data is presented. % specific activity is plotted on Y axis. To calculate % specific activity, initial rate of unmodified enzyme was referenced at 100% and all other samples were compared to that. In above figure % specific activity of HRP containing samples (A), LDH containing samples (B) and Lip containing samples (C) were presented. 5-P, 5-S are represented as green and black. HRP, HRP-PAA, LDH, LDH-PAA, Lip and Lip-PAA are represented as red, blue, red, blue, red and blue respectively.

**4.4.7.2 Activity studies at 65 °C.** The activity at room temperature was followed by testing the activity of samples at high temperature. The activity retention at high temperature is desired as this improves the power density of biofuel cell by many folds. Error! Bookmark not defined. The activity studies were carried out with the similar methods as described in experimental sections at 65 °C. The samples were incubated in the cuvette such that temperature is stable at 65 °C and then substrate is added and product formation is monitored. Figure 4.8 shows the % specific activity plots for GOx and AP samples. Plots for other enzymes such as HRP, LDH and Lip are given in Figure 4.9.

Activity studies at high temperature were carried out for all samples. GOx containing samples showed complete deactivation in case of unmodified GOx. Although GOx-PAA, 5-P and 5-S showed 136, 132 and 112% activity retention (Figure 4.8A). In case of AP, unmodified AP showed deactivation, whereas, AP-PAA, 5-P and 5-S showed 106, 103 and 298% activity retention (Figure 4.8B). HRP was the only enzyme which retained 47% of its activity at 65 °C. HRP-PAA, 5-P and 5-S displayed activity retention of 149, 98 and 138% (Figure 4.9A). In case of LDH and Lip, both unmodified enzymes lost its activity at 65 °C, also, LDH and Lip containing MEC showed peculiar behavior, where, 5-P lost its activity at 65 °C (Figure 4.9B-C). LDH-PAA and 5-S exhibited 146 and 77% activity retention for LDH enzymatic activity. Whereas, Lip-PAA and 5-S showed 78 and 540% activity retention for Lip enzymatic activity. Effect of the polymer scaffolding on enzymatic rate constants was evaluated using Lineweaver Burk plots to extract kinetic

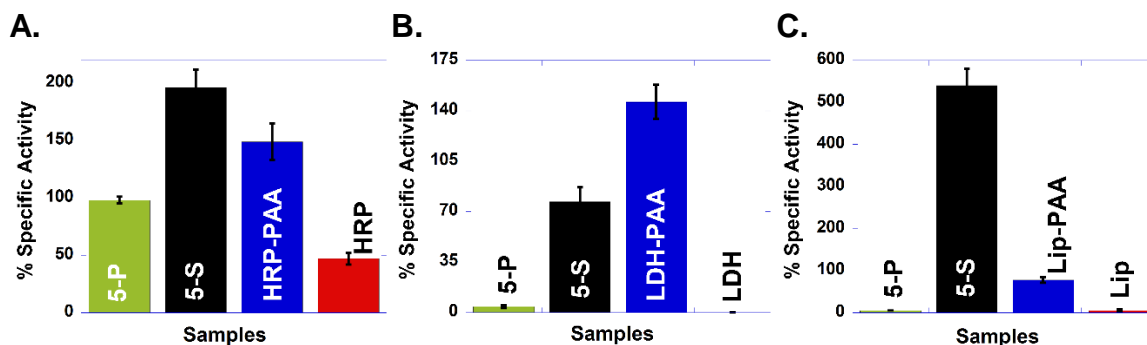


constants such as  $K_M$ ,  $V_{max}$ , Catalytic efficiency and  $K_{cat}$ . This data is presented below.



**Figure 4.8.** Activity studies were carried out at room temperature (65 °C) in pH 7.4, 10 mM, PB for GOx and AP containing samples and data is presented. % specific activity is plotted on Y axis. To calculate % specific activity, initial rate of unmodified enzyme at 25 °C was referenced at 100% and all other samples were compared to that. In above figure % specific activity of GOx containing samples (A) and AP containing samples (B) were presented 5-P, 5-S are represented as green and black. GOx, GOx-PAA, AP and AP-PAA are represented as red, blue, red and blue respectively.

### High Temperature (65 °C) Activity Studies



**Figure 4.9.** Activity studies were carried out at room temperature (65 °C) in pH 7.4, 10 mM, PB for HRP, LDH and Lip containing samples and data is presented. % specific activity is plotted on Y axis. To calculate % specific activity, initial rate of unmodified enzyme at 25 °C was referenced at 100% and all other samples were compared to that. In above figure % specific activity of HRP containing samples (A), LDH containing samples (B) and Lip containing samples (C) were presented. 5-P, 5-S are represented as green and black. HRP, HRP-PAA, LDH, LDH-PAA, Lip and Lip-PAA are represented as red, blue, red, blue, red and blue respectively.

**4.4.8 Kinetic studies.** Enzymatic catalytic rates were used to assemble the Lineweaver Burk plots which were then used to compute kinetic parameters such as  $K_M$ ,  $V_{max}$ ,  $K_{cat}$  and catalytic efficiency. Lineweaver Burk plots of GOx and AP containing samples are presented in Figure 4.10. Lineweaver Burk plots were gathered by plotting  $1/\text{initial rate}$  vs  $1/\text{substrate concentration}$ . Using these plots,  $K_M$  and  $V_{max}$  values were gathered.  $K_M$  value is the reciprocal of negative Y-intercept, whereas,  $V_{max}$  value is the reciprocal of X intercept of Lineweaver Burk plots.  $K_M$  values signifies the affinity of the substrate towards the enzymes and higher  $K_M$  value indicates lower affinity of substrate to enzymes. While,  $V_{max}$  value denotes the maximum velocity of the enzymatic reaction. Based on  $K_M$  and  $V_{max}$  values, other parameters were gathered. Turnover numbers were given in terms on  $K_{cat}$  values and catalytic efficiency was calculated by taking ratio of  $K_{cat}/K_M$ .

Lineweaver Burk plots of GOx and AP containing samples are given in Figure 4.10 and that of HRP, LDH and Lip are given in Figure 4.11. The kinetic parameters of all the samples using 5 different enzymatic assays are given in Table 4.2. According to Figure 4.10A and Table 4.2, GOx, GOx-PAA, 5-P and 5-S showed  $K_M$  values of 5.17, 0.844, 5.93 and 1.98 mM, respectively. Same samples showed catalytic efficiencies of 0.103, 0.096, 0.050 and 0.064 in the same order. In case of  $K_{cat}$ , GOx showed highest value of 0.533 and GOx-PAA showed lowest value of  $0.081\text{ s}^{-1}$ .

Similarly, studies were carried out for AP containing samples (Figure 4.10 and Table 4.2).  $K_M$  values of AP, AP-PAA, 5-P and 5-S were 21.9, 43.0, 12.9 and 6.55 mM, respectively. AP showed lowest  $K_{cat}$  and catalytic efficiency which was, 0.002

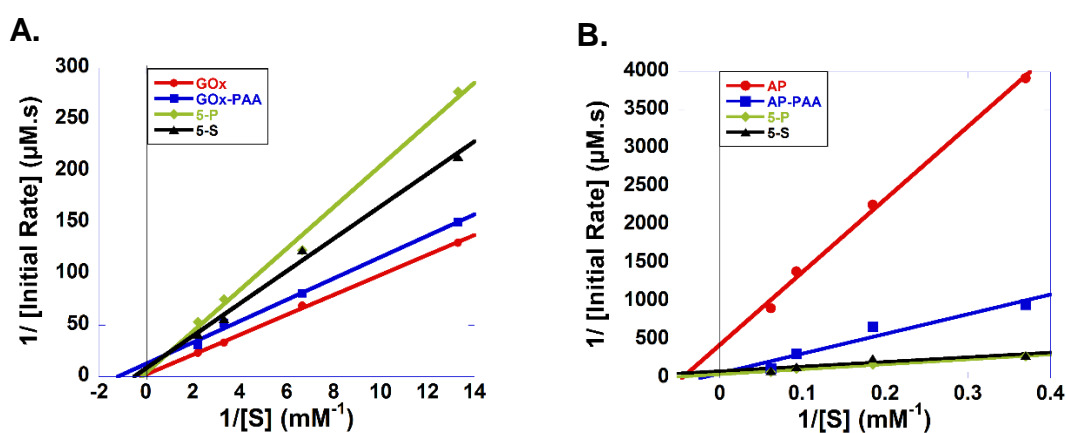
$\text{s}^{-1}$  and  $9.11 \times 10^{-5}$ . While, 5-P and 5-S showed highest  $K_{\text{cat}}$  and catalytic efficiency values.  $K_{\text{cat}}$  values of 5-P and 5-S were  $0.020$  and  $0.011 \text{ s}^{-1}$ , respectively and catalytic efficiency values were  $1.55 \times 10^{-3}$  and  $1.68 \times 10^{-3}$ , respectively.  $K_{\text{cat}}$  value for AP-PAA was  $0.020 \text{ s}^{-1}$  and catalytic efficiency was  $3.96 \times 10^{-4}$ .

Likewise studies were performed and Lineweaver Burk plots were gathered for HRP containing samples and  $K_{\text{M}}$  values for HRP, HRP-PAA, 5-P and 5-S were  $0.107$ ,  $0.461$ ,  $0.796$  and  $0.330 \text{ mM}$ , respectively (Figure 4.11A and Table 4.2). HRP and HRP-PAA showed very similar catalytic efficiency values of  $0.318$  and  $0.308$ . Whereas, catalytic efficiency decreased for 5-P and 5-S and it was  $0.155$  and  $0.097$ , respectively. In case of  $K_{\text{cat}}$ , HRP-PAA and 5-P showed similar values of  $0.142$  and  $0.123 \text{ s}^{-1}$ . Similarly,  $K_{\text{cat}}$  for HRP and 5-S  $K_{\text{cat}}$  was very close, having the value of  $0.034$  and  $0.032 \text{ s}^{-1}$ , respectively.

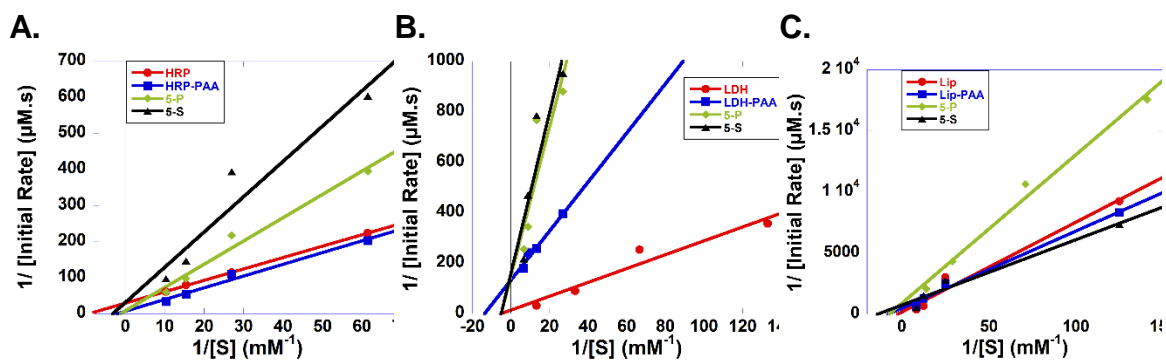
Similarly, Lineweaver Burk plots for LDH containing enzymes were assembled and kinetic values were extracted (Figure 4.11B and Table 4.2).  $K_{\text{M}}$  values for LDH, LDH-PAA, 5-P and 5-S were  $0.198$ ,  $0.073$ ,  $0.196$  and  $0.196 \text{ mM}$  and catalytic efficiencies were  $0.364$ ,  $0.096$ ,  $0.036$  and  $0.031$  in the same order. LDH exhibited highest  $K_{\text{cat}}$  of  $0.072 \text{ s}^{-1}$ , whereas, LDH-PAA, 5-P and 5-S showed  $K_{\text{cat}}$  values of  $0.007$ ,  $0.007$  and  $0.006 \text{ s}^{-1}$ , respectively.

In the same manner Lineweaver Burk plots for Lip were assembled (Figure 4.11C and Table 4.2). Accordingly,  $K_{\text{M}}$  values of Lip, Lip-PAA, 5-P and 5-S were  $0.372$ ,  $0.122$ ,  $0.133$  and  $0.070 \text{ mM}$  and catalytic efficiencies were  $0.013$ ,  $0.016$ ,  $0.007$  and  $0.014$ , respectively. Lip exhibited highest turnover number ( $K_{\text{cat}}$ ) of  $0.005$

s<sup>-1</sup>, whereas, Lip-PAA, 5-P and 5-S exhibited similar  $K_{cat}$  values of 0.002, 0.001 and 0.001, respectively.



**Figure 4.10.** (A) Lineweaver burk plots of GOx (red), GOx-PAA (blue), 5-P (green) and 5-S (black) with increasing glucose (0.075 – 0.45 mM). (B) Lineweaver Burk plots of AP (red), AP-PAA (blue), 5-P (green) and 5-S (black) with increasing 4-nitrophenylphosphate (2.7 – 16.2 mM). Studies were carried out in pH 7.4, 10 mM PB.



**Figure 4.11.** (A) Lineweaver burk plots of HRP (red), HRP-PAA (blue), 5-P (green) and 5-S (black) with increasing o-methoxyphenol (0.0163 – 0.097 mM). (B) Lineweaver Burk plots of LDH (red), LDH-PAA (blue), 5-P (green) and 5-S (black) with increasing NADH (0.007 – 0.15 mM). (C) Lineweaver Burk plots of Lip (red), Lip-PAA (blue), 5-P (green) and 5-S (black) with increasing 4-nitrophenylacetate (0.008 – 0.12 mM). Studies were carried out in pH 7.4, 10 mM PB/ Tris acetate.

**Table 4.2.** Kinetic parameters such  $K_M$ ,  $V_{max}$ ,  $K_{cat}$  and catalytic efficiency of all the enzymes, enzyme-PAA, 5-P and 5-S. All the kinetic parameters were gathered in pH 7.4, 10 mM Tris/ phosphate buffer.

	$K_M$ (mM)	$V_{max}$ ( $\mu\text{M}^{-1}\text{s}^{-1}$ )	$K_{cat}$ ( $\text{s}^{-1}$ )	Catalytic Efficiency
<b>GOx enzymatic assay</b>				
GOx	5.17	0.533	0.533	0.103
GOx-PAA	0.844	0.081	0.081	0.096
5-P	5.93	0.294	0.294	0.050
5-S	1.98	0.126	0.126	0.064
<b>AP enzymatic assay</b>				
AP	21.9	0.002	0.002	$9.11 \times 10^{-5}$
AP-PAA	43.0	0.017	0.017	$3.96 \times 10^{-4}$
5-P	12.9	0.020	0.020	$1.55 \times 10^{-3}$
5-S	6.55	0.011	0.011	$1.68 \times 10^{-3}$
<b>Lip enzymatic assay</b>				
Lip	0.373	0.005	0.005	0.013
Lip-PAA	0.122	0.002	0.002	0.016
5-P	0.133	0.001	0.001	0.007
5-S	0.070	0.001	0.001	0.014
<b>HRP enzymatic assay</b>				
HRP	0.107	0.034	0.034	0.318
HRP-PAA	0.461	0.142	0.142	0.308
5-P	0.796	0.123	0.123	0.155
5-S	0.330	0.032	0.032	0.097
<b>LDH enzymatic assay</b>				
LDH	0.198	0.072	0.072	0.364
LDH-PAA	0.073	0.007	0.007	0.096
5-P	0.196	0.007	0.007	0.036
5-S	0.196	0.006	0.006	0.031

## 4.5 Discussion.

Here 5 enzymes were conjugated to form MEC's using two different techniques such as parallel and sequential synthesis. In case of parallel synthesis, two step synthesis methodology was followed. In first step enzyme-PAA conjugates were made using EDC chemistry by covalently crosslinking lysine amino ( $\text{NH}_2$ ) groups from enzyme and carboxyl ( $-\text{COOH}$ ) groups from PAA. In second step these enzyme-PAA conjugates were further conjugated using crosslinked EDC to form MEC, 5-P, where 5 denotes number of enzymes present in MEC and P denotes the parallel synthesis method. In sequential synthesis, one step synthesis is followed and all 5 enzymes and PAA was added to form the mixture which was crosslinked using EDC by crosslinking lysine  $\text{NH}_2$  from enzymes and  $-\text{COOH}$  from PAA. This MEC was denoted as 5-S, where 5 signifies number of enzymes present in MEC and S denotes sequential synthesis method for production of MEC. Previously, we have shown the use of PAA for covalently modifying enzymes for improving its stability and activity. Here, we want to progress towards stabilizing and retaining the activity of more than one enzyme using hydrophilic matrix of PAA for use in multiple applications of biocatalysis and expanding it for biofuel cell.

Successful syntheses of 5-P, 5-S and enzyme-PAA conjugates were evaluated using agarose gel electrophoresis, TEM, DLS and zeta potential studies. Covalent conjugation of enzymes to PAA was confirmed using agarose gel electrophoresis and zeta potential. Agarose gel electrophoresis studies were based on the size and charge of the samples. MEC's carry more negative charge due to carboxyl groups from PAA and they are larger in size compared to individual enzymes.



Therefore, increased negative charge should propel the MEC's towards positive electrode of the gel but the increased size of the MEC's can hamper its movement. Therefore, decreased mobility of 5-P and 5-S is possible and can be attributed to increased size of the MEC as seen in Figure 4.1A. Due to this the MEC's were stuck in the well of the agarose gel (Lane 6 and 7). This data was corroborated by TEM images. As can be seen from Figure 4.3A and B, 5-P and 5-S showed extensively crosslinked nanogel morphological structure on TEM grid. Whereas, GOx showed discreet aggregated particles. The aggregation of the proteins can be due to the stain or TEM grid itself. Similar nanogels morphological structures were reported for enzyme-PAA samples previously. Error! Bookmark not defined.

Zeta potential was used for measuring the surface charge on the MEC's, enzyme-PAA conjugates and enzymes. It is an important tool that can generate an extensive information regarding the surface electrostatic environment of the samples. The covalent conjugation of PAA to enzyme should result in increased negative surface charge on the MEC's and the enzyme-PAA conjugates. This was confirmed using zeta potential measurements. MEC's and enzyme-PAA conjugates showed increased negative zeta potential compared to unmodified enzymes (Figure 4.1B) which established the covalent nature of conjugation of PAA to enzymes. The increase in size of the MEC's and enzyme-PAA conjugates were confirmed using DLS studies (Table 4.1). DLS data showed the increased size of unmodified enzymes after initial conjugation to PAA in first step of synthesis of 5-P. The enzyme size of all 5 enzymes were in the range of 1-10 nm, which was increased for enzyme-PAA conjugates. The range of sizes for enzyme-PAA

conjugates were in the range of 10-35 nm. The 5-P and 5-S showed further increase in hydrodynamic size due to extensive polymer crosslinking to ~100 nm. This proves the successful synthesis of enzyme-PAA and MEC's. Further the effect of polymer conjugation on enzyme structure was tested by evaluating enzyme secondary structure using CD studies.

CD studies were carried out to test the secondary structure of the enzymes after PAA conjugation and consequent synthesis of MEC's, which is necessary for retention of bio catalytic activity. PAA conjugation resulted in 30-40% reduction in secondary structure in case of all 5 enzymes (Figure 4.4, 4.5). This reduction in secondary structures can be attributed to the structural constraints put on the enzymes due to hydrophilic PAA matrix by covalent conjugation. CD studies were also performed on 5-P and 5-S to check the retention of the secondary structure. The CD spectra of MEC's were not compared with individual enzymes or enzyme-PAA since MEC's contained all 5 enzymes in solution and it will be difficult to resolve the spectra for individual enzymes. Although, CD spectra for 5-P and 5-S showed retention of shape for secondary structure of all 5 enzymes combined. This proves that the enzymes in MEC's retained its secondary structure to considerable amount. Therefore, CD studies confirmed the retention in secondary structure of enzymes in PAA matrix for enzyme-PAA and MEC's. Further the effect of loss of 30-40% secondary structure of enzymes in PAA matrix on biological activity of enzymes were tested. Biological activity of MEC's, enzyme-PAA and unmodified enzymes were carried out at room temperature and at high temperature at pH 7.4.

Catalytic activity of conjugates were reported previously at room and high temperature. Although, catalytic activity of an enzyme in presence of other enzymes were not reported before. Here, effect of presence of multiple enzymes on activity of one of the enzymes was tested. Also, in case of 5-P, domain formation of each enzyme-PAA was expected as each enzyme-PAA was synthesized in first step which was extensively crosslinked in second step (Scheme 4.1). This domain formation will result in patches of individual enzymes together. This scenario was not foreseen in case of 5-S as all 5 enzymes were mixed along with PAA and MEC, 5-S was synthesized in single step. Therefore, domain formation of enzyme-PAA was avoided in case of 5-S. Therefore effect of presence and absence of domains were tested on biocatalysis at room and high temperatures.

Room temperature activities were carried out using 5 different enzymatic assays corresponding to individual enzymes. Enzymatic assay for GOx showed that GOx-PAA, 5-P and 5-S showed reduction in % specific activity to 80, 78 and 91 %, respectively. In case of GOx activity assay the reduction in activity was not considerable. But, in case of HRP and LDH the reduction in activities were notable. In case of HRP; HRP-PAA, 5-P and 5-S showed activities of 60, 49 and 48%, respectively. While, in case of LDH; LDH-PAA, 5-P and 5-S showed activities of 30, 57 and 40%, respectively. Therefore PAA conjugation doesn't affect the enzymatic assay of GOx in of GOx-PAA, 5-P and 5-S. Although in case of HRP and LDH, HRP-PAA, 5-P and 5-S resulted in loss of considerable amount of activity over ~ 60 -65%. The loss in activity in case of enzyme-PAA, 5-P and 5-S

for HRP and LDH containing conjugates and MEC's can be attributed to extensive network of PAA. Therefore, substrates take time to reach the active site and subsequently rate of enzymatic reaction is reduced, considerably. While, in case of GOx enzymatic assay, samples such as GOx-PAA, 5-P and 5-S, the enzymatic activity was not affected. Therefore, GOx, HRP and LDH assays showed no difference in % specific activity for enzyme-PAA, 5-P and 5-S. Therefore, presence or absence of domains of enzymes in MEC's did not affect the enzymatic activities of GOx, HRP or LDH, as both 5-P and 5-S showed similar % specific activities at room temperature.

On the other hand enzymatic assays for AP and Lip showed unprecedented increase in the % specific activity for enzyme-PAA and MEC's. Enzymatic assays for AP showed very high increase in activity in case of AP-PAA, 5-P and 5-S to 626, 1948 and 680%, respectively. In case of lipase assay; Lip-PAA, 5-S and 5-S showed activities of 114, 89 and 450%, respectively. The enhancement in the enzymatic activity of AP and Lip was corroborated by the previous findings in the literature.<sup>25, 26</sup> This very high enhancement in the activity could be attributed to the exposure of the active site to the substrate. To test the robustness of these enzyme-PAA and MEC's activity studies were performed at high temperature (65 °C).

High temperature activity studies proved that PAA conjugation to enzymes in individual and multienzyme fashion improved its stability and activity retention. GOx activity assay proved that hydrophilic matrix around the enzyme resulted in retention of its > 100% of the activity for GOx-PAA, 5-P and 5-S samples. Similar

observations were made for AP and HRP activity assays where, AP-PAA, HRP-PAA, 5-P and 5-S samples retained more than 100% of the activity. The activity of 5-S in case of AP and HRP activity assay was enhanced to 300 and 200%, respectively. The higher kinetics rates could be suspected for such increase in activity. Also, increase in activity was only observed in case of 5-S, therefore, domain formation as in case of 5-P seemed to be unnecessary for augmentation of activity at high temperatures. At the same time domain formation did not negatively impact the activity of 5-P in case of GOx, AP or HRP activity assays.

Peculiar behavior was observed in case of LDH and Lip activity assays, where, 5-P at high temperature did not show any activity. Therefore, domain formation from 5-P in case of LDH and Lip activity assay adversely affected the activity at high temperatures. This proves synthesis of MEC's in sequential fashion is the superior method for retention of activity at higher temperatures for certain enzymes. This was proved as 5-S in case of LDH and Lip activity assay showed 77% and 540% of activity which was better compared to 5-P. To eliminate the activity enhancement by increased temperature, resulting in, product formation due to substrate degradation, controls were carried out without incorporation of enzyme samples. The resulting initial rate was computed after subtraction of initial rate when enzymatic samples were not present in the activity assay to eliminate the false enhancement in activity. This showed systematically the effect of domain formation on activity of MEC's at room and high temperatures. Further, to find out the reason behind the activity enhancement at room temperature kinetics studies were carried out. This was done by use of Lineweaver Burk plots. Systematic

changes in  $K_M$ ,  $V_{max}$ ,  $K_{cat}$  and catalytic efficiencies were monitored after conjugation of enzymes to PAA in enzymes-PAA, 5-P and 5-S samples.

Kinetic data showed that, for GOx containing samples,  $K_M$  values of GOx-PAA and 5-S were 0.844 and 1.98 mM that were very low compared to  $K_M$  values of GOx (5.17 mM) this explains the increased substrate affinity. 5-P showed slightly higher  $K_M$  (5.93 mM) compared to GOx. The reduced  $K_M$  explains the retention of activity at high temperature where GOx loses its activity completely. The huge enhancement of activity retention in case of AP activity assay for AP-PAA, 5-P and 5-S can be explained based on  $K_M$  and catalytic efficiency. At room temperature, AP-PAA and 5-S had 6 times higher and 5-P had 20 times higher activity compared to AP. This correlates to that of catalytic efficiency of these samples. AP had catalytic efficiency of  $9.11 \times 10^{-5}$  which increased to  $3.96 \times 10^{-4}$  for AP-PAA and  $1.55 \times 10^{-3}$  and  $1.68 \times 10^{-3}$  for 5-P and 5-S, respectively. 5-S and 5-P showed higher substrate affinity as their  $K_M$  values were 12.9 and 6.55 mM, respectively, which were lower than that of AP (21.9 mM).

Reduction in activity of LDH and HRP containing samples after polymer conjugation and MEC's formation can be explained via changes in  $K_M$  and catalytic efficiency values. As, catalytic efficiency decreased in case of HRP-PAA, 5-P and 5-S to 0.308, 0.155 and 0.097 from 0.318 of HRP. This explains the reduction in activity of HRP (100%) to (45- 60%) for HRP-PAA, 5-P and 5-S. Similar trend can be found in case of LDH containing enzymes. Catalytic efficiencies decreased drastically from 0.364 of LDH to 0.03-0.09 in case of LDH-PAA, 5-P and 5-S. Similarly, activity retention of LDH-PAA, 5-P and 5-S reduced by 40-60%

compared to LDH. Also,  $V_{\max}$  decreased after PAA conjugation to LDH. LDH showed  $V_{\max}$  of 0.072 which decreased to 0.006-0.007 in case of LDH-PAA, 5-P and 5-S. Lip containing samples also showed increase in catalytic efficiencies after polymer conjugation for Lip-PAA and 5-S. Catalytic efficiency of Lip (0.013) increased for Lip-PAA (0.016) and 5-S (0.014), which correlates to increase in activity of Lip-PAA (114 %) and 5-S (450 %). Similarly, decrease in activity of 5-P (89 %) can be related to its decrease in catalytic efficiency (0.007).

#### **4.6 Conclusion.**

This is the first reported method where 5 non cascading enzymes with different pI values were stabilized using polymer encapsulation to form multienzyme complexes (MEC's). MEC synthesis was done using 2 different ways. In parallel synthesis protocol, firstly, individual enzyme-PAA complexes are made by covalent conjugation of primary amine groups of enzymes and carboxylic acid groups on PAA. Further, these enzyme-PAA conjugates were crosslinked by EDC chemistry and 5-P MEC is obtained. In sequential method of synthesis of MEC, all 5 enzymes were mixed with PAA and stirred and then crosslinked using EDC to obtain 5-S. GOx, HRP, Lip, LDH and AP were used as model enzymes and PAA was used as hydrophilic polymer for enzyme stabilization. The synthesis of MEC's and enzyme-PAA were confirmed using agarose gel electrophoresis, zeta potential, DLS and structural and morphological features of the conjugates were studied using CD spectroscopy and TEM. These robust MEC's were used for room and high temperature catalysis which is highly desirable in biofuel cell applications. The difference in synthesis protocols on the MEC microenvironments were

evaluated by its effect on its kinetic parameters by assembling Lineweaver Burk plots. Room temperature activity studies showed that MEC formation enhanced the activity of 5-P and 5-S 5-20 folds compared to unmodified enzyme for AP and Lip. MEC formation had no effect on activity of 5-P and 5-S for GOx activity. Activity of 5-P and 5-S decreased by about 40-50% for LDH and HRP activity assays. At high temperature all the unmodified enzymes lost its activity, except HRP, which retained ~40% of its activity. 5-P and 5-S showed 1 to 3 fold increase inactivity for AP, GOx and HRP activity assay. LDH and Lip showed peculiar behavior where 5-P completely lost its activity and domain formation in case of 5-P proved detrimental for activity retention at high temperature. Although, 5-S retained 70 % in case of LDH and 540 % activity in case of Lip. The variations in activity retentions are explained based on changes in kinetic parameters. As, huge enhancement of activity of AP at room temperature is due to 10-20 fold enhancement in catalytic efficiency of AP-PAA, 5-P and 5-S. This method of polymer encapsulation of 5 enzymes opens up new avenues for stabilization of multienzymes for diverse applications in catalysis and biofuel cells. High temperature applicability of this system can be used in enhancement of power density in case of biofuel cell. Therefore, this strategy can be used in production of bio based fuels in environmentally friendly, benign and biologically compatible methods.

#### 4.7 References

- 
1. Bio Based Economy. [http://www.bioeconomy.net/applications/applications\\_enzymes.html](http://www.bioeconomy.net/applications/applications_enzymes.html) (accessed February 25, **2016**).
  2. Gurung N.; Ray S.; Bose S.; Rai V. *Biomed Res Int.* **2013**, 2013, 1-18



- 
3. Li S.; Yang X.; Yang S.; Zhu M.; Wang X. *Comput Struct biotechnol J.* **2012**, 2, 1-10
  4. Zore O. V.; Pattammattel A.; Gnanaguru S.; Kumar C. V.; Kasi R. M. *ACS Catal.* **2015**, 5, 4979-4988.
  5. Cao X.; Li Y.; Zhang Z.; Yu J.; Qian J.; Liu S. *Analyst.* **2012**, 137, 5785-5791.
  6. Heller A.; Feldman B. *Chem Rev.* **2008**, 108, 2482-2505
  7. Huber C.; Preis M.; Harvey P. J.; Grosse S.; Letzel T.; Schroder P. *Chemosphere.* **2016**, 146, 435-441.
  8. Gong J.; Lee C. S.; Kim E. J.; Chang Y. Y.; Chang Y. S. *J Hazard Mater.* **2016**, 310, 135-142
  9. Karaguler, N.G., Sessions, R.B. & Binay, B. *Biochem. Soc. Trans.* **2007**, 35, 1610-1615.
  10. Claire M. PhD Thesis, University of Birmingham, UK, **2011**.
  11. Tanaka H.; Horiuchi Y.; Konishi K. *Anal. Biochem.* **1975**, 66, 489-497.
  12. Gandhi N. N. Applications of Lipase. *J. Am. Oil Chem. Soc.* **1997**, 74, 621-63.
  13. Gray C. J.; Narang J. S.; Barker S. A. *Enzyme Microb Technol.* **1990**, 12, 800-807.
  14. Negishi S.; Shirasawa S.; Arai Y.; Suzuki J.; Mukataka S. *Enzyme Microb. Technol.* **2003**, 32, 66-70.
  15. Huang J.; Huang Y.; Wu X.; Du W.; Yu X.; Hu X. *Prasiton Res.* **2009**, 104, 287-293.
  16. Nguyen, L.; Dao, T.; Zivkovic, T.; Fehrholz, M.; Schaefer, W.; Salomon, S. *Enzyme Microb. Technol.* **2010**, 46, 479-486

- 
17. Zhang, G.Q.; Chen, Q.J.; Sun, J.; Wang, H.X.; Han, C.H. *J. Basic Microbiol.* **2013**, 53, 868-875.
18. Sung W. J.; Bae Y. H. *Sensor Actuat. B-Chem.* **2006**, 114, 164-169
19. Zhu Z.; Tam T. K.; Sun F.; You C.; Zhang Y. H. P. *Nat. Commun.* **2014**, doi:10.1038/ncomms4026
20. Zore O. V.; Pattammattel A.; Gnanaguru S.; Kumar C. V.; Kasi R. M. *ACS Catal.* **2015**, 5, 4979-4988.
21. Kumar C V.; Chaudhari A. *Chem Comm.* **2002**, 2382-2383.
22. Ramakrishnan V.; Goveas L. C.; Suralikerimath N.; Jampani C.; Halami P. M.; Narayan B. *Biocatal Agric Biotechnol.* **2016**, 6, 19-27.
23. Majumder S. P.; Das A. C. *Ecotoxicol Environ Saf*, **2016**, 126, 56-61.
24. Gordon G. L.; Doelle H. W. *Eur J Biochem*, **1976**, 67, 543-555.
25. Abel B.; Aslan K. *J Colloid Interface Sci.* **2014**, 415, 133-142
26. Lee E. H.; Tsujimoto T.; Uyama H.; Sung M. H.; Kim K.; Kuramitsu S. *Polym J.* **2010**, 42, 818-822

## Chapter 5

### 5. Summary and Proposal of Future Work

#### 5.1 Summary

The thesis presented the various enzyme stabilization strategies using hydrophilic polymer- polyacrylic acid (PAA) and in certain cases using 2D material – graphene oxide. Thus, enzyme-PAA synthesized have shown to be active in organic solvents, lower pH's, higher temperatures, in presence of denaturant and multiple enzymes. Specific strategies are used to stabilize the enzymes in each of the mentioned challenging conditions. For enzymes to be stabilized in organic solvents, Hb was used as a model enzyme and it was covalently conjugated to PAA. To enhance solubility and in turn the activity of Hb the Hb-PAA conjugate was esterified using ethanol (EtOH) and 1-propanol (1-prop). <sup>1</sup> The esterification was performed on the unreacted carboxyl acid groups on PAA and Hb. The Hb-PAA conjugation and esterification was done using EDC chemistry. The synthesis of these conjugates were tested using zeta potential, dynamic light scattering (DLS), infrared (IR) spectroscopy and transmission electron microscopy (TEM). The 3D structural changes after conjugation were monitored using circular dichroism (CD) spectroscopy. Four different organic solvents such as MeOH, EtOH, dimethylformamide (DMF) and acetonitrile (ACN) were used to test the activity of Hb. Esterified conjugates of Hb-PAA showed major activity retention followed by Hb-PAA, whereas, Hb showed least retention in activity in organic solvents. This retention of activity of esterified conjugates and Hb-PAA were

examined further using measuring the kinetic parameters of the Hb and Hb-PAA and Hb-PAA-ester conjugates. These showed that the esterified conjugates and Hb-PAA had superior catalytic efficiency in organic solvents in most of the cases. This showed the very first robust and easy method of using hydrophilic polymer conjugation for organic solvent activity of enzymes.

In next case, enzyme stability of two enzymes were improved in low pH, high temperature and in presence of denaturants. Glucose oxidase (GOx) and horseradish peroxidase (HRP) were used as model enzymes and PAA was used to conjugate to enzymes.<sup>2</sup> To further protect the enzymes 2D material – graphene oxide (GO) was used. In this study, bienzyme- GOx and HRP were first encapsulated covalently using PAA and the resultant bienzyme-PAA conjugate was physically conjugated to GO using non covalent interactions. The synthesis of bienzyme conjugates and bienzyme conjugate hybrids were confirmed using agarose gel electrophoresis, zeta potential and TEM micrographs. Tertiary structural changes of the enzymes were examined using CD spectroscopy. The biocatalysis applicability of these conjugates and conjugate hybrids were tested at high temperature, in presence of denaturant and at low pH. In all of the above cases, bienzyme conjugate hybrids – samples encapsulated both by PAA and GO proved greater in biocatalysis application. Also, these samples were recyclable up to 2-4 cycles depending upon the conditions. These robust, green and biocompatible bienzyme conjugate hybrids are useful in future for biocatalysis, energy and sensing applications.

Further the strategy of polymer encapsulation for enzyme stabilization was applied to stabilization of more than two enzymes. In this study total of 5 enzymes were stabilized using PAA. Industrially important enzymes were picked for this studies, such as, GOx, HRP, acid phosphatase (AP), lactate dehydrogenase (LDH) and lipase (Lip).<sup>3, 4, 5, 6, 7, 8, 9, 10</sup> The multienzyme conjugates are synthesized using 2 different routes such as, (1) parallel synthesis and (2) sequential synthesis. In case of parallel synthesis individual enzyme-PAA conjugates were synthesized in first step and in second step each 5 enzyme-PAA conjugates were extensively crosslinked to form multienzyme complex (MEC) 5-P. Sequential synthesis of MEC was done using one step conjugation. In this case all the enzymes and PAA was mixed in specific proportion and conjugated by adding cross-linker. This MEC was named 5-S. The synthesis of MEC and enzyme-PAA was confirmed using agarose gel electrophoresis, zeta potential, DLS. Morphology and structural studies were performed using TEM and CD spectroscopy. These conjugates were tested for room temperature and high temperature activity and it was seen that, MEC's performed superior in case of all enzymes at high temperature. At room temperature, MEC's showed decrease in activity for LDH and HRP, while in case of Lip and AP there was unprecedented increase in activity was observed. The impact of conjugation and multienzyme formation on enzyme kinetics was tested by assembling Lineweaver Burk plots and extracting useful parameters such as,  $K_M$ ,  $V_{max}$ ,  $K_{cat}$  and catalytic efficiency. These strategy of multienzyme formation can be used in biofuel cell or biobatteries. All the constituents used in this synthesis

were biologically compatible and green, therefore, it can be used for implantable devices such as pacemakers, which can derive energy from body fluids.

## **5.2 Proposal of Future Work**

Based on studies conducted and hypothesis tested as of now I am proposing some future experiments to be conducted that can solve some of the problems in biocatalysis, sensing and biofuel cell areas which are to be completed by my predecessors.

### **5.2.1 Biocatalysis**

In next round of studies biocatalysis of enzymes with various aspects can be tested, such as-

1. Recyclability of the biocatalysts
2. Long term storage stability of the biocatalysts
3. Stimuli responsive biocatalysts

These aspects can be improved on existing systems. The recyclability and stimuli responsiveness of the biocatalysts can be solved in conjunction where stimuli responsive polymer can be used that only responds to certain stimuli such as- temperature, pH, ionic strength or magnetism. This in turn can be helpful in recyclability aspect, where, these stimuli can make the whole biocatalyst easily separable from other media. Long term stability is a huge challenge in enzyme industry due to enzyme denaturation on storage at ambient temperatures. In our lab, we have enhanced the stability of the enzyme at room as well as low temperatures (8 °C) for up to 8 weeks.<sup>11</sup> The future aim is to stabilize the enzyme conjugates for longer duration up to few months.

### **5.2.2 Sensing**

The current method of multienzyme conjugation can be used for bio sensing of certain biologically relevant biomarkers. In our lab, a method for detection of glucose at micro molar level has been developed using paper based sensing. The multienzyme conjugates can be immobilized on paper as a cheap and robust sensing platform for quick and efficient sensing of different biomarkers.

### **5.2.3 Biofuel Cell Application**

The next study will be focused on development of biofuel cell using multienzyme conjugate as an anode and artificial hydrogenase as a cathode. Hydrogenases are an expensive enzyme, therefore, our lab focuses on synthesis of artificial hydrogenases using BSA as a platform for production of iron-sulfur cluster which will act as an artificial hydrogenase. While at an anode multienzyme complex can be used that catalyzes glucose or simple sugars to give electrons. These electrons can be shuttled through biofuel cell to get electrical energy. Therefore, simple biological feed can be used as an energy production medium. Hence, it is a cheap, green and environmentally friendly way of production of energy which is biologically compatible as well. This can be used for various energy production applications in batteries as well as in human implants such as pacemakers or insulin pumps.

In next set of experiments we plan to do collaboration with Prof Zhang from Virginia Tech institute. Their group uses 13 different enzymes for biofuel cell production from simple sugars. But the lack of heat and long term stability has limited the application of the biofuel cell. Therefore, in future, we plan to modify 13

different enzymes by conjugating them in similar fashion as we do for multienzyme conjugate formation consisting of 5 enzymes. There can be few different synthesis strategies used, such as, parallel/ sequential multienzyme synthesis. The high temperature workability of this system will enhance the power density of the sugar biobattery. This will be a first green, biocompatible, biodegradable and environmentally friendly biofuel cell that can be used for various applications.

### 5.3 References

---

1. Zore O. V.; Lenehan P. J.; Kumar C. V.; Kasi R. M. Efficient Biocatalysis in Organic Media with Hemoglobin and Poly(acrylic acid) Nanogels. *Langmuir*. **2014**, 30, 5176-5184.
- 2 Zore O. V.; Pattammattel A.; Gnanaguru S.; Kumar C. V.; Kasi R. M. Bienzyme–Polymer–Graphene Oxide Quaternary Hybrid Biocatalysts: Efficient Substrate Channeling under Chemically and Thermally Denaturing Conditions. *ACS Catal*. **2015**, 5, 4979-4988.
3. Cao X.; Li Y.; Zhang Z.; Yu J.; Qian J.; Liu S. Catalytic activity and stability of glucose oxidase/horseradish peroxidase co-confined in macroporous silica foam. *Analyst*. **2012**, 137, 5785-5791.
4. Heller A.; Feldman B. Electrochemical Glucose Sensors and Their Applications in Diabetes Management. *Chem Rev*. **2008**, 108, 2482-2505
5. Huber C.; Preis M.; Harvey P. J.; Grosse S.; Letzel T.; Schroder P. Emerging pollutants and plants – Metabolic activation of diclofenac by peroxidases. *Chemosphere*. **2016**, 146, 435-441.



- 
6. Huber C.; Preis M.; Harvey P. J.; Grosse S.; Letzel T.; Schroder P. Emerging pollutants and plants – Metabolic activation of diclofenac by peroxidases. *Chemosphere*. **2016**, 146, 435-441.
  7. Karaguler, N.G., Sessions, R.B. & Binay, B. Protein engineering applications of industrially exploitable enzymes: *Geobacillus stearothermophilus* LDH and *Candida methylica* FDH. *Biochem. Soc. Trans.* **2007**, 35, 1610-1615.
  8. Claire M. Bacterial acid phosphatase and its application to waste remediation and metal recovery. PhD Thesis, University of Birmingham, UK, **2011**.
  9. Tanaka H.; Horiuchi Y.; Konishi K. Determination of surfactants by use of acid phosphatase. *Anal. Biochem.* **1975**, 66, 489-497.
  10. Gandhi N. N. Applications of Lipase. *J. Am. Oil Chem. Soc.* **1997**, 74, 621-63.
  11. Riccardi C. M.; Cole K. S.; Benson K. R.; Ward J. R.; Bassett K. M.; Zhang Y.; Zore O. V.; Stromer B.; Kasi R. M.; Kumar C. V. Toward “Stable-on-the-Table” Enzymes: Improving Key Properties of Catalase by Covalent Conjugation with Poly(acrylic acid). *Bioconjugate Chem.* **2014**, 25, 1501-1510.